

MINISTRY OF EDUCATION AND SCIENCE OF UKRAINE
SUMY NATIONAL AGRARIAN UNIVERSITY

Qualifying scientific work on the
rights of the manuscript

LI FANG

UDC: 632.911.2: 632.951: 632.95.028

DISSERTATION

**COMPARATIVE EVALUATION OF DIFFERENT METHODS OF
DETERMINING PESTICIDE RESIDUES IN PLANT PRODUCTS**

Speciality: 202 Plant protection and quarantine

Field of knowledge: 20 Agricultural sciences and food

Submitted for a scientific degree of Doctor of philosophy

The dissertation contains the results of own research. The use of ideas, results and texts of other authors have references to the relevant source

_____ Li Fang

Scientific supervisor Volodymyr Dubovyk, PhD, Associate Professor

Sumy 2023

АНОТАЦІЯ

Лі Фанг. Порівняльна оцінка різних методів визначення залишків пестицидів у рослинній продукції. – Кваліфікаційна наукова праця на правах рукопису. Дисертація на здобуття ступеня доктора філософії за спеціальністю 202 «Захист та карантин рослин». Сумський національний аграрний університет, Суми, 2023.

Пестициди відіграють важливу роль у підвищенні врожайності сільськогосподарських культур та контролі шкідників і хвороб у сучасному сільськогосподарському виробництві. Однак порушення регламентів застосування пестицидів часто призводить до надмірного накопичення залишкових кількостей пестицидів, які завдають серйозної шкоди здоров'ю людей та навколишньому середовищу. Листові овочі мають сезонність і економічність, обсяги посівів не такі великі, як у зернових культур, і цикл їх росту короткий, тому вимоги до зовнішніх умов навколишнього середовища суворіші. Науковці вивчають відмінності та закономірності поглинання і транспортування пестицидів листовими овочами, що є важливим для контролю за забрудненням пестицидами. У зв'язку з цим, особливо актуальною є розробка простої, ефективної та недорогої технології виявлення залишків пестицидів, для аналізу рослинної продукції, з метою суворого контролю надлишкової кількості залишків пестицидів. Порівняно з традиційними методами виявлення, технологія електрохімічного сенсорного аналізу має ряд переваг, таких як висока ефективність, простота технології проведення аналізу та недороге обладнання. У цій роботі вивчені відмінності поглинання і перенесення пестицидів у різних листових овочах, а також досліджені особливості динамічного поглинання і накопичення пестицидів у гідропонному салаті. Крім того, для виявлення пестицидів застосували серію електрохімічних сенсорів з використанням декількох нанокompозитних матеріалів в якості модифікаційних матеріалів чутливих електродів. За оптимальних умов, виготовлені електрохімічні сенсори показали

високочутливу ефективність виявлення залишків пестицидів із задовільними показниками значень та з низькою межею виявлення (LOD). Виготовлені сенсори мають хорошу повторюваність, відтворюваність, стабільність та стійкість до перешкод. Крім того, на виготовленому сенсорі можна отримати точні та чутливі результати кількісного аналізу виявлення залишків пестицидів у реальних зразках. Основний зміст дослідження полягає в наступному:

(1) В якості дослідного пестициду обрано імідаклоприд (ІМІ), а в якості експериментальних об'єктів - салат-латук, пакчой-шанхайцин, пакчой-джимаокай, капуста ГаоГенг та зелені овочі, при цьому основна увага приділялася відмінностям поглинання та розповсюдження пестициду ІМІ в різних листових овочах, а також вивченню особливостей динамічного поглинання та накопичення. Результати показали, що коріння овочів поглинає пестициди з культуральної води, а потім переміщує їх у стебло, листя, старе листя, нове листя та інші частини. Залишок ІМІ в різних частинах салату був різним. Зі збільшенням експозиції ІМІ постійно накопичувався в листі, і залишкова концентрація ІМІ в листі поступово підвищувалась, порівняно з іншими частинами, а концентрація ІМІ в старому листі була вищою, ніж у нових листках.

(2) Карбоксильовані багатостінні вуглецеві нанотрубки (MWCNT-COOH) показали високу електропровідність і хороші диспергуючі властивості, завдяки одновимірній порожнистій провідній вуглецевій структурі та карбоксильній функціоналізації. MWCNT-COOH використали для модифікації склоподібного вуглецевого електрода (GCE) при виготовленні сенсора MWCNT-COOH/GCE для виявлення карбендазиму (CBZ). Присутність карбоксильної групи, певною мірою, покращила ступінь дисперсності вуглецевих нанотрубок, що дозволило досягти рівномірного розподілу вуглецевого матеріалу. Одновимірна порожниста провідна вуглецева структура сприяє ефективному транспортуванню заряду на поверхні

чутливого електрода, що покращує електрохімічну реакцію. За оптимальних умов виготовлений датчик MWCNT-COOH/GCE демонструє хорошу ефективність виявлення CBZ з низьким значенням LOD (6,7 нМ). Виготовлений датчик використовували для виявлення CBZ у зразках капусти, огірків та картоплі. Отримані результати мали низьке відносне стандартне відхилення (RSD) від 1,95% до 4,78% та високу точність визначення від 93,6 до 104,4%. В подальшому результати оцінили за допомогою високоефективної рідинної хроматографії (HPLC) для підтвердження точності електрохімічного виявлення CBZ.

(3) Пористий вуглець, отриманий з біомаси, є доступним і дешевим джерелом вуглецю. Пористий вуглець з сої (SDPC) з тривимірною (3D) взаємопов'язаною пористою структурою був отриманий шляхом використання некондиційної сої, як джерела вуглецю, за допомогою високотемпературного процесу карбонізації. SDPC був використаний для модифікації склоподібного вуглецевого електрода (GCE) при виготовленні сенсора SDPC/GCE для визначення імідаклоприду (ІМІ). Тривимірна взаємопов'язана пориста структура SDPC значно покращила електропровідність та здатність до поглинання ІМІ завдяки взаємопов'язаній вуглецевій провідній системі та великій питомій поверхні. За оптимальних умов виготовлений SDPC/GCE сенсор показав низьке значення LOD (5,18 нМ) в широкому діапазоні лінійних концентрацій ІМІ 0,3-75 мкМ. Виготовлений датчик використовували для виявлення ІМІ у зразках томатів та огірків. Потім оцінили результати за допомогою високоефективної рідинної хроматографії HPLC, щоб підтвердити точність електрохімічного виявлення ІМІ.

(4) Ефективність електрохімічного виявлення пестицидів можна покращити за допомогою синергетичного ефекту нанокompозитного сенсорибілізатора. Багатофункціональний нанокompозит надпровідної сажі (SCB) та ZrO_2 був отриманий за допомогою простої та ефективної технології з використанням ультразвуку. Нанокompозит SCB@ ZrO_2 був використаний для

модифікації склоподібного вуглецевого електрода (GCE) при виготовленні сенсора SCB@ZrO₂/GCE для визначення метилпаратіону (МП). Наночастинки SCB показали високу електропровідність, що сприяло ефективному транспортуванню заряду, а наночастинки ZrO₂ мали сильну спорідненість до фосфорних груп МП, що підвищувало здатність до накопичення МП. За оптимальних умов, виготовлений сенсор SCB@ZrO₂/GCE демонстрував низьке значення LOD (0,045 мкМ) у лінійному діапазоні концентрацій МП 0,03-10 мкМ. На виготовленому сенсорі отримали добрі результати виявлення МП у зразках салату, огірків і томатів. Потім оцінили результати за допомогою HPLC для підтвердження точності електрохімічного виявлення МП.

(5) Пористі вуглецеві сфери (PCS), отримані з простроченого соку цукрової тростини (SJ), готували гідротермічним методом і надалі модифікували β-циклодекстрином (β-CD). Нанокмпозит SJPCS@β-CD використали для модифікації склоподібного вуглецевого електрода (GCE) при виготовленні сенсора SJPCS@β-CD/GCE для визначення метилпаратіону (МП). SJPCS із взаємопов'язаною пористою структурою демонструє відмінну електропровідність, сильну адсорбційну властивість і високу питому поверхню, в той час як β-CD, з властивістю молекулярного розпізнавання, забезпечує рівномірну дисперсію SJPCS і сприяє розпізнаванню та адсорбції молекул МП. Завдяки синергетичному поєднанню SJPCS та β-CD, датчик SJPCS@β-CD/GCE продемонстрував високу ефективність визначення МП з нижньою межею виявлення 5,87 нМ в діапазоні концентрацій МП 0,01-10 мкМ. Для визначення МП в овочах (цибуля, капуста, шпинат) виготовлений сенсор показав хорошу практичність з відносним стандартним відхиленням від 1,06% до 4,25% і задовільною точністю визначення від 96,5 до 100,5%. Потім результати оцінили за допомогою HPLC для підтвердження точності електрохімічного визначення МП. Розроблено перспективну технологію швидкого визначення метилпаратіону в харчових продуктах.

Ключові слова: залишки пестицидів; інсектициди; карбендазим; імідаклоприд; метилпаратіон; електрохімічний сенсорний аналіз; електропровідні вуглецеві матеріали; пористий вуглець з біомаси; нанокompозит; синергічний ефект; високоефективна рідинна хроматографія; соя; картопля; огірок; захист рослин.

ANNOTATION

Li Fang Comparative evaluation of different methods of determining pesticide residues in plant product. - Qualifying scientific work on the rights of the manuscript.

Dissertation for the degree of Doctor of Philosophy in specialty 202 - "Plant protection and quarantine " - Sumy National Agrarian University, Sumy, 2023.

Pesticides have played an important role in improving the crop yield and eliminating the pests and diseases in modern agricultural production. However, the improper use of pesticides often leads to the excessive pesticide residues, which cause serious harm to human health and ecological environment. As we all known, leafy vegetables have obvious seasonality and economy, and the planting scale is not as large as that of grain crops, and their growth cycle is short, so the requirements for external environmental conditions are stricter. Therefore, the differences and laws of pesticide absorption and transport of leafy vegetables are studied, which are important for pesticide pollution control. Additionally, it is particularly urgent to develop a simple, efficient, and low-cost detection technology for analysing the pesticide residues to strictly control the excessive pesticide residues. Compared with traditional detection methods, the electrochemical sensing analysis technology has several advantages such as high efficiency, simple analysis operation, and inexpensive measurement equipment. In this work, the differences of pesticide absorption and transfer in different leaf vegetables were studied, and the dynamic absorption and accumulation rules were explored in hydroponic lettuce.

Otherwise, a series of electrochemical sensor by using several nanocomposite materials as modification materials of sensing electrodes were proposed for the pesticide detection. Under the optimal conditions, the fabricated electrochemical sensors showed highly sensitive pesticide detection performance with satisfactory recovery rates and low limit of detection (LOD) values. The good repeatability, reproducibility, stability, and anti-interference can be achieved at the fabricated sensors. Moreover, the accurate and sensitive quantitative analysis performance can be obtained at the fabricated sensor for the detection of pesticide residues in real samples. The main research contents are as follows:

(1) IMI was taken as the test pesticide, and Lettuce, pakchoi-Shanghaiqing, pakchoi-Jimaocai, GaoGeng Cabbage and Greengrocery were taken as the experimental objects, focusing on the differences of IMI pesticide absorption and transfection in different leafy vegetables, and exploring the dynamic absorption and accumulation law. The results showed that the roots of vegetable could absorb pesticides in culture water, and then transfer to stem, leaves, old leaves, new leaves and other parts. The residue of IMI in different parts of lettuce was different. With the increase of days, IMI was continually accumulated in the leaves, and the residual concentration of IMI in the leaves was gradually higher than that in other parts, and the concentration of old leaves was higher than that in new leaves.

(2) Carboxylated multi-walled carbon nanotubes (MWCNT-COOH) showed high electrical conductivity and good dispersing property due to the one-dimensional hollow conductive carbon structure and carboxyl functionalization. MWCNT-COOH was used to modify the glassy carbon electrode (GCE) for the fabrication of MWCNT-COOH/GCE sensor towards carbendazim (CBZ). The presence of carboxyl group improved the dispersion degree of carbon nanotubes to a certain extent, which could realize the uniform distribution of carbon material, and the one-dimensional hollow conductive carbon structure contributes to the efficient charge transport on the sensing electrode surface, which could enhance the electrochemical response. Under the optimal conditions, the fabricated MWCNT-

COOH/GCE sensor exhibited good CBZ detection performance with low LOD value (6.7nM). The good practical feasibility can be obtained at the fabricated sensor for the detection of CBZ in cabbage, cucumber and potato samples with low RSD from 1.95% to 4.78% and good recoveries from 93.6 to 104.4%, and then the results are evaluated by using HPLC to confirm the accuracy of CBZ electrochemical detection.

(3) Biomass-derived porous carbon possessed abundant low-cost biomass carbon source. Soybean-derived porous carbon (SDPC) with three-dimensional (3D) interconnected porous structure was prepared by using the expired soybean as carbon source through a high-temperature carbonization process. SDPC was used to modify the glassy carbon electrode (GCE) for the fabrication of SDPC/GCE sensor towards imidacloprid (IMI). The 3D interconnected porous structure of SDPC significantly improved the electrical conductivity and good absorption capability for IMI due to the interconnected carbon conductive network and large specific surface area. Under the optimal conditions, the fabricated SDPC/GCE sensor exhibited a low LOD value (5.18 nM) in wide IMI linear concentration range of 0.3-75 μ M. The good practical feasibility can be obtained at the fabricated sensor for the detection of IMI in tomato and cucumber samples, and then the results are evaluated by using HPLC to confirm the accuracy of IMI electrochemical detection.

(4) The pesticide electrochemical detection performance can be improved based on the synergistic effect of nanocomposite sensitizer. The multifunctional nanocomposite of superconductive carbon black (SCB) and ZrO₂ was prepared by a simple and efficient ultrasound-assisted strategy. The SCB@ZrO₂ nanocomposite was used to modify the glassy carbon electrode (GCE) for the fabrication of SCB@ZrO₂/GCE sensor towards methyl parathion (MP). SCB nanoparticles showed high electrical conductivity, which promoted the efficient charge transport, and ZrO₂ nanoparticles possessed strong affinity towards the phosphorus groups of MP, which enhanced the accumulation ability of MP. Under the optimal conditions, the fabricated SCB@ZrO₂/GCE sensor exhibited a low LOD value (0.045 μ M) in

MP linear concentration range of 0.03-10 μM . The good practical feasibility can be obtained at the fabricated sensor for the detection of MP in lettuce, cucumber and tomato samples, and then the results are evaluated by using HPLC to confirm the accuracy of MP electrochemical detection.

(5) The expired sugarcane juice (SJ)-derived porous carbon spheres (PCS) were prepared by hydrothermal method and further modified with β -cyclodextrin (β -CD). The SJPCS@ β -CD nanocomposite was used to modify the glassy carbon electrode (GCE) for the fabrication of SJPCS@ β -CD/GCE sensor towards methyl parathion (MP). SJPCS with interconnected porous structure exhibits excellent electrical conductivity, strong adsorption property, and high specific surface area, while β -CD with molecular recognition property achieves the uniform dispersion of SJPCS and promotes the recognition and adsorption of MP molecules. Thanks to the synergistic combination of SJPCS and β -CD, the SJPCS@ β -CD/GCE sensor exhibited respectable MP determination performance with low limit of detection of 5.87 nM in the MP concentration range of 0.01-10 μM . For the MP detection in vegetables (onion, cabbage, spinach), the fabricated sensor showed good practicability with adequate relative standard deviation of 1.06% to 4.25% and satisfactory recoveries of 96.5 to 100.5%, and then the results are evaluated by using HPLC to confirm the accuracy of MP electrochemical detection. A promising strategy for the rapid determination of methyl parathion in food products was developed.

Keywords: Pesticide residue; insecticides; Carbendazim; Imidacloprid; Methyl parathion; Electrochemical sensing analysis; Conductive carbon materials; Biomass-derived porous carbon; Nanocomposite; Synergistic effect; High Performance Liquid Chromatography; soya; Potato; cucumber; Plant protection.

LIST OF PUBLICATIONS

a. Publications that reflect the main scientific results of the dissertation;

• In foreign scientific professional journals indexed by Scopus and Web of Science Core Collection

1. **Fang Li**, Runqiang Liu, Volodymyr Dubovyk, Qiwen Ran, Bo Li, etc.. Three-dimensional hierarchical porous carbon coupled with chitosan based electrochemical sensor for sensitive determination of niclosamide, Food Chemistry. 2022,366:130563. (**Web of Science Core Collection, Q1**). (The applicant participated in research, analysis of the results and writing the article).
2. **Fang Li**, Runqiang Liu, Volodymyr Dubovyk, Qiwen Ran, etc.. Rapid determination of methyl parathion in vegetables using electrochemical sensor fabricated from biomass-derived and beta-cyclodextrin functionalized porous carbon spheres. Food Chemistry, 2022,384: 132573. (**Web of Science Core Collection, Q1**). (The applicant participated in research, analysis of the results and writing the article).
3. Runqiang Liu, Bo Li, **Fang Li**, Volodymyr Dubovyk, etc.. A novel electrochemical sensor based on beta-cyclodextrin functionalized carbon nanosheets@carbon nanotubes for sensitive detection of bactericide carbendazim in apple juice. Food Chemistry. 2022,384:132573. (**Web of Science Core Collection, Q1**). (The applicant participated in research, analysis of the results, writing the article and as corresponding author).
4. Liu Runqiang, Chang Yuqi, **Li Fang**, Dubovyk Volodymyr, Li Dongdong, Ran Qiwen, Zhao Hongyuan. Highly sensitive detection of carbendazim in juices based on mung bean-derived porous carbon@chitosan composite modified electrochemical sensor. Food Chemistry, 2022,133301. (**Web of Science Core Collection, Q1**). (The applicant participated in research, analysis of the results, writing the article and as corresponding author).
5. Wang Zhankui, Liu Yunhang, **Li Fang**, Dubovyk Volodymyr, etc.. Electrochemical sensing platform based on graphitized and carboxylated multi-

walled carbon nanotubes decorated with cerium oxide nanoparticles for sensitive detection of methyl parathion. *Journal of Materials Research and Technology*, 2022, 19, 3738-3748. (**Web of Science Core Collection, Q2**). (The applicant participated in research, analysis of the results, writing the article and as corresponding author).

- **Articles in scientific journals included in the list of scientific professional journals of Ukraine ranked category "B"**

6. **Li Fang**, Dubovyk Volodymyr, Liu Runqiang. Study of mathematical methods and models usage in the pesticide degradation and residue prediction. *Bulletin of Sumy National Agrarian University*, 2019, 35-36(1-2):67-71. (The applicant participated in research, analysis of the results and writing the article).
7. **Li Fang**, Dubovyk Volodymyr, Liu Runqiang. A review of rapid pesticide residues determination in vegetables and fruits. *Bulletin of Sumy National Agrarian University*. 2020, 42(4):40-47. (The applicant participated in research, analysis of the results and writing the article).
8. **Li Fang**, Dubovyk Volodymyr, Liu Runqiang. Rapid Electrochemical Detection of Carbendazim in Vegetables Based on Carboxyl Functionalized Multi-Walled Carbon Nanotubes. *Bulletin of Sumy National Agrarian University*. 2021, 4(46), 76-82. (The applicant participated in research, analysis of the results and writing the article).
9. **Li Fang**. Determination of methyl parathion in vegetables by high performance liquid chromatography. *Bulletin of Sumy National Agrarian University*. 2022, 3(49), 3-8. (The applicant participated in research, analysis of the results and writing the article, **Sole author**).

b. Publications that certify the approbation of the dissertation materials;

- **Conference papers**

10. **Li Fang**, Dubovyk Volodymyr, Liu Runqiang. Progress electrochemical sensor based on carbon nanotubes for pesticide residual detection. The 4th International scientific and practical conference "Fundamental and applied research in the

- modern world”,2020,11-18~19. (PhD participant in carrying out of experimental research, processing of results, and writing the article).
- 11.**Li Fang**, Dubovyk Volodymyr, Liu Runqiang. Present situation of pesticides uses and pesticides residue problems, Proceedings of the International Scientific and Practical CONFERENCE «HONCHARIVSKI CHYTANNYA» dedicated to the 92th anniversary of Doctor of Agricultural Sciences professor Mykolay Dem'yanovych Honcharov, 2021-5-25. (PhD participant in carrying out of experimental research, processing of results, and writing the article).
 - 12.**Li Fang**, Dubovyk Volodymyr, Liu Runqiang. The use of pesticides and the hazards caused by pesticide residues. fundamental and applied problems of modern ecology and plant protection, International scientific-practical conference, 2021-10-21~22. (PhD participant in carrying out of experimental research, processing of results, and writing the article).
 - 13.**Li Fang**, Dubovyk Volodymyr, Liu Runqiang. The principle of gas chromatography and its application in the analysis of pesticide residues. The 2nd International scientific and practical conference “Modern science: innovations and prospects”.2021-11-7~9. (PhD participant in carrying out of experimental research, processing of results, and writing the article).
 14. **Li Fang**, Dubovyk Volodymyr, Liu Runqiang. A review about the application of high performance liquid chromatography in pesticide residue detection. The 4th International scientific and practical conference “Science, innovations and education: problems and prospects”.2021-11-10~12. (PhD participant in carrying out of experimental research, processing of results, and writing the article).
 15. **Li Fang**, Wang Xinfu, Liu Dongmei, Dubovyk Volodymyr. A review of purified materials in QuEChERS pre-treatment method for pesticide residue detection. Proceedings of the International Scientific and Practical CONFERENCE «HONCHARIVSKI CHYTANNYA» dedicated to the 93rd anniversary of Doctor of Agricultural Sciences professor Mykolay Dem'yanovych Honcharov, 2022-5-25.(PhD participant in carrying out of experimental research, processing of results, and writing the article).

TABLE OF CONTENTS

INTRODUCTION.....	19
SECTION 1. LITERATURE REVIEW ON THE TOPIC AND CHOICE OF RESEARCH DIRECTIONS	26
1.1 Current situation, harm, and source of pesticide residues and the accumulation and transfer of pesticides in vegetables.....	26
1.1.1 Current situation of pesticide residues	26
1.1.2 Harm of pesticide residues	28
1.1.3 Source of pesticide residues	30
1.1.4 The accumulation and transfer of pesticides in plants	31
1.2 Typical pesticide residue detection techniques.....	33
1.2.1 Gas chromatography.....	33
1.2.2 High performance liquid chromatography	34
1.2.3 Chromatograph-mass spectrometry.....	35
1.2.4 Fluorescence detection techniques	37
1.2.5 Enzyme inhibition detection techniques.....	37
1.2.6 Biosensor techniques	38
1.3 New electrochemical sensing detection technology	39
1.3.1 Principle of electrochemical sensor.....	39
1.3.2 Classification of electrochemical sensors.....	40
1.3.3 Application of nanomaterials in electrochemical sensors	41
1.3.4 Application of electrochemical sensor in pesticide residue detection	46
1.4 Main research content	52
1.5 Conclusions in section 1	55
SECTION 2 ORGANIZATION, SUBJECTS, MATERIALS AND METHODS RESEARCH	57
2.1 Objects of research and Materials.....	57
2.2 Research methods	60
2.2.1 X-ray photoelectron spectroscopy (XPS) test	60

2.2.2 Infrared spectrometer (FT-IR) test	60
2.2.3 Scanning electron microscopy (SEM) - Transmission electron microscopy (TEM) test.....	60
2.2.4 X-ray diffractometer (XRD) test	61
2.2.4 Raman spectroscopy analysis	61
2.2.5 Electrochemical performance test	61
2.2.6 Surface pretreatment of glassy carbon electrode.....	62
2.2.7 Pretreatment of vegetable and fruit samples for electrochemical sensor detection.....	62
2.2.8 QuEChERS method.....	63
2.2.9 Pretreatment of vegetable samples for HPLC	63
2.2.10 Pretreatment of culture solution samples for HPLC	63
2.2.11 Calculation method of Limit of Detection	64
2.2.12 Statistical evaluation.....	64
2.3 The research route.....	65
2.4 Conclusions in section 2	66
SECTION 3 The Absorption and Accumulation of Imidacloprid Pesticide in several Hydroponic Leaf Vegetables	67
3.1 Instrument conditions and pretreatment methods.....	68
3.1.1 Chromatographic conditions and Chromatographs.....	68
3.1.2 Standard curve	68
3.1.3 The results of spiked recovery.....	69
3.1.4 Sample collection	70
3.2 Experimental results and analysis.....	71
3.2.1 Variety differences of IMI absorbed and accumulated in different leafy vegetables	71
3.2.2 Absorption and transfer dynamics of IMI in hydroponic lettuce.	73
3.3 Conclusion in section 3.....	75

SECTION 4 Determination of Carbendazim in Vegetables by electrochemical sensor based on MWCNTs-COOH and evaluated by High Performance Liquid Chromatography	78
4.1 Materials and Preparation Methods for electrochemical sensor.....	79
4.1.1 Fabrication of MWCNTs-COOH/GCE sensor.....	79
4.1.2 Detection method of MWCNTS-COOH/GCE Sensor for CBZ	80
4.2 Experimental results and analysis of electrochemical sensor detection	80
4.2.1 Microstructure and morphology of MWCNTS-COOH	80
4.2.2 Electrochemical properties of MWCNTS-COOH /GCE	81
4.2.3 Electrochemical behavior of CBZ	82
4.2.4 Optimization of detection conditions	83
4.2.5 Analytical performance of MWCNTS-COOH /GCE sensor	86
4.2.6 Reproducibility, stability and anti-interference.....	87
4.3 Detection of CBZ in vegetable samples and evaluated by HPLC	88
4.3.1 Detection of CBZ by electrochemical sensor based on MWCNT-COOH in vegetable samples.....	88
4.3.2 Determination of CBZ by HPLC in vegetable samples	89
4.3.3 Comparative evaluation on electrochemical sensor based on MWCNTs-COOH and HPLC for CBZ detection in Vegetables	91
4.4 Conclusion in section 4	91
SECTION 5 Determination of Imidacloprid in Vegetables by electrochemical sensor based on Soybean-derived Porous Carbon and evaluated by High Performance Liquid Chromatography.....	93
5.1 Materials and Preparation Methods for electrochemical sensor.....	95
5.1.1 Preparation of nanocomposites SDPC	95
5.1.2 Fabrication of SDPC/GCE sensor	95
5.2 Experimental results and analysis of electrochemical sensor detection	96
5.2.1 Microstructure and morphology of SDPC.....	96
5.2.2 Electrochemical characterization.....	97
5.2.3 Electrochemical behavior of IMI.....	99

5.2.4 Optimization of detection conditions	100
5.2.5 Analytical performance of SDPC /GCE sensor	102
5.2.6 Reproducibility, repeatability, and anti-interference.....	104
5.3 Detection of IMI in vegetable samples and evaluated by HPLC	105
5.3.1 Determination of IMI by electrochemical sensor based on SDPC in vegetable samples	105
5.3.2 Determination of IMI by HPLC in vegetable samples.....	105
5.3.3 Comparative evaluation on electrochemical sensor based on SDPC and HPLC for IMI detection in Vegetables	107
5.4 Conclusion in section 5	108
Section 6 Determination of Methyl parathion in Vegetables by electrochemical sensor based on Superconductive carbon black@ zirconia and evaluated by High Performance Liquid Chromatography.....	109
6.1 Materials and Preparation Methods for electrochemical sensor.....	111
6.1.1 Fabrication of SCB@ZrO ₂ /GCE sensor	111
6.2.2 Detection method of SCB@ZrO ₂ /GCE Sensor for MP	112
6.2 Experimental results and analysis of electrochemical sensor detection	112
6.2.1 Microstructure and morphology of SCB@ZrO ₂	112
6.2.2 Electrochemical characterization.....	113
6.2.3 Electrochemical behavior of MP	114
6.2.4 Optimization of detection conditions	115
6.2.5 Analytical performance of SCB@ZrO ₂ /GCE sensor	118
6.2.6 Reproducibility, repeatability, and anti-interference.....	119
6.3 Detection of MP in vegetable samples and evaluated by High Performance Liquid Chromatography	120
6.3.1 Determination of MP by electrochemical sensor based on SCB@ZrO ₂ in vegetable samples	120
6.3.2 Determination of MP by HPLC.....	121
6.3.3 Comparative evaluation on electrochemical sensor based on SCB@ZrO ₂ and HPLC for MP detection in Vegetables.....	123

6.4 Conclusion in selection 6	124
SECTION 7 Determination of Methyl parathion in Vegetables by electrochemical sensor fabricated from biomass-derived and β -cyclodextrin functionalized porous carbon spheres and evaluated by High Performance Liquid Chromatography	125
7.1 Materials and Preparation Methods for electrochemical sensor.....	128
7.1.1. Preparation of nanocomposites SJCS.....	128
7.1.2. Fabrication of SJPCS@ β -CD sensor.....	129
7.2. Experimental results and analysis of electrochemical sensor detection	129
7.2.1. Microstructure and morphology of SJPCS.....	129
7.2.2. Electrochemical characterization.....	134
7.2.3. Electrochemical behavior of MP	135
7.3.5. The optimization of detection conditions	138
7.3.6. Analytical performance of SJPCS@ β -CD/GCE	140
7.3.7. Reproducibility, repeatability, and anti-interference.....	142
7.3 Detection of MP in vegetable samples and evaluated by High Performance Liquid Chromatography	144
7.3.1 Determination of MP by electrochemical sensor based on SJPCS@ β -CD in vegetable samples	144
7.3.2 Determination of MP by HPLC.....	144
7.3.3 Comparative evaluation on electrochemical sensor based on SJPCS@ β -CD and HPLC for MP detection in Vegetables	145
7.4. Conclusion in section 7	145
CONCLUSIONS	147
Reference.....	150

THE LIST OF SYMBOLS

Abbreviation	Full name
MWCNTs	Multi-walled carbon nanotubes
ZrO ₂	Nano zirconia
β-CD	β-cyclodextrin
SCB	Superconductive carbon black
CTS	Chitosan
CBZ	Carbendazim
IMI	Imidacloprid
MP	Methyl parathion
NA	Niclosamide
IMI	Imidacloprid
SEM	Scanning electron microscope
TEM	Transmission electron microscope
XRD	X-ray diffraction
XPS	X-ray photoelectron spectroscopy
FT-IR	Fourier Transform Infrared spectoscopy
CV	Cyclic voltammetry
DPV	Differential pulse voltammetry
GCE	Glass carbon electrode
HPLC	High performance liquid chromatography
HPLC-MS/MS	High performance liquid chromatography-tandem mass spectrometry
RSD	Relative standard deviations
GC-MS	Gas chromatography - mass spectrometry
LC-MS	Liquid chromatography - mass

	spectrometry
LOD	Limit of Detection
MWCNTs-COOH	Carboxyl Functionalized Multi-Walled Carbon Nanotubes
SJPCS	the expired sugarcane juice-derived three-dimensional porous carbon spheres
3DHPC	three-dimensional hierarchical porous carbon
EIS	electrochemical impedance spectroscopy
PSA	Primary secondary amine
GCB	Graphitized carbon black

INTRODUCTION

Relvance of topic. Pesticides are widely used in agricultural production and bring huge economic benefits to society. According to the existing survey, in recent ten years, the problem of pesticide residues in soil and water is more serious, and crops can absorb and transport pesticides in soil and water, which leads to the hidden danger of pesticide residues exceeding the standard in crops with or without reasonable application of pesticides, and causes great harm to the ecological environment and human health. Compared with grain crops such as rice and wheat, leafy vegetables have obvious seasonality and economy, and the planting scale is not as large as that of grain crops, and their growth cycle is short, so the requirements for external environmental conditions are stricter. There are many pests and diseases, and pesticides are widely used in leafy vegetables production, which has caused frequent ecological environmental pollution problems, and the safe cultivation and planting of leafy vegetables has also received widespread attention from the society. Therefore, the study of differences and laws of pesticide absorption and transport in leafy vegetables are important for pesticide pollution control.

Commonly used detection methods of pesticide residues, such as High Performance Liquid Chromatography and Gas Chromatography, are subject to many limitations because of their expensive equipment, long analysis period, high technical content and special detect conditions. Therefore, it is of great significance to develop an analytical method for rapid detection of pesticide residues. Electrochemical sensing technology is an important method for rapid detection of pesticide residues. In recent years, with the development of nanotechnology, it has become the research and development direction to construct a rapid, efficient, sensitive and suitable electrochemical sensor based on the characteristics of nanomaterials for rapid detection technology of pesticide residues.

In this dissertation, the differences of pesticide absorption and transfer in different leaf vegetables were studied, and the dynamic absorption and accumulation rules were explored in hydroponic lettuce. In addition, four kinds of electrochemical sensors were prepared based on carbon-based nanomaterials/composites for the detection of carbendazim, imidacloprid and methyl parathion respectively, and satisfactory results were obtained in vegetable samples. HPLC method was conducted to confirm the accuracy of pesticide residues by electrochemical detection, and those experimental results showed that electrochemical sensing technology can meet the requirements of pesticide residue detection in actual vegetable samples. Moreover, those advantages of simple operation and fast response in electrochemical sensor provide the possibility for on-site detection of pesticide residues in agricultural products.

Connection of work with scientific programs, plans, and topic.The research work was carried out in accordance with the main direction of scientific research of Sumy National Agrarian University and Henan Institute of Science and Technology within the framework of scientific topics: National Key R&D Program of China (No. 2017YFD0301104), Project of Plant Protection Key Discipline of Henan Province (1070202190011005), and Zhongyuan Thousand Talents Program of Henan Province (ZYQR201810142).

The Aim and Objectives of the study.The purpose of the dissertation is to study the differences and rules of pesticide absorption and transport by different leafy vegetables, control pesticide pollution and guide agricultural safety production; and then to achieve rapid, sensitive and accurate determination in plant products by using new electrochemical sensing technology, and compare and confirm the accuracy of experimental results by using common Liquid Chromatography detection method.

To achieve the main goal, it was necessary to solve a number of interrelated tasks.

- 1, Determination of pesticide residues in hydroponic leaf vegetables by liquid chromatography;
- 2, The electrochemical reaction mechanisms of the three kinds of pesticides (Carbendazim, Imidacloprid, Methyl Parathion);
- 3, The physical characterization of carbon-based materials (composites) used to fabricate electrochemical sensors;
- 4, The electrochemical behaviors of the three kinds of pesticides (Carbendazim, Imidacloprid, Methyl Parathion) at modified electrodes;
- 5, The pretreatment process of plant products samples to be detected;
- 6, The exploration of chromatographic conditions, including Chromatographic column, mobile phase, flow rate and sample size.

Research Object. Focusing on the differences of IMI pesticide absorption and transfer in different leafy vegetables, and exploring its dynamic absorption and accumulation law; the electrochemical sensors based on carbon-based nanomaterials/composites were prepared for three kinds of pesticides (Carbendazim, Imidacloprid, Methyl Parathion) detection, and the results were evaluate by using HPLC to confirm the accuracy of pesticides electrochemical detection.

Research Subject. The differences of pesticide absorption and transfer in different leaf vegetables, and the dynamic absorption and accumulation rules in hydroponic lettuce; Comparative evaluation of electrochemical sensor technology and chromatography for the detection of pesticide residues in vegetable samples.

Research methods. Scanning electron microscope, Transmission electron microscope, X-ray diffraction (XRD) analysis, X-ray photoelectron spectroscopy, Raman spectroscopy analysis, Infrared spectrometer analysis, Cyclic voltammetry, High performance liquid chromatograph(HPLC), Differential pulse voltammetry and Statistical evaluation. The experimental data were processed by Microsoft Office Excel and Origin Pro8.0 for statistical analysis.

Scientific novelty of the obtained results.

- (1) There are variety differences of IMI pesticide residues in different leafy vegetables. According to the residue of IMI in different parts of different leafy vegetables, high residue varieties and low residue varieties were screen out. In addition, the absorption, transport and accumulation of IMI pesticides in vegetables were related to the treatment time of IMI. The results of this experiment showed that the residue of IMI could be detected in all parts of lettuce at 1 day after the root of lettuce was treated with a certain concentration of IMI culture solution; the concentration of IMI in old leaves was higher than that in any part of lettuce plants after 7 days; both new leaves and old leaves reached the peak after 10 days, and the content of IMI in new leaves was slightly lower than that in old leaves; after 15 days, the residual concentration of IMI in new leaves and old leaves of lettuce decreased compared with that in 10 days, which may be related to the degradation mechanism in plants, leaf surface area and transpiration of leaves.
- (2) The simple and efficient electrochemical detection of CBZ was realized based on the MWCNT-COOH/GCE sensor. The hollow conductive carbon structure and carboxyl functionalization of MWCNT-COOH synergistically enhanced the CBZ detection property. The CBZ detection result of the MWCNT-COOH/GCE sensor was evaluated by using HPLC to confirm the accuracy of CBZ electrochemical detection in vegetable samples.
- (3) The low-cost electrochemical detection of IMI was realized based on the SDPC/GCE sensor. The SDPC with 3D interconnected porous structure was prepared by using the expired soybean as carbon source. Thanks to the advantages of highly conductive porous carbon network and large specific surface area, the SDPC/GCE sensor exhibited good IMI detection performance. The IMI detection result of the SDPC/GCE sensor was evaluated by using HPLC to confirm the accuracy of IMI electrochemical detection.

(4) The highly sensitive electrochemical detection of MP was realized based on the SCB@ZrO₂/GCE sensor. SCB nanoparticles showed high electrical conductivity, which promoted the efficient charge transport, and ZrO₂ nanoparticles possessed strong affinity towards the phosphorus groups of MP, which enhanced the accumulation ability of MP. The combination of SCB nanoparticles and ZrO₂ nanoparticles significantly enhanced the MP detection property of the SCB@ZrO₂/GCE sensor. The MP detection result of the SCB@ZrO₂/GCE sensor was evaluated by using HPLC to confirm the accuracy of MP electrochemical detection.

(5) The highly sensitive electrochemical detection of MP was realized based on the SJPCS@β-CD/GCE sensor. SJPCS was prepared by hydrothermal method and further modified with β-CD. SJPCS with interconnected porous structure exhibits excellent electrical conductivity, strong adsorption property, and high specific surface area, while β-CD with molecular recognition property achieves the uniform dispersion of SJPCS and promotes the recognition and adsorption of MP molecules. The SJPCS@β-CD/GCE sensor exhibited respectable MP determination performance. The MP detection result of the SJPCS@β-CD/GCE sensor was evaluated by using HPLC to confirm the accuracy of MP electrochemical detection.

Practical significance of the obtained results. The residues of IMI in leafy vegetables were different among different vegetable varieties, because of their different abilities to absorb and transport IM. Through the hydroponic experiment of leafy vegetables, the distribution, transfer differences and laws of IMI residues in leafy vegetables-water system were preliminarily found out, which provided scientific basis for guiding the rational and safe use of imidacloprid and other common leafy pesticides.

Based on the characteristics of pesticide molecular structure and functional nano materials/composite coupling electrochemical sensing technology, the novel electrochemical sensors were constructed for rapid, sensitive and accurate detection

of pesticide residues, including three kinds of pesticide: Carbendazim, Imidacloprid and Methyl Parathion. It provided guarantee for the safety of plant products.

1, The MWCNT-COOH/GCE sensor was built for the detection of CBZ. Under the optimal experimental conditions, this sensor presented a low LOD value of 6.7 nM within an acceptable linear CBZ concentration range of 0.03-20 μ M. Moreover, the good practical feasibility can be obtained at the fabricated sensor for the detection of CBZ in cabbage, cucumber and potato samples, with low RSD from 1.95% to 4.78% and good recoveries from 91% and 104.7%, and then the results are evaluate by using HPLC to confirm the accuracy of CBZ electrochemical detection.

2, The SDPC/GCE sensor was built for the detection of IMI. Under the optimal experimental conditions, this sensor presented a low LOD value of 5.18 μ M within an linear CBZ concentration range of 0.3-75 μ M. Moreover, the decent practicability can be achieved at the SDPC/GCE sensor for the detection of IMI in tomato and Cabbage samples with low RSD from 1.67% to 4.63% and good recoveries from 94% and 108%, and then the results are evaluate by using HPLC to confirm the accuracy of IMI electrochemical detection.

3, The SCB@ZrO₂/GCE sensor was built for the detection of MP. Under the optimal experimental conditions, this sensor presented a low LOD value of 0.016 μ M within an linear MP concentration range of 0.03~10 μ M. Moreover, the decent practicability can be achieved at the SCB@ZrO₂/GCE sensor for the detection of MP in lettuce, cucumber and tomato samples with low RSD from 1.18% to 5.37% and good recoveries from 95.33% and 107.25%, and then the results are evaluate by using HPLC to confirm the accuracy of MP electrochemical detection.

4, In order to further explore the detection of MP by sensors, SJPCS@ β -CD/GCE sensor was built. The experiment results showed that the SJPCS@ β -CD/GCE sensor exhibited a relatively low LOD (5.87 nM) and wide linear concentration range (0.01-10 μ M) towards the determination of MP. Moreover, the decent practicability can be achieved at the SJPCS@ β -CD/GCE sensor for the detection of MP in three

kinds of vegetables -onion, cabbage and spinach samples with low RSD from 1.06% to 4.25% and good recoveries from 96.5% and 100.5%,and then the results are evaluate by using HPLC to confirm the accuracy of MP electrochemical detection..

Personal contribution of the applicant. The Ph.D. student conducted extensive literature search and analysis work around the research topic, formed a review of the research field; then optimized research technique and methods by experimental and laboratory studies, statistical processing and results analysis. Under the guidance of the supervisor, the experiment results were detailed explained and summarized, the conclusions of the dissertation was formulated, and practical suggestions were put forward.

Publication. According to the research results of the dissertation work, **15** articles were published in scientific journals. There were 5 scientific articles indexed by Web of Science Core Collection(Q1,Q2); 4 scientific articles published in Ukrainian scientific professional journal (category“B”) (of which one was sole author) , and the remaining 6 publiations were international conference papers.

Structure and scope of the dissertation. This dissertation was 168 pages in total, including annotation, introduction, 7 sections,conclusion and the list of used sources of literature included 291 groups of foreign authors. The main body of the dissertation was printed in 126 pages, including 5 Schemes, 20 tables and 92 figures.

SECTION 1. LITERATURE REVIEW ON THE TOPIC AND CHOICE OF RESEARCH DIRECTIONS

1.1 Current situation, harm, and source of pesticide residues and the accumulation and transfer of pesticides in vegetables

1.1.1 Current situation of pesticide residues

With the rapid growth of population in the world, human beings need more food and agricultural products. Pesticides have played an irreplaceable role in increasing the crop yield and eliminating the pests and weeds. However, the nonstandard abuse of pesticides always causes serious environmental pollution and food safety risks, which produce a serious threat to human health (Hughes et al., 2021; Jian-yong, 2018; Z. J. Liu & Cao, 2015; F. H. M. Tang, Lenzen, McBratney, & Maggi, 2021; Zuniga-Venegas et al., 2021). According to the authoritative statistics (Aslan et al., 2011), the loss of grain output, caused by various diseases, insects, and weeds in the field every year, can reach up to about 50% of the total yield. It is important to note that the pesticides can recover about 30% of the loss of grain output by preventing and killing the pests and diseases.

As a large agricultural country, China has a very vast land area, which supports a wide variety of cultivated crops (J. J. Gao, Gai, Liu, & Shi, 2021). The corresponding agricultural output lies front rank in the world. The annual application amount of pesticides in China is about 1.8 million tons. The application area reaches up to 300 million hm², which shows a trend of continuous growth every year (C. Ding & Cao, 2005). The use of pesticides has brought huge economic benefits in modern agricultural production. However, the negative impact of pesticide residues has been increasingly affecting the ecological environment, human health and international trade (de Medeiros, Acayaba, & Montagner, 2021; Farina, Abdullah, Bibi, & Khalik, 2017).

Pesticide residues refer to the general term of prototype, poisonous metabolin, degradations and impurities in living body, byproducts, and ecological environment.

There are four main categories of pesticide residues in China: organophosphorus pesticides, carbamate pesticides, and nicotinoid pesticides.

Organophosphorus pesticides are one kind of high efficiency, rapid, and wide spectrum pesticides, which have been widely used as insecticides. These pesticides mostly involve the phosphate esters and thiophosphorus esters. The commonly used organophosphorus pesticides are dimethoate, methyl parathion, malathion, trichlorfon, phoxim, parathion, etc. Organophosphorus pesticides are unstable in nature and volatile in alkaline media. Compared with other types of pesticides, the residual time of these pesticides is short and less pollution to the environment, but great harm can be produced for the human body. After entering the human body, organophosphorus pesticides can combine with cholinesterase to form phosphorylated cholinesterase. As a result, the activity of acetylcholinesterase is inhibited, and a large amount of acetylcholine is accumulated in the human body, which causes the serious damage on the nervous system.

Carbamate pesticides are one kind of organic synthetic compound pesticides with carbamate structure, which mainly involves the carbofuran, carbamide, carboxycarb, aphidiocarb, carbamide, etc. Carbamate pesticides with no special odor are stable under acidic conditions and decomposable under alkaline conditions. These pesticides are widely used for the prevention and control of plant diseases and insect pests in modern food and fruit and vegetable production due to the fast decomposition speed, high efficiency, low toxicity and strong anti-interference. Common pesticides of this type are carbofuran, Carbendazim and aldicarb etc.

Nicotinoid pesticides with nicotine structure are new type of insecticides with high efficiency, low toxicity, strong endotoxicity and high anti-interference. These pesticides have been used in more than 120 countries. The commonly used nicotinic pesticides mainly include imidacloprid, thiamethoxam, dinotefuran and acetamiprid, etc. The mechanism of their action is to prevent the normal transmission between nerve cells by affecting the synapses of the central nervous system of insects.

All kinds of pesticides may produce serious residual pollution to a certain extent in modern green agricultural production. Although the wide application of pesticides can improve the yield of agricultural products, we should also protect human life and ecological environment. Therefore, it is very important to reduce the amount of pesticide residues in modern food and fruit and vegetable production.

1.1.2 Harm of pesticide residues

Pesticides are used to prevent diseases and insect pests on crops, garden plants and cash crops so as to ensure the crop yield and improve economic benefits and commercial value. However, the irrational use of pesticides will cause harm to the environment, pollute the soil, water and air, and then directly or indirectly cause harm to human health. At present, 10%-20% of pesticides are effectively used to prevent diseases and insect pests. 5%-30% of pesticides enter into the atmosphere through volatilization. 40%-60% of pesticides penetrate into soil and groundwater (Jing, 2017). The pesticide residues and its harmful degradation products in grains (Popp, Peto, & Nagy, 2013), fruits (Govindasamy, Mani, Chen, Chen, & Sundramoorthy, 2017a; Sarangapani, O'Toole, Cullen, & Bourke, 2017), water, oil and other related products may cause serious harm to human health and food safety (Mie et al., 2017).

There are two main ways of pesticide poisoning in daily life. The pesticide residues can enter the human body through biological enrichment in the food chain. For example, vegetables, fruits, animals, and other animals containing pesticides are consumed in daily life. Moreover, the living environment is polluted by pesticides. For example, there are pesticide production factories or crops planted in a large area, which need many pesticides to prevent and control the pests. The human body inhales pesticides in the environment, which leads to the pesticide poisoning. Among them, the pesticide poisoning caused by pesticides entering human body through the food chain is the most common pesticide poisoning phenomenon. In recent years, the excessive pesticide residues have attracted widespread attention. The main harm as described as follows:

1.1.2.1 Harm of pesticide residues to ecological environment

In the process of agricultural production, most pesticides can't used directly act on target organisms but enter into the surrounding environment through various ways including the direct application, seed dressing, spraying, water flow, and other ways into the ecological environment, which cause serious pollution of soil (V. Silva et al., 2019), air, water and so on. Some pesticide residues remain in ecological environment for a long time, even for many years. It's easy for pests and bacteria in the environment to develop drug resistance, and even cause the destruction of the ecological balance and the loss of harmony in nature, resulting in a vicious circle (Rasheed, Bilal, Nabeel, Adeel, & Iqbal, 2019).

1.1.2.2. Harm of pesticide residues to human health

Pesticide residues can enter into the human body through the respiratory tract, digestive tract, skin and other ways, which cause different degrees of harm to human body. The serious harm mainly involve four aspects: gastrointestinal diseases (Jones, Everard, & Harding, 2014), cirrhosis (Teixeira et al., 2018), hydronephrosis, low human immunity, dizziness, amnesia (Taghizadeh et al., 2021), cancer and fetal deformities (Calaf, Bleak, & Roy, 2021). The common pesticide acute poisoning is mainly caused by the ingestion of food contaminated with pesticides. Serious harm may lead to the lifelong disability or even death.

1.1.2.3. Harm of pesticide residue to agricultural development

Under the condition of market economy, the pesticide residues affected the development of agriculture in China. Especially, the unreasonable use of pesticides may lead to the low germination rate, poor quality and late mature (Tudi et al., 2021). At present, green agriculture is the ultimate development trend of agricultural economy in the world. Pesticide residues may lead to the lack of market

competitiveness of agricultural products, which affect the development of green agriculture.

1.1.2.4. Harm of pesticide residues to export trade of agricultural and sideline products

Many countries have formulated several strict standards and laws to ensure the correct use of pesticides, which can decrease the pesticide residues in agricultural products (Ferro, Otsuki, & Wilson, 2015). However, the development level of different countries are different, and the provisions of pesticide residue limit vary greatly, which hinders the trade of agricultural products a certain extent, which causes great economic losses (P. Liu, Guo, & Iop, 2019). With the rapid development of society, people pay more attention to health and safety than ever before. The non-standard management and use of pesticides seriously threaten the safety of video and agricultural ecological environment, and potentially threaten the health of human beings. Therefore, the rapid, efficient, and practical pesticide residue analysis methods has great practical significance for the protection of ecological environment and food safety strategy.

1.1.3 Source of pesticide residues

There are three main sources of pesticide residues in modern agricultural production. The direct pollution of pesticides on agricultural products is one kind of common sources of pesticide residues (Szpyrka et al., 2015). The spraying pesticide can cause pesticide adhesion pollution on the surface of crops, which will be absorbed by crops and transferred to various parts. The direct pollution mainly involves the surface adhesion and inhalation pollution. Moreover, the indirect pollution caused by pesticides in the environment is one kind of common sources of pesticide residues. Due to the massive application of pesticides, a large number of pesticides enter into air (Gallart-Mateu, Armenta, & de la Guardia, 2016), water (Sjerps, Kooij, van Loon, & Van Wezel, 2019; Syafrudin et al., 2021; Tan, Ahmad, Abd Shukor, & Yeap, 2019) and soil (Davie-Martin, Hageman, Chin, Rouge, &

Fujita, 2015), which may lead to the environmental pollutant. Crops absorbed pesticides from the polluted environment for a long time, which can cause secondary contamination of food. In addition, contaminate food is aslo an important sources of pesticide residues through food chain and biological enrichment. It is estimated that about 30% of pesticides load the surface of crops after spraying, while the remaining 70% fall into the soil, water, and atmosphere, forming pesticide residues through indirect pollution of crops, or through the accumulation of food chain and biological enrichment effects. Food chain refers to the clothing moth ecological chain which is connected as food from lower to higher order in the animal ecosystem. Biological enrichment occurs in the process of chemical substances moving along the food chain. Therefore, human bodies at the top of the food chain are exposed to the most pollutants. The analysis of source of pesticides is shown in **Fig.1-1**.

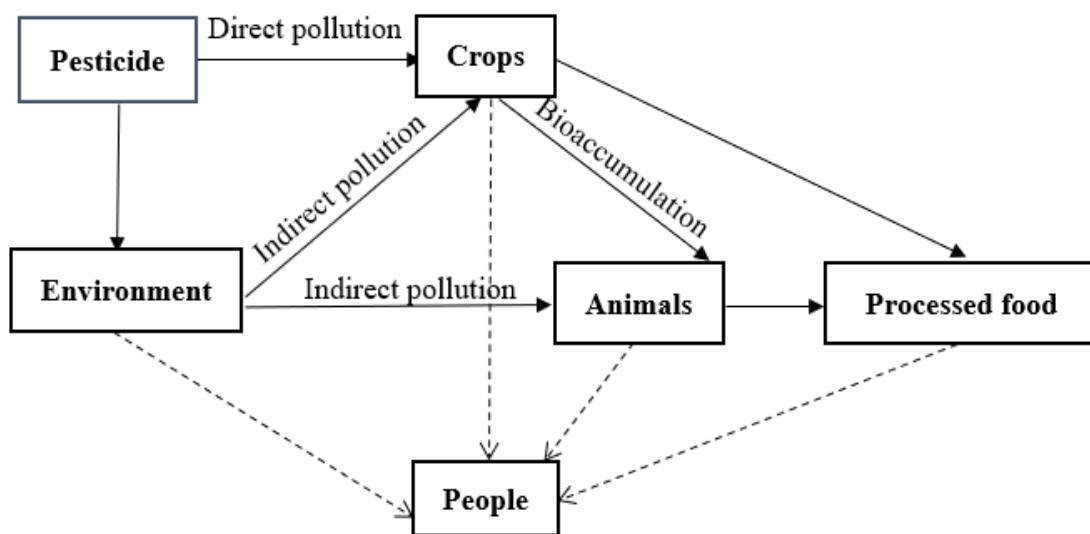


Fig. 1-1. The analysis of sources of pesticide residues

1.1.4 The accumulation and transfer of pesticides in plants

With the increasing variety of vegetables and the diversification of vegetable cultivation methods, there are more and more factors affecting the residue and

transfer of pesticides in vegetables. The absorption, enrichment and transfer of pesticides in plants often cause some physiological changes in plants. Almost all plants can absorb, enrich and transfer pesticides in a certain range. Due to the difference of plant species and varieties, the best growth period and the parts that absorb pesticides will also be different. The factors affecting the absorption, enrichment and transfer of pesticides in plants can be summarized as follows: vegetable varieties, cultivation methods, pesticide types and application methods, growth environment and so on.

Vegetable varieties. There are many kinds of vegetables, and the same kind of vegetables are divided into many varieties because of the shape and quantity of leaves and the specific resistance and tolerance of vegetables. The research shows that the pesticide residues and the degradation half-life of pesticides on different vegetables are different due to the differences of crop factors such as vegetable types and growth cycles.

Pesticide. Under the same inorganic environment, the absorption, degradation and residual amount of pesticides in vegetable plants are different due to the differences in chemical elements, substance structure and physicochemical properties of pesticides. The content of pesticide residues in vegetables increases with the increase of the original deposition of pesticides in vegetables. When spraying different concentrations of pesticides on the same vegetable, the original amount of pesticides deposited varies with the level of pesticide treatment. The amount of pesticide residues in vegetables is closely related to the spraying of pesticides on the leaves of crops or the irrigation of pesticides on the roots.

Growing environment. From the research of many scholars, inorganic environmental factors have an important influence on pesticide residues on plants, among which the main environmental factors are temperature, humidity, light, pH and so on. In order to study the factors affecting the degradation of neonicotinoid pesticides in the soil of *Lycium barbarum* plantation in Zhongning, Ningxia, the

residues of imidacloprid and acetamiprid under different soil temperature, humidity, pH value, salt content, initial concentration and microbial conditions were determined by HPLC-MS(Han, 2022). The results showed that soil microorganisms were the primary factors affecting the degradation of neonicotinoid pesticides in the soil of Zhongning Lycium barbarum plantation in Ningxia, and the initial concentration, temperature and humidity of pesticides also had significant effects, while the pH value and salt content of soil had relatively little effects.

1.2 Typical pesticide residue detection techniques

At present, many methods have been used to detect pesticide residue in agricultural products, including but not limited to Gas Chromatography (Pinho, Neves, Queiroz, & Silverio, 2009; Saka, 2010; B. Wang et al., 2010), High Performance Liquid Chromatography (Albaiges, 2016; Koo, Lee, Yang, Kim, & Shin, 2010), Chromatograph-mass Spectrometry (Covaciu, Magdas, Marincas, & Moldovan, 2017; Ueno, 2011), enzyme inhibition (Sulak, 2010; Upadhyay & Verma, 2013), fluorescence sensor(D. D. Su, Li, Yan, Lin, & Lu, 2021; Q. Wang et al., 2019), spectrophotometric and biosensor detection technology (Gong, Guo, Sun, Cao, & Wang, 2014; Kaewvimol, 2018; G. Zhao, Wang, & Liu, 2015). These methods have been widely used in pesticide residue detection because of their high sensitivity and high accuracy. Therefore, a series of important scientific research achievements have been made, which have opened a broad road for pesticide residue detection of crops.

1.2.1 Gas chromatography

Gas chromatography (GC) is a kind of chromatography, which uses gas as mobile phase for chromatographic separation and analysis, and is suitable for separation and analysis of volatile and difficult-to-decompose compounds. At present, GC is widely used in the detection and analysis of pesticide residues, and its detection effect is good well (Jian-yong, 2018). The separation efficiency is high, and that GC can separate complex mixture with very close boiling point. Usually, a chromatographic column with a length of 1 ~ 2 meters has the separation efficiency

of thousands of theoretical plates, and some longer chromatographic columns have the separation efficiency of hundreds of thousands or even millions of theoretical plates. The substances with very close or very complicated distribution coefficients that are difficult to separate can be separated accurately through repeated distribution and balance.

GC has the characteristic of fast analysis, usually a sample analysis can be completed in a few minutes to dozens of minutes, and the rapid analysis can be completed in a few seconds. In the analysis of some samples with very similar properties, samples can be injected at one time. GC has the characteristic of high selectivity, it can separate and analyze substances with similar boiling points, and it has a strong analytical ability for hydrocarbon isomers, optical isomers, isotopes and so on which are very similar in nature (Mei-yang, 2015).

In the direct qualitative analysis of components by GC, known substances or known data must be compared with corresponding chromatographic peaks, or combined with other methods (such as mass spectrometry and spectroscopy) to get direct positive results. In quantitative analysis, it is often necessary to use known pure samples to correct the detected output signals. In addition, GC analysis equipment is complex, expensive and expensive to use, and the operation is complex, professional and requires high personnel.

1.2.2 High performance liquid chromatography

High performance liquid chromatography (HPLC) is a new separation technology developed based on the classical liquid chromatography and meteorological chromatography. The high-efficiency stationary phase of ultra-fine particles is used in liquid column chromatography, and the whole separation process is controlled by computer. This method not only has high separation speed and detection efficiency, but also achieves the level of meteorological chromatography automation. At the same time, it maintains the advantages of liquid chromatography, such as wide application range of samples, flexibility of mobile phase change and

convenient mass preparation. HPLC is characterized by its ability to analyze pesticides at room temperature, especially for nonvolatile and thermally unstable pesticides. Due to the advantages of both liquid and gas chromatography, HPLC has been used and developed rapidly in recent years for the determination of pesticide residues. Mammana (Mammana, Berton, Camargo, Lascalea, & Altamirano, 2017) built a method based on coprecipitation-assisted cocervated extraction coupled to HPLC-UV, to detect 5 kinds of organophosphorus pesticides in water samples, including fenitrothion, guthion, parathion, methidathion, and chlorpyrifos. Under optimized conditions, The resulting LODs ranged within 0.7-2.5 ng/mL and the achieved RSD and recovery values were <8% (n = 3) and >81%, respectively.

HPLC has a wide selection of mobile phase and a wide variety of stationary phase, which is not limited by the volatility of the sample, so it can separate unstable and non-volatile substances. With the development of the stationary phase, it is possible to separate the sublimated substances with sufficient activity. Therefore, HPLC has great practical significance in the field of pesticide residue detection. The detect result by HPLC is highly accurate and sensitive, however, it is complicated to operate and requires high instruments.

1.2.3 Chromatograph-mass spectrometry

Chromatography-mass spectrometry is a combination of chromatography with high separation capability and mass spectrometry with high identification ability. This method has the characteristic of strong identification ability, fast analyze speed and high sensitivity, which can be used to separate and detect components under test at the same time. It's suitable for qualitative and quantitative analysis of unknown components in multi-component mixtures apply to multicomponent mixture of unknown components in qualitative and quantitative analysis, determination of molecular structure of compounds and determination of molecular weight of compounds.

Gas chromatography - mass spectrometry (GC-MS), combined with the high separation performance of GC and the ability to accurately identify compounds of MS, can be used to detect the components qualitatively and quantitatively, improving the sensitivity of the instrument, and have the effect of reducing interfering substances. GC-MS can serve for simultaneous qualitative and quantitative detection of multiple pesticide residues, which makes it very important in pesticide residue detection. Theurillat (Theurillat, Dubois, & Huertas-Perez, 2021) established a multi residue analysis method based on QuEChERS (Quick, Easy, Cheap, Effective, Rugged, and Safe). Pesticides in fatty matrices were extracted and determined by gas chromatography-mass spectrometry (GC-MS). Camara (Camara, Fuster, & Oliva, 2020) developed a QuEChERS multi-residue GC-MS/MS method for the detection of pesticides in fresh edible snails. There were quantified 27 different pesticides in the 824 samples analyzed. Among them, 22.09% contained pesticide residues.

Liquid chromatography - mass spectrometry (LC-MS) can be used to analyze easy volatile, thermally unstable, highly polar and low concentration pesticides. LC-MS has the advantages of good detection selectivity, high sensitivity, simultaneous qualitative and quantitative analysis, reliable results, and has a good ability to detect multiple pesticide residues. However, due to the high price of the instrument, the immature technologies and other shortcomings, The use of GC-MS and LC-MS is limited. Golge (Golge, 2021) developed a novel and sensitive chromatography method with modified Quick Polar Pesticide (QuPPE) sample preparation for determination of eight high polar pesticides in cherries by liquid chromatography-triple quadrupole mass spectrometry (LC-MS/MS). Good linearity ($R^2 > 0.99$) was observed, and the residuals were lower than +/- 20%. Average recoveries ranged from 70.2 to 105.1%, and LOQ values ranged from 1.77 to 12.13 mg/kg. The repeatability and reproducibility are in range of 1.57-15.56% and 3.51-16.17% separately. All measurement uncertainty values were lower than 50% for all polar pesticides.

1.2.4 Fluorescence detection techniques

Fluorescence detection method is based on the absorption and reaction of different substance molecules to light with different wavelengths. This technology has high sensitivity, but it is limited to the luminous pesticide, and the non-luminous pesticide still needs to be added with fluorescent agent, so it is easy to be interfered by external factors, and its adaptability is poor (Ouyang et al., 2021; S. Wang et al., 2021). The fluorescence sensor consists of fluorescence signal element and identification element. Enzymes, antibodies, aptamers and molecularly imprinted polymers (MIP) are combined with nanomaterials to further enrich the types of fluorescence sensors (Y.-z. ZHOU, WANG, LIU, & Industry, 2018) . Hou(Hou et al., 2015) used tyrosinase to catalyze the oxidation of tyrosine methyl ester on the surface of carbon dots to corresponding quinone products, which can quench the fluorescence of carbon dots, and the enzyme inhibition rate is proportional to the logarithm of the methyl parathion concentration in the range 1.0×10^{-10} – 1.0×10^{-4} M with the detection limit (S/N=3) of 4.8×10^{-11} M. Luo (Luo, Lai, Qiu, Wang, & Chemical, 2018) proposed a simple method for the preparation of highly selective and sensitive fluorescent probes based on Rhodamine B (RB) modified silver/gold bimetal nanoparticles (RB-Ag/Au NPs). Because that the coordination ability of Ag/Au NPs and organophosphorus pesticides is stronger than that of Ag/Au NPs and RB, RB will be displaced from the Ag/Au NPs surface, accompanied by the fluorescence recovery of RB. It can be applied to the determination of Organophosphorus Pesticides in real fruit and water samples with the limit of detection (LOD) as low as 0.0018 ng/mL.

1.2.5 Enzyme inhibition detection techniques

Enzyme inhibition method is a relatively mature detection technology. This method is based on the toxicological principle that organophosphorus and carbamate pesticides can specifically inhibit the activity of acetylcholinesterase (AChE) in the central and peripheral nervous system of insects, destroy the normal conduction of nerves, and make insects die of poisoning, so that AChE can react with the inhibitor

in the sample. According to the inhibition of AChE activity, it can be judged whether the sample contains organophosphorus and carbamate pesticides. According to the different detection methods, enzyme inhibition method can be divided into enzyme slice method and colorimetric method. Yang (X.-m. Yang, Gu, Wu, Feng, & Xie, 2019) proposed an enzyme inhibition method to detect the pesticide residues of the milk. He established a system to study the inhibitory reactions of organic phosphorus and aminofosphate residues in milk. The analysis of color reactions of milk showed a good correlation between color intensity and content of tolclofos-methyl, methamidophos and isoprocarb 1-naphthalenyl methyl carbamate, and the detection range of four kinds of pesticides is 0.5 ~ 1.0 mg/kg.

Although the detection technology of enzyme inhibition method is low in cost and convenient to operate, the results can be obtained in a short time, but the types of pesticides and samples suitable for this method are limited, and it can only be used for the residue detection of organophosphorus and carbamate pesticides at present. Recently, many researchers study the selective purification of enzyme, effective oxidation pretreatment, colorimetric signal enhancement and false positives elimination. The sensitivity of enzyme inhibition method is influenced by the purity of the enzyme, the concentration of substrate and environmental factors, etc., and the stability and sensitivity of the enzyme suppression method are need to be higher (Arduini et al., 2019; Pundir, Malik, & Preeti, 2019; Sgobbi & Machado, 2018).

1.2.6 Biosensor techniques

Biosensory method combines biochemical technology and electrochemical reaction principle, and uses bioactive substances such as antigens, antibodies, nucleic acids, enzymes and cells with molecular recognition function as sensitive elements to convert the concentration of the measured object into electrical signals (T. S. E. Silva et al., 2020; J. Tang et al., 2020). However, the sensitive elements of this method is not easy to obtain, which limits the widening of its application range. Recently, biosensors based on nanomaterials have developed

rapidly in pesticide detection, and more and more new nanomaterials have been used to prepare electrochemical biosensors, which greatly promoted the development of the biosensor technology (Akdag, Isik, & Goktas, 2020; Ayat, Ayouz, Yaddadene, Berouaken, & Gabouze, 2021; Chouichit, Whangsuk, Sallabhan, Mongkolsuk, & Loprasert, 2020; Jain, Yadav, Joshi, Joshi, & Kodgire, 2021; Lah, Ahmad, & Low, 2021). The electrochemical biosensor based on the inhibition of acetylcholinesterase is a promising method for the detection of organophosphorus. The irreversible oxidation peak of the active product thiocholine is an important marker for the detection of organophosphorus (Alex & Mukherjee, 2021; Cao et al., 2020; Caratelli et al., 2020; Davletshina, Ivanov, Shamagsumova, Evtugyn, & Evtugyn, 2020; T. S. E. Silva et al., 2020; A. P. Singh, Balayan, Hooda, Sarin, & Chauhan, 2020). Zhao (H. Zhao et al., 2015) constructed an ultra-sensitive current sensor by using Au nanoparticles (AuNPs)- β -cyclodextrin (β -CD) and Prussian blue-chitosan (PB-CS) and acetylcholinesterase (AChE), and realized the high sensitivity detection of malathion and carbaryl through the synergic action of multiple components, with detection limit as low as 4.14 pg/mL and 1.15 pg/mL, respectively. By cross-linking acetylcholinesterase onto the IL-GR/Co₃O₄ / CHI electrode constructed from ionic liquid modified graphene (IL-GR) and Co₃O₄ nanoparticles, Zheng (Zheng, Liu, Zhan, Li, & Zhang, 2016) was able to effectively reduce the loss of enzyme activity and improve the detection sensitivity. A linear relationship between the inhibition percentage (I%) and logarithm of the concentration of dimethoate was found in the range from 5.0×10^{-12} to 1.0×10^{-7} M, with a detection limit of 1.0×10^{-13} M (S/N = 3).

1.3 New electrochemical sensing detection technology

1.3.1 Principle of electrochemical sensor

The working principle of the electrochemical sensor is that the target substance generates electrochemical reaction on the surface of a specific electrode, generating electrochemical signals, which are converted into electrical signals by a transducer, and the electrical signals are amplified, filtered and converted to analog-digital by a

detector and then output to a computer. Electrochemical sensors generally adopt a three-electrode system, including working electrode, counter electrode and reference electrode.

The main components of electrochemical sensors are Sensing elements and transducer, and their basic structure and principle are shown in **Fig 1-2**. The materials with specific recognition function are fixed on the surface of the bare electrode to form a sensing element, which reacts with the target substance to be measured and converts the obtained reaction parameters into perceptual signals. The transducer receives the sensing signal, converts it into measurable electrical signal and electrochemical signal, and then outputs the obtained electrical signal after secondary amplification and processing by the electronic system, and finally displays and records it by the computer. According to the linear relationship between the electrical signal and the concentration of the target substance, the measured substance can be analyzed.

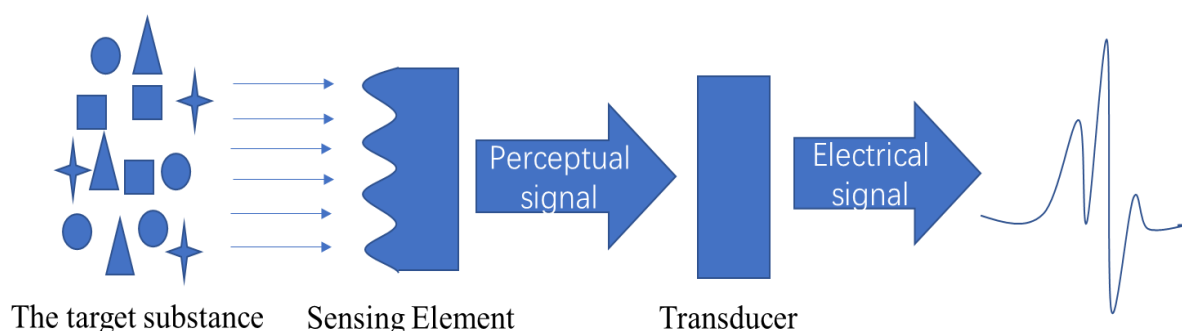


Fig.1-2. The structure and working principle of electrochemical sensor.

1.3.2 Classification of electrochemical sensors

The signal detected by electrochemical sensor includes potential, current, resistance, capacitance, and frequency, etc., and the changes of these electrochemical signals can be directly measured. According to the different electrochemical response mechanism, electrochemical sensors can be divided into current type, potential type, conductivity type and other electrochemical sensors.

1.3.3 Application of nanomaterials in electrochemical sensors

The sensitivity of electrochemical sensor can be improved by chemically modified electrode. By physical and chemical methods, some substances with special properties are given to the electrode to improve its function, and some new chemical and electrochemical properties are given to the electrode to improve the selectivity and sensitivity of the instrument. In the detection of pesticide residues in agricultural products, the electrode can be modified with inorganic materials, organic materials, and other materials, or the electrode can be combined with biological sensitive elements (such as enzymes, DNA, etc.), through the interaction between pesticide molecules and biological sensitive elements, indirectly feedback the change of the target to be measured.

Nanomaterial electrochemical sensor is an electrode conversion element, and the electrochemical performance of the sensor can be significantly improved by modifying the nanomaterial or its composite material on the electrode surface, to achieve high efficiency and sensitive detection of the target compound. Due to the unique properties and excellent electrochemical properties of nano-materials, the sensitivity, stability and selectivity of electrochemical sensors can be significantly improved after modification of nano-materials, which makes the modification of electrochemical sensors by nano-materials become a hot research topic at present. (Dominguez, 2003; Merkoci, 2002). Nanomaterials widely used in the field of electrode modification materials can be divided into carbon nanomaterials (carbon nanotubes, graphene), metal oxide nanomaterials, conductive polymers, etc. There are fewer and fewer single nanomaterials used as electrode modification materials, and compounds of nanomaterials, macromolecular nanomaterials with other functions, and combinations of biomolecules are often used, so that we can fully give play to the role of the synergies between the two, and then improve the detection performance of electrochemical sensor. With the rapid development of materials science, many nanoscale materials have been used to construct

electrochemical sensors, such as carbon-based materials, nano metals, metal oxides, composite materials etc..

1.3.3.1 Application of carbon-based nanomaterials in electrochemical sensors

Carbon nanotubes, discovered by Japanese electron microscope scientist Iijima in 1991, has attracted much attention (Iijima, 1991). As one of the great discoveries in the field of nanomaterials in the 20th century, the p electrons of carbon atoms on carbon nanotubes form a wide range of delocalized π structures, which make them have obvious conjugation effect and promote the special electrochemical properties of carbon nanotubes. Carbon nanotubes are often used as catalysts or supporting materials in electrochemical sensors due to their large specific surface area, good electrical conductivity, and strong electrochemical stability. According to the number of graphite layers, carbon nanotubes can be divided into multi-walled carbon nanotubes (MWCNTs) and single-walled carbon nanotubes (SWCNTs). Due to the special structure and electrochemical performance of carbon nanotubes, they can often be loaded or filled with other special materials, and better performance of carbon nanotubes composites can be prepared to improve their electrochemical performance (N. Liu, 2018). There are two known composite forms of carbon nanotubes and composite materials. One is carbon nanotubes as the main body, and other materials are modified on carbon nanotubes to increase their solubility and make them evenly dispersed. The other takes polymer as the main body and carbon nanotubes as the filling material, which can significantly improve the stability and conductivity of composite materials (Xiaomiao Feng, Li, Yang, & Hou, 2012). Polymers are mainly conductive polymers, such as polyaniline (PAn), polypyrrole (PPy), and poly-p-benzene (PPP). Carbon nanotube composites have attracted extensive attention from many researchers due to their superior electrocatalytic properties and significantly improved detection performance of sensors.

Messaoud et al. (Ben Messaoud, Ghica, Dridi, Ben Ali, & Brett, 2017) successfully prepared a novel electrochemical sensor for the highly sensitive

detection of bisphenol by using multi-walled carbon nanotubes (MWCNTs) and AuNPs modified GCE. The properties of the modified electrode were better than those of the unmodified electrode. Under the optimal conditions, when the concentration of the detected substance is in the range of 0.01 μM to 0.7 μM , the peak current and its concentration show a good linear relationship, the detection limit is 4 nM, and the electrochemical sensor has good reproducibility and stability.

Wang et al. (D. Y. Wang et al., 2018) successfully constructed a novel electrochemical sensor of MWCNTs/Cu@Ni by combining multi-walled carbon nanotubes (MWCNTs) with copper-nickel nanoparticles (Cu@Ni). Both guanine (G) and adenine (A) were detected under optimal conditions, the electrochemical signals showed a linear relationship in the concentration range of 5-18 μM and 8-15 μM , respectively. The detection limits were 0.35 μM and 0.56 μM (S/N=3), respectively. The linear ranges of G and A were 1-18 μM and 2-15 μM , respectively, and the detection limits were 0.17 μM and 0.33 μM (S/N=3), respectively. The sensor has been successfully used for the quantitative detection of G and A in actual samples, which indicates that the composite MWCNTs/Cu@Ni has a broad application prospect.

Li Wenjin et al. (J. Li, 2014) modified GCE with nano-composite MWCNTs/poly (2-acetyl-5-bromothiapan) and successfully prepared a novel electrochemical sensor capable of simultaneously detecting hydroquinone (HQ), catechol (CC) and p-methylphenol (PC). The concentrations of HQ, CC and PC within 1×10^{-5} - 8×10^{-4} mol/L, 5×10^{-6} - 5.5×10^{-4} mol/L and 5×10^{-6} - 7×10^{-4} mol/L showed a good linear relationship with peak current. The results show that the sensor has high sensitivity and high selectivity.

1.3.3.2 Application of metal oxide nanomaterials in electrochemical sensors

Metal oxide nanomaterials are an important part of nanomaterials. With the development and research of nanotechnology, more and more metal oxide materials have been developed. Common metal oxide nanomaterials mainly include ZrO_2 ,

TiO₂, ZnO, MnO₂ and so on. Because of the good electric catalytic activity, unique biological compatibility, and higher specific surface area, metal oxide nanomaterials are used as the electrode modification material, which can obviously accelerate the electron transfer rate, and the electrochemical performance is significantly improved.

Kumaravel et al. (Kumaravel & Chandrasekaran, 2011) modified GCE with TiO₂/Nafion nanocomposite material with good biocompatibility, and successfully prepared an electrochemical sensor for the highly sensitive detection of Sumithion. The DPV method was used to detect the electrochemical performance of the modified electrode. In the range of 0.2 ~ 4 μM, the linear relationship between the response current and the concentration was obvious. The limits of detection and quantification were 0.0866 μM and 0.2889 μM, respectively, and the relative standard deviation was 5.1%. The peak current measured by CV method remains stable after 50 cycles, indicating that it has good stability.

Wang et al. (Y. L. Wang et al., 2015) successfully prepared ZrO₂/OMP nanocomposites by modifying ordered mesoporous polyaniline (OMP) with ZrO₂ nanoparticles, and constructed a new electrochemical sensor for the rapid detection of MP. The sensor makes full use of the strong affinity of ZrO₂ for phosphate groups and the synergistic effect of OMP with high catalytic activity and strong conductivity. Therefore, the constructed sensor shows good electrochemical response. Under the optimal conditions, the MP limit of detection was as low as 2.28×10^{-10} mol/L (S/N=3). In addition, the sensor has good selectivity, reproducibility, and stability, and has been successfully used for the detection of MP in apples and cabbage.

ReddyPrasad et al. (ReddyPrasad, Naidoo, & Sreedhar, 2019) prepared C-dots/ZrO₂ nanocomposites by electrochemical deposition method to modify GCE and successfully constructed a new electrochemical sensor for highly sensitive detection of methyl parathion (MP). Under the optimal conditions, DPV method was used to detect MP, and the concentration range was 0.2-48 ng/mL. There was a

good linear relationship between current and MP concentration, and the detection limit was 0.056 ng/mL. In addition, the novel electrochemical sensor was applied to the determination of methyl parathion in rice samples, and satisfactory results were obtained.

1.3.3.3 Application of conductive polymer nanocomposites in electrochemical sensors

Conductive polymer is a kind of conductive polymer material prepared by chemical or electrochemical "doping" of polymer with conjugated chain structure, which has both the properties of polymer material and the strong conductivity of metal compounds (Hui, 2017). Conductive polymers mainly include polyaniline (PAn), polypyrrole (PPy), poly-thiophene (PTi), and poly-p-benzene (PPP), etc., which are widely used in the field of electrochemical sensors due to their good conductivity, catalytic performance, and environmental stability.

Conductive polymer nanocomposite refers to the composite of conductive polymer and other materials in the nanometer scale, which has both excellent properties. The synergistic effect produced by the composite can significantly improve the performance of conductive polymer nanocomposites and expand their application. For example, conductive polymer and carbon nanotube doping can significantly improve their dispersion and processing performance. In addition, there is a strong interaction between the conjugated π electrons of the main chain of conductive polymerization and the free P electrons of carbon nanotube, and the combination of the two can significantly improve the conductivity. Currently, composites of conductive polymers with carbon materials (carbon nanotubes and graphene), metal nanoparticles, metal sulfides and oxides are widely used.

Dai et al. (H. Dai, 2018) first prepared polypyrrole (PPy/ graphene (GO) nanocomposites by electrochemical polymerization method, then used phytic acid (PA) molecules to carry out electrostatic adsorption functionalization of PPy/GO nanocomposites, and successfully prepared a PA/PPy/GO based electrochemical

sensor for detecting heavy metal ions. Electrochemical test results show that PA/PPy/GO modified electrode has higher conductivity and larger peak current. Differential pulse voltammetry (DPV) was used for electrochemical detection of heavy metal ions lead (Cd) and Cadmium (Pb). The corresponding linear range was 5-150 $\mu\text{g/L}$. In addition, the preparation of PA/PPy/GO nanocomposite electrochemical sensor provides a simple, rapid, and sensitive electrochemical method for high sensitivity detection of heavy metal ions.

Mahmoudian et al.(Mahmoudian, Basirun, & Alias, 2016) firstly prepared gold nanoparticles/polypyrrole composite by electrochemical method, and successfully constructed an electrochemical sensor with high sensitivity and high selectivity for rapid detection of serotonin. The synergistic effect of polypyrrole and gold nanoparticles on the surface activity of the modified electrode was fully utilized. When the sensor is used to detect serotonin in serum samples in the presence of interfering substances, the analytical performance is 320 times that of the bare electrode.

Tertis et al. (Tertis et al., 2017)prepared an electrochemical sensor for mercury ion detection by using platinum/polypyrrole nanosphere composite material (Pt/PPy NSS). The composite was synthesized by direct reduction of potassium tetrachloroplatinate (II) in the presence of pyrrole monomer in sodium hydroxide solution. DPV method was used to detect mercury ions. The linear concentration range was 5-500 nM and the detection limit was 0.27 nM (S/N=3). In addition, the sensor has high sensitivity and strong anti-interference ability.

1.3.4 Application of electrochemical sensor in pesticide residue detection

Electrochemical sensor is a very important sensor which integrates sensing technology and electrochemical analysis technology, and has been successfully applied to the rapid analysis and detection of various pesticide residues in agricultural products.

1.3.3.1 Application of electrochemical sensor in organophosphorus pesticide detection

Pesticides can effectively reduce plant diseases and insect pests, provide a good environment for the growth of crops, so that the output of crops increased significantly, agricultural production cannot do without pesticides. At present, organophosphorus pesticides are widely used, with many categories, good effects, short residual time, rapid decomposition by microorganisms and strong selectivity. The usage of Organophosphorus Pesticides in agricultural production also shows an increasing trend year by year. Organophosphorus Pesticides can inhibit acetylcholinesterase, so the enzyme electrode is constructed to indirectly reflect the content of organophosphorus pesticides with the help of the inhibition rate of the enzyme electrode, namely electrochemical biosensor. However, electrochemical biosensors also have its shortcomings, such as enzyme is easily soluble in water, easy to inactivate, and enzyme immobilization has high composition, low repeatability, poor stability, etc. Therefore, people began to build pesticide residues electrochemical sensors that do not rely on enzymes.

Huo et al. (Huo, Li, Zhang, Hou, & Lei, 2014) developed a novel electrochemical sensor based on a hybrid nanocomposite composed of copper oxide nanowires (CuO NWs) and single-walled carbon nanotubes (SWCNTs) for the detection of organophosphorus pesticides. Hybrid nanocomposites are highly stable and have special affinity for Malathion, which provides a basis for electrochemical quantitative analysis of Malathion. Under optimized operating conditions, differential pulse voltammetry (DPV) was further used to detect malathion. Its dynamic range was wide and the detection limit was as low as 0.1ppb (0.3nm). It showed good selectivity to other common pesticides, inorganic ions, and sugars, as well as good stability and reproducibility.

Based on synthetic peptide nanotubes (PNTs) and modified graphite electrode (PGE), Bolat et al. (Bolat, Abaci, Vural, Bozdogan, & Denkbaz, 2018) developed a novel, simple and sensitive insecticidal thionophos (FT) sensor. Under optimal

conditions, the electrochemical response of PNT/PGE was linearly proportional to the concentration of FT in the range of 0.114 μM to 1.712 μM , with a detection limit of 0.0196 μM ($S/N = 3$). The sensor is also used to detect fenitrothion in tap water. The recoveries of the spiked water were between 94.9% and 103.6%. The sensor was also applied for the detection of fenazion in tap water. The recoveries of the spiked water samples ranged from 94.9 to 103.6%.

Gao et al. (N. Gao et al., 2019) first synthesized graphene nanosheets modified with gold and zirconia nanocomposites by simple electrochemical co-deposition on glassy carbon electrodes (Au-ZrO₂-GNS /GCE) for electrocatalytic analysis of methyl parathion (MP). The sensor based on AuZrO₂-GNS /GCE shows excellent MP detection capability due to the strong affinity of zirconia for phosphate groups, as well as the high catalytic activity and good electrical conductivity of Au-GNs. Then the optimum manufacturing and operating conditions were obtained by systematically optimizing the electrodeposition process, pH value and enrichment time. The sensor response current of square wave voltammetry is highly linearly correlated with the MP concentration range of 1-100 ng/mL and 100-2400 ng/mL, and the detection limit is 1 ng/mL. Au-ZrO₂-gns/GCE nanocomposite sensor showed excellent accuracy and reproducibility in detecting MP in Chinese cabbage samples, which provided a new method for efficient pesticide detection in practical application.

Chen (Z. F. Chen et al., 2021) successfully developed a high-performance nitrogen-doped holey graphene (N-HG) electrochemical sensor for determination of methyl parathion based on a hierarchical macro and nanoporous 3-D architecture. The influence of various N-configurations on electron transfer kinetics and the sensing performance of the N-HG modified electrode was investigated systematically through combined practical and theoretical studies. It was found that N-HG with a high pyrrolic-N content exhibited the largest electron transfer rate and the best sensing performance (ultralow detection limits: 3.5 $\text{pg}\cdot\text{ml}^{-1}$; wide linear range: 1 $\text{ng}\cdot\text{ml}^{-1}$ –150 $\mu\text{g}\cdot\text{ml}^{-1}$).

Renganathan(Renganathan, Balaji, Chen, & Kokulnathan, 2020) developed a simple strategy for construction of palladium nanoparticles (Pd NPs) adorned on the boron nitride (BN) heterojunction (HJ) for electrochemical detection of paraoxon ethyl (PXL). It is found that the Pd NPs/BN HJ electrocatalyst exhibited an outstanding performance for PXL detection due to the synergetic effect, large surface area, high electrical conductivity, and numerous active sites. The fabricated Pd NPs/BN HJ modified electrode can detect trace level of PXL from 0.01-210 μM with low detection limit of 0.003 μM and sensitivity of 2.23 $\mu\text{A } \mu\text{M}^{-1} \text{ cm}^{-2}$.

1.3.3.2 Application of electrochemical sensor in organochlorine pesticide detection

Organochlorine pesticides are organic compounds containing organochlorine elements that are used to control plant diseases and insect pests. The toxicity of organochlorine pesticides to human body is mainly manifested in the invasion of nerves and substantial organs. It has been reported that some organochlorine pesticides are carcinogenic to experimental animals(Adeleye, Sosan, & Oyekunle, 2019; Jorfi, Atashi, Akhbarizadeh, Khorasgani, & Ahmadi, 2019).

Yu et al. (G. X. Yu et al., 2016) prepared the electrochemical sensor to detection hexachlorobenzene (HCB) by the surface of nitrogen-doped graphene (NG) and chitosan modified glassy carbon electrode. Under the optimized conditions, the modified electrode has good sensing performance for hexachlorobenzene, the linear range is from 3 $\mu\text{g/L}$ to 10 mg/L , and the detection limit is as low as 1.72 $\mu\text{g/L}$. HCB sensors are constructed using a layer-by-layer assembly technique. In this sensor, NG not only provides electrocatalytic activity for the reduction of hexachlorobenzene, but also shows good adsorption affinity for hexachlorobenzene, thus improving the sensitivity of the sensor. The sensor has been successfully used to detect hexachlorobenzene in real water samples and provides a promising alternative for environmental monitoring.

Akilarasan et al.(Akilarasan et al., 2021) used a low-temperature synthesis of graphene oxide-wrapped perovskite-type strontium titanate nanocomposites

(GO@SrTiO₃-NC) to prepare electrochemical sensor for the detection of organochlorine pesticide 2,4, 6-trichlorophenol (TCP). The prepared GO@SrTiO₃ nanocomposites have large surface area, excellent electrical conductivity, and active sites, which are more conducive to the catalysis of TCP. The synergistic effect between GO and perovskite SrTiO₃ results in an extended operating range of 0.01 to 1.47 and 1.47 to 434.4 μ M, with a very low detection limit of 3.21 nM for TCP detection. In addition, the sensor has good selectivity and long-term stability.

1.3.3.3 Application of electrochemical sensors in nicotinic pesticide detection

Nicotinic pesticides are a new type of broad-spectrum insecticides with high efficiency, low toxicity, strong endoscopy, long residual effect period and low residues. They occupy a high share in the market with an annual sales volume of 6 billion Euros (Yingchun Zhou, Jiang, Xiong, & Liu, 2018). At present, the sales volume in the world pesticide market exceeds that of carbamates. Neonicotinoid pesticides include imidacloprid, insect amidine, thiamethoxam, thiamethoxam lamictal, etc. Among them, imidacloprid, with high efficiency, low toxicity, broad-spectrum, systemic strong, long effect time, is one of the world's bestselling varieties of pesticides, but because of its heat stability, strong polarity and difficult volatile characteristics, not appropriate to use GC - MC analysis, and electrochemical sensor method has some advantages.

Paula et al. (Paula, Ferreira, & Cesar, 2020) developed a glassy carbon electrode electrochemical sensor modified with reduced graphene oxide and Manganese (II) phthalocyanine (GCE/rGO/MnPc) for the determination of imidacloprid in honey samples. In the presence of imidacloprid, a higher peak current change is obtained using the proposed sensor compared to bare GCE. The optimized results were obtained by experiments: the reduced concentration of go (2.0 mg/mL), manganese (II) phthalocyanine (1.5 mg/mL), electrolyte pH (6.5) and electrolyte concentration (1,50 mol/L). The study also showed that the reduction process of imidacloprid is irreversible and diffuse-controlled, with a single reduction

peak of approximately -0.9V corresponding to the reduction of nitro (-NO₂) present in the structure, resulting in the formation of hydroxylamine-derived in a process involving approximately four electrons. Determination of imidacloprid in honey samples showed recovery values in the EPA range (90.5 to 101.9%).

Liu et al.(L. Liu, J. Guo, & L. Ding, 2021) constructed an electrochemical sensor based on raffia derived porous carbon (RPC) and polyaniline (PANI) composite functional glass carbon electrode (GCE) for the determination of imidacloprid (IMI). PANI nanowire arrays were uniformly deposited on the surface of RPC without aggregation. The electrochemical response of IMI on RPC@PANI/GCE is about four times that of bare GCE, indicating that RPC@PANI has high electrocatalytic activity for IMI reduction. DPV method was used to detect the electrochemical performance of the modified electrode. The linear relationship between the response current and the concentration was obvious in the range of 0.1 ~ 70 µg/ mL, and the detection limit was as low as 0.03µg/ mL. In addition, it provides high recovery rates by testing real samples.

1.3.3.4 Application of electrochemical sensor in fungicide pesticide detection

Fresh fruits and vegetables have high moisture content and are easily contaminated by microorganisms after harvest, such as bananas and oranges, which should be treated with fungicides to reduce losses. Commonly used fungicides include carbendazim, thiabendazole and propimidazole. Benazol can inhibit the growth and reproduction of mold and is often used for fruit preservation. However, the residual benazol in fruits is toxic to our, mainly affecting the liver, nervous system and bone marrow of human body.

Razzino et al. (Razzino, Sgobbi, Canevari, Cancino, & Machado, 2015) described the determination of the fungicide Carbendazim (CBZ) using a glassy carbon electrode modified with a thin film of mesoporous silica/multiwalled carbon nanotubes. The mixed material (SiO₂/MWCNT) was prepared by sol-gel process using HF as catalyst. Under the optimal conditions, the current reaction of

SiO₂/MWCNT/GCE in the range of carbendazim concentration of 0.2 ~4.0 μmol L⁻¹ showed a good linear relationship. The calculated detection limit is 0.056 μmol L⁻¹. The main characteristics of the SiO₂/MWCNT/GCE sensor are its high sensitivity, low detection limit and robustness, allowing the determination of CBZ in untreated actual samples. What's more, this strategy provides CBZ with significant selectivity to ascorbic acid and citric acid, the major compounds in orange juice. CBZ has obvious selectivity to ascorbic acid and citric acid, the main compounds in orange juice. The excellent sensitivity and selectivity provide a feasible application for CBZ detection in orange juice samples.

Zhang et al. (X. Zhang et al., 2021) developed OD/1D nanohybrid by anchoring 1T phase Molybdenum disulfide quantum dots (QD) on multi-walled carbon nanotubes (MWCNT) through simple assembly method. The microstructure of the material showed that 1T phase-determined QD can be anchored to the MWCNT by van der Waals forces, and anchoring improves the surface area and conductivity of the nanohybrid. Therefore, the electrochemical sensor based on MoS₂ QDs@MWCNT nanohybrid shows excellent catalytic activity for Carbendazim oxidation. Under optimized conditions, the sensor showed linear voltammetry response to Carbendazim concentration from 0.04 to 1.00 μmol/L, LOD as low as 2.6*10⁻⁸ mol/L, and high selectivity, good reproducibility, and long-term stability. In addition, the sensor has been successfully used for the determination of Carbendazim in two typical Chinese medicines, and the recoveries obtained are in good agreement with the HPLC results, indicating that the sensor plate constructed has important practical application in the analysis of Carbendazim in complex matrix.

1.4 Main research content

In this dissertation, the differences of pesticide absorption and transfer in different leaf vegetables were studied, and the dynamic absorption and accumulation rules were explored in hydroponic lettuce. In addition, electrochemical sensors based on carbon-based materials/composites are used to detect three kinds of

pesticides (including CBZ, IMI and MP) residue in common vegetables, and satisfactory recoveries were obtained, in good agreement with the results obtained via HPLC, proving that the proposed sensor shows high potential for practical application in pesticides screening.

(1) IMI was taken as the test pesticide, and Lettuce, pakchoi-Shanghaiqing, pakchoi-Jimaocai, GaoGeng Cabbage and Greengrocery were taken as the experimental objects, focusing on the differences of IMI pesticide absorption and transfection in different leafy vegetables, and exploring the dynamic absorption and accumulation law. The results showed that the roots of lettuce could absorb in culture water, and then transfer to stem, leaves, old leaves, new leaves and other parts. The residue of IMI in different parts of lettuce was different. With the increase of days, IMI was continually accumulated in the leaves, and the residual concentration of IMI in the leaves was gradually higher than that in other parts, and the concentration of old leaves was higher than that in new leaves.

(2) Carboxylated multi-walled carbon nanotubes (MWCNT-COOH) showed high electrical conductivity and good dispersing property due to the one-dimensional hollow conductive carbon structure and carboxyl functionalization. MWCNT-COOH was used to modify the glassy carbon electrode (GCE) for the fabrication of MWCNT-COOH/GCE sensor towards carbendazim (CBZ). The presence of carboxyl group improved the dispersion degree of carbon nanotubes to a certain extent, which could realize the uniform distribution of carbon material, and the one-dimensional hollow conductive carbon structure contributes to the efficient charge transport on the sensing electrode surface, which could enhance the electrochemical response. Under the optimal conditions, the fabricated MWCNT-COOH/GCE sensor exhibited good CBZ detection performance with low LOD value (6.7 nM). The good practical feasibility can be obtained at the fabricated sensor for the detection of CBZ in cabbage, cucumber and potato samples, and then the results are evaluated by using HPLC to confirm the accuracy of CBZ electrochemical detection.

(3) Biomass-derived porous carbon possessed abundant low-cost biomass carbon source. Soybean-derived porous carbon (SDPC) with three-dimensional (3D) interconnected porous structure was prepared by using the expired soybean as carbon source through a high-temperature carbonization process. SDPC was used to modify the glassy carbon electrode (GCE) for the fabrication of SDPC/GCE sensor towards imidacloprid (IMI). The 3D interconnected porous structure of SDPC significantly improved the electrical conductivity and good absorption capability for IMI due to the interconnected carbon conductive network and large specific surface area. Under the optimal conditions, the fabricated SDPC/GCE sensor exhibited a low LOD value (5.18 μM) in wide IMI linear concentration range of 0.3-75 μM . Moreover, the sensor has been successfully applied to the determination of IMI in tomato and lettuce samples, and its recovery rate is in good agreement with that of HPLC, indicating that the constructed sensor has good practical application value in the analysis of IMI in complex matrices.

(4) The pesticide electrochemical detection performance can be improved based on the synergistic effect of nanocomposite sensitizer. The multifunctional nanocomposite of superconductive carbon black (SCB) and ZrO_2 was prepared by a simple and efficient ultrasound-assisted strategy. The SCB@ ZrO_2 nanocomposite was used to modify the glassy carbon electrode (GCE) for the fabrication of SCB@ ZrO_2 /GCE sensor towards methyl parathion (MP). SCB nanoparticles showed high electrical conductivity, which promoted the efficient charge transport, and ZrO_2 nanoparticles possessed strong affinity towards the phosphorus groups of MP, which enhanced the accumulation ability of MP. Under the optimal conditions, the fabricated SCB@ ZrO_2 /GCE sensor exhibited a low LOD value (16 nM) in MP linear concentration range of 0.03-10 μM . Moreover, it can be found that the obtained recoveries of MP are well comparable with the recoveries obtained from HPLC. The sensor has good practical feasibility for the detection of MP in lettuce, cucumber, and tomato samples. The detection results were evaluated by HPLC, verifying the accuracy of MP electrochemical detection.

(5) The expired sugarcane juice (SJ)-derived porous carbon spheres (PCS) were prepared by hydrothermal method and further modified with β -cyclodextrin (β -CD). The SJPCS@ β -CD nanocomposite was used to modify the glassy carbon electrode (GCE) for the fabrication of SJPCS@ β -CD/GCE sensor towards methyl parathion (MP). SJPCS with interconnected porous structure exhibits excellent electrical conductivity, strong adsorption property, and high specific surface area, while β -CD with molecular recognition property achieves the uniform dispersion of SJPCS and promotes the recognition and adsorption of MP molecules. Thanks to the synergistic combination of SJPCS and β -CD, the SJPCS@ β -CD/GCE sensor exhibited respectable MP determination performance with low limit of detection of 5.87 nM in the MP concentration range of 0.01-10 μ M. For the MP detection in vegetables (onion, cabbage, spinach), the fabricated sensor showed good practicability with adequate relative standard deviation of 1.06% to 4.25% and satisfactory recoveries of 96.5 to 100.5%. A promising strategy for the rapid determination of methyl parathion in food products was developed. Moreover, it can be found that the obtained recoveries of MP are well comparable with the recoveries obtained from HPLC. These results indicate that the good practical feasibility of the fabricated SCB@ZrO₂/GCE sensor can be achieved for the MP determination in vegetables. The good practical feasibility can be obtained at the fabricated sensor for the detection of MP in onion, cabbage and spinach samples, and then the results are evaluate by using HPLC to confirm the accuracy of MP electrochemical detection.

1.5 Conclusions in section 1

1. We introduced the use status of pesticide residues, and described the harm of pesticide residues in detail from four aspects: ecological environment, human health, agricultural development and international trade. In addition, the sources of pesticide residues and the factors of accumulation and transfer of pesticides in plants were analyzed.

2. The typical detection techniques of pesticide residues were reviewed, including GC, HPLC, Chromatograph-mass spectrometry, Fluorescence detection techniques, Enzyme inhibition detection techniques and Biosensor techniques.
3. The principle and classification of electrochemical sensor were introduced, and then the application of electrochemical sensor in pesticide residue detection was summarized.
4. The main research content of this dissertation is summarized.

SECTION 2 ORGANIZATION, SUBJECTS, MATERIALS AND METHODS RESEARCH

2.1 Objects of research and Materials

The differences of pesticide absorption and transfer in different leaf vegetables were studied, and the dynamic absorption and accumulation rules were explored in hydroponic lettuce. In addition, the electrochemical sensors were prepared for the three kinds of pesticides (Carbendazim, Imidacloprid, Methyl Parathion) residual detection, and the experimental results were compared with those of HPLC methods. The mainly used reagents and instruments to prepare electrochemical sensors and optimize experimental conditions are introduced below. **Table 2-1** shows the main reagents used in the experiment and **Table 2-2** shows the major instruments used in the experiment.

Table 2-1 The main reagents used in the experiment.

Name(Abbreviation molecular	Manufacturer
N, N-Dimethylformamide(DMF)	Aladdin Reagent Co., LTD
Acetone(CH ₃ COCH ₃)	Sinopharm Group Co. LTD
Potassium ferricyanide(K ₃ FeC ₆ N ₆)	Aladdin Reagent Co., LTD
Potassium ferrocyanide K ₄ [Fe(CN) ₆]	Aladdin Reagent Co., LTD
Sodium hydroxide(NaOH)	Aladdin Reagent Co., LTD
Phosphoric acid(H ₃ PO ₄)	Tianjin KaitongChemical Reagent Co. LTD
Nitric acid(HNO ₃)	Aladdin Reagent Co., LTD
ADSP(Na ₂ HPO ₄)	Aladdin Reagent Co., LTD
Absolute alcohol(CH ₃ CH ₂ OH)	Aladdin Reagent Co., LTD
AMSP(NaH ₂ PO ₄)	Aladdin Reagent Co., LTD
Potassium chloride(KCl)	Aladdin Reagent Co., LTD
Potassium hydroxide(KOH)	Aladdin Reagent Co., LTD
Concentrated hydrochloric	Aladdin Reagent Co., LTD
Alumina powder(Al ₂ O ₃)	Shanghai Chenhua Instrument Co., LTD
Multi-walled carbon nanotubes (MWCNTs)	Aladdin Reagent Co., LTD
HPLC-grade acetonitrile	MREDA Technology Inc, USA
Nano zirconia(ZrO ₂)	Aladdin Reagent Co., LTD
Methanol	Dikma Beijing, China
Primary secondary amine (PSA)	Tianjin Bona Aijer Technology Co., LTD
Graphitized carbon black (GCB)	Hangzhou Micron Pie Technology Co.,
Superconductive carbon black(SCB)	TIMCAL
NaCl	Sinopharm Chemical Reagent Co. LTD
β-cyclodextrin(β-CD)	Aladdin Reagent Co., LTD
Chitosan (CTS)	Aladdin Reagent Co., LTD
Carbendazim(CBZ)	Aladdin Reagent Co., LTD
Imidacloprid(IMI)	Aladdin Reagent Co., LTD
Methyl parathion (MP)	Aladdin Reagent Co., LTD
Niclosamide(NA)	Aladdin Reagent Co., LTD

Table 2-2 The major instruments used in the experiment.

Instruments name	Model
Electrochemical workstation	Shanghai Chen hua CHI660E
Scanning electron microscope(SEM)	Gemini SEM 300
Transmission electron microscope(TEM)	FEI Talos F-2000S
Infrared spectrometer	Bruker Vertex 70 FT-IR Infrared spectrometer
UV-visible absorption spectrometer	Perkin Elmer Lamda 900 UV-vis-NIR spectrograph
X-ray diffractometer(XRD)	Bruker DX-1000, Germany
X-ray photoelectron spectroscopy (XPS)	PHI X-tool
pH meter	Shanghai Lei Ci PHs-2F
Pipette	ThermoFisher Scientific Pipette
Electronic Balance	Mettler Toledo electronic balance
CNC ultrasonic cleaning instrument	Kunshan ultrasonic instrument co., LTD.
Infrared heat lamp	Philips Infrared infrared grill lamp
Heat collection constant temperature heating magnetic stirrer	Lichen technologyDF-101S
Electric constant temperature drying oven	YLE-2000
Vacuum tube furnace	GWG-1/1600
Glassy carbon electrode(GCE)	CHI104
Vacuum drying oven	DHG-9140A
Centrifuge	Sigma 3K 30, Germany
UPLC-PDA	I-Class PLUS, Waters
Vortex Shaker	IKA Vortex 3, Germany
Millipore filter system	Millipore Corporation, Bedford, MA, USA
NOVA-2200e instrument	Quantachrome, USA

The chemical reagents used in the experiment were analytically pure, which could be used directly without further purification. All the water used was ultra-pure water. 0.1Mol phosphate buffer solution (PBS) was prepared as the electrolyte solution for pesticide residue detection. The pH value of PBS was adjusted by adding H_3PO_4 or NaOH solution. In addition, 5 mM $\text{K}_3[\text{Fe}(\text{CN})_6]/\text{K}_4[\text{Fe}(\text{CN})_6]$ solutions containing 0.3M KCl was used as standard electrolyte solution.

2.2 Research methods

2.2.1 X-ray photoelectron spectroscopy (XPS) test

The basic principle of X-ray photoelectron spectroscopy (XPS) technology is that when the X-ray radiates the sample, the photoelectric effect will occur on the surface of the sample, and the inner electrons or valence electrons in the atoms or molecules in the sample will be excited and emitted, and the energy of the photoelectrons generated can be measured. Then the energy distribution of these photoelectrons is analyzed, and the photoelectron energy spectrum can be drawn with the kinetic energy/binding energy of the photoelectrons as the abscissa and the relative intensity as the ordinate. Through XPS test, the elemental composition, content, and chemical bond of compounds can be obtained.

2.2.2 Infrared spectrometer (FT-IR) test

The composite materials were dried in a blast drying oven, and then mixed with KBr at a rate of about 2mg:100mg fully, and evenly dispersed. After that, a tablet press was used to press the mixture into slices. Finally, a Bruker Vertx 70 FT-IR spectrometer was used for testing with a scanning range of $500\text{-}4000\text{ cm}^{-1}$ and the infrared absorption spectrum was recorded and saved.

2.2.3 Scanning electron microscopy (SEM) - Transmission electron microscopy (TEM) test

The modified material is drip-coated on the surface of ordinary glass, and the surface morphology of the modified electrode is observed by scanning electron microscope (SEM) after natural air drying. After using the same treatment method,

the internal fine structure is observed by transmission electron microscopy (TEM), and then the surface morphology electron microscopy and internal fine structure are compared and analyzed.

2.2.4 X-ray diffractometer (XRD) test

X-ray diffractometer is used to scan and analyze the materials. The incident light source is CuK α ray, the scanning range is 5-80°, and the tube pressure/tube flow was 40 KV/30mA. Diffraction intensity is recorded by scintillation counter of graphite monochromatic detector.

2.2.4 Raman spectroscopy analysis

Raman spectrum analysis method is an analysis method of Raman scattering effect applied to the study of molecular structure. Through Raman spectrum analysis, people can know the state information of vibration and rotation energy levels of substances. It is mainly used for quantitative analysis and molecular structure identification of substances in different phases.

2.2.5 Electrochemical performance test

The electrochemical performance test, parameter optimization and impedance characterization of the modified electrode are carried out under the control of CHI660B electrochemical workstation, using a classical three-electrode system (Show as **Fig. 2-1**). The modified or bare electrode ($\Phi=3\text{mm}$) is working electrode, platinum wire electrode ($\Phi=1\text{mm}$) is counter electrode, and saturated calomel electrode(SCE) is reference electrode. Electrochemical impedance characterization, the three-electrode system is placed in the base solution of 5mM $[\text{Fe}(\text{CN})_6]^{4-/3-}$ and 0.3M KCl, frequency range of 100mHz~10kHz. Cyclic voltammetry (CV) and differential pulse voltammetry (DPV) are used to detect pesticide residues, and the detection performance of the sensor was verified.

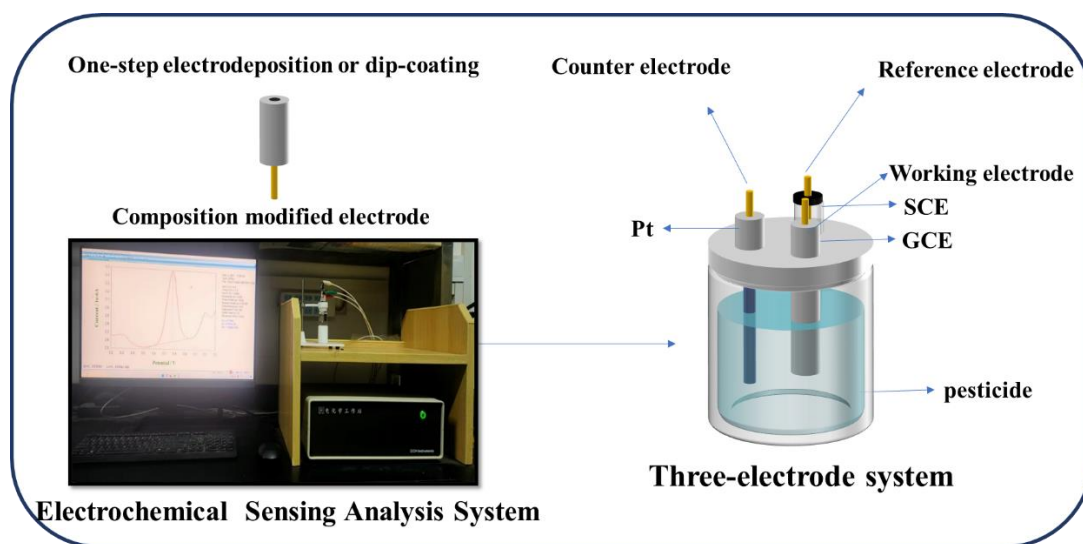


Fig. 2-1. Electrochemical sensing analysis system for pesticide detection

2.2.6 Surface pretreatment of glassy carbon electrode

Before modifying the electrode, the glassy carbon electrode with a diameter of 3mm was polished on deerskin with alumina powder with a particle size of 0.05, 0.3 and 1.0 μm in turn until a smooth mirror appeared, followed by ultrasonic cleaning in anhydrous ethanol and deionized water for 3 min successively, and then dried with an infrared lamp for later use. The platinum wire electrode should be burned with alcohol lamp to remove impurities on the surface, then cleaned with ethanol in turn and dried naturally before use.

2.2.7 Pretreatment of vegetable and fruit samples for electrochemical sensor detection

The vegetable samples to be tested were obtained from the Plant factory in Henan Institute of Science and Technology, so as to ensure that the vegetables do not contain any pesticide residues. The constructed sensor was applied for the quantitative analysis of pesticide residues in vegetable and fruit samples. For the all vegetable samples, it was crushed by homogenizer to get homogenate respectively. After centrifugation, the supernatant of the homogenate was taken, and 2 g NaCl and 10 mL acetonitrile were added successively. After vortex and high speed centrifugation, the supernatant was taken and then filtered by a 0.22 μm filter membrane, and the collected filtrate was diluted 100 times with PBS solution (0.1 M,

pH value was selected the optimal one). The pretreatment method of fruit sample is same with that of the above.

2.2.8 QuEChERS method

The QuEChERS method (Quick, Easy, Cheap, Effective, Rugged and Safe) utilizes the adsorption between adsorbents and impurities to remove impurities in the matrix, thus purifying the sample. QuEChERS method can be summarized as the following steps: (1) pulverizing the sample to be tested; (2) adding extractant acetonitrile, etc. for extraction and separation; (3) adding salt to remove water (MgSO_4 , etc.); (4) adding adsorbent to remove impurities (ethylenediamine-propyl silane, etc.); and (5) taking supernatant for detection.

2.2.9 Pretreatment of vegetable samples for HPLC

Each vegetable sample was washed and dried, and then cut them into pieces and put them into a homogenizer for homogenization. 10 g sample were weighed into a 50 ml centrifuge tube; 2 g NaCl and 10 mL acetonitrile are added, blended, and vortexed for 3 min, then centrifuged for 5min at 3,500 rpm. An aliquot of 2 ml was transferred from the supernatant to a new clean 2 ml centrifuge tube containing a certain amount of PSA and GCB purification material. The samples were again vortexed for 3min and then centrifuged at 10,000 rpm for 5 min. Afterwards, 2 ml supernatant was taken and filter them through 0.02 μM filter membrane before sampling. Generally, vegetable samples without any pesticides were taken, a certain amount of standard mixture was added, and the determination was repeated for 3 times according to the given chromatographic conditions.

2.2.10 Pretreatment of culture solution samples for HPLC

5 ml culture solution was taken and filter them through 0.02 μM filter membrane before sampling. The determination was repeated for 3 times according to the given chromatographic conditions by HPLC-UV.

2.2.11 Calculation method of Limit of Detection

According to the methods recommended by the International Union of Pure Applied Chemistry, the calculation method of LOD is:

$$\text{LOD}=3S_0/S$$

S_0 is the standard deviation of the determination of the blank solution, and S is the sensitivity, which is the slope of the standard curve.

2.2.12 Statistical evaluation

The statistical evaluation was applied to investigate the reproducibility, repeatability, anti-interference, and practical feasibility of the fabricated electrochemical sensors. For the reproducibility measurement, five or six different electrode sensors were used to detect the pesticide residual. In order to analyze the repeatability, selectivity, and practical feasibility, the individual sensor was applied to detect pesticide residual for each performance. The obtained relative standard deviation (RSD) value and recoveries can reflect the reproducibility, repeatability, selectivity, and practical feasibility of the fabricated sensor.

2.3 The research route

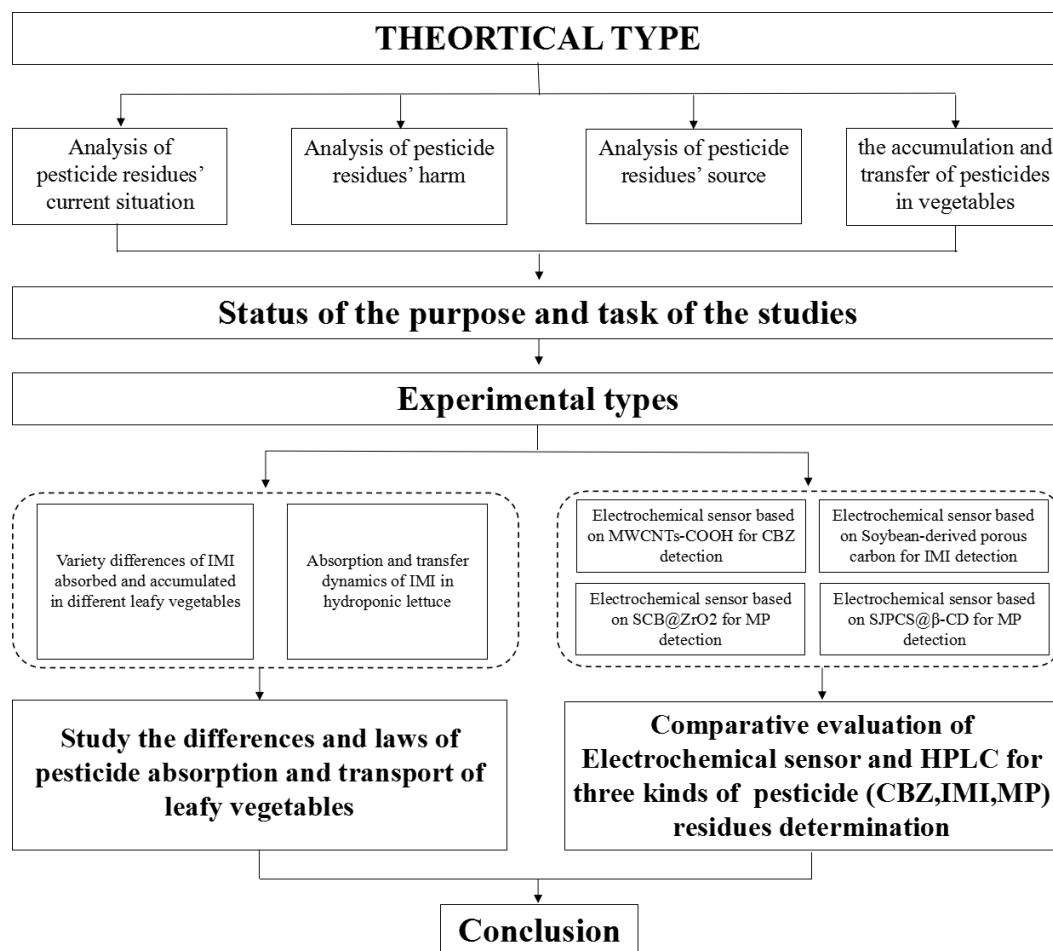


Fig. 2-2 The research route of study

Firstly, the differences of pesticide absorption and transfer in different leaf vegetables were studied, and the dynamic absorption and accumulation rules were explored in hydroponic lettuce.

Second, in order to meet the requirements of pesticide residue detection, nano materials/composites were selected to modify glassy carbon electrode, and the nano materials/composites electrochemical sensors with excellent performance were successfully constructed. The conditions affecting the detection performance were optimized systematically, and nanocomposites were used for sensitive detection of pesticide residues. The reproducibility, anti-interference and stability of the modified sensor were tested and applied to the detection of pesticide residues in actual samples, and the obtained recoveries are in good accordance with the results

achieved by HPLC, showing that the constructed sensor holds great practical application in pesticide analysis.

2.4 Conclusions in section 2

The differences of pesticide absorption and transfer in different leaf vegetables were studied, and the dynamic absorption and accumulation rules were explored in hydroponic lettuce.

1. The objects of research consists of two parts. One is the absorption and transfer of pesticide in different leaf vegetables, the other is the electrochemical sensors prepared for three kinds of pesticides (Carbendazim, Imidacloprid and Methyl Parathion) residual detection, then the main list of reagents and instruments used in the experiment are summarised.
2. The methods used in the experiment are described, including electrochemical sensor and high performance liquid chromatography.
3. The research route and experimental procedure are described briefly.

SECTION 3 THE ABSORPTION AND ACCUMULATION OF IMIDACLOPRID PESTICIDE IN SEVERAL HYDROPONIC LEAF VEGETABLES

The growth cycle of leafy vegetables is short, and the interval of pesticide application is shortened accordingly. Because there is not enough time for pesticide degradation and metabolism, the risk of pesticide residue in leafy vegetables is higher than that in other kinds of vegetables(S. Liu et al., 2021). Therefore, the safe use of pesticides in leafy vegetables has become a prominent problem in the healthy development of vegetable industry.

Imidacloprid (IMI) is a representative pesticide of a new generation of nicotinic insecticides. Its pharmacodynamic group is nitroimine, and the heterocyclic part is 6-chloro-3-pyridine methyl (CPM). Its pure product is a colorless crystalline solid, and its original drug is a colorless crystal with a slightly special smell. IMI has many characteristics, such as high efficiency, quick effect, low toxicity, broad spectrum and low residue, and has no cross-resistance with other pesticides. IMI has multiple effects on pests, such as systemic absorption, contact toxicity and stomach toxicity. It mainly inhibits nicotinic acid acetylcholinesterase receptor in pests, which hinders the information transmission function of their motor nervous system and makes pests die of nerve paralysis. IMI can effectively control insect infestation in rice, wheat, corn, potato, cotton, fruit trees, vegetables, beets and other crops, such as aphids, thrips, planthoppers, rice weevils, leafhoppers, rice negative worms, whiteflies, leaf miners and other HOMOPTERA, thysanoptera, COLEOPTERA and LEPIDOPTERA insects, and pests are not easy to develop drug resistance(Sun et al., 2014).

In this part, IMI was taken as the test pesticide, and Lettuce, Pakchoi-ShangHaiQing, Pakchoi-JiMaoCai, GaoGeng Cabbage and Greengrocery were taken as the experimental objects, focusing on the differences of IMI pesticide

absorption and transfer in different leafy vegetables, and exploring its dynamic absorption and accumulation law.

3.1 Instrument conditions and pretreatment methods

In this experiment, the pretreatment method of QuEehERS was optimized. Acetonitrile was used to extract IMI pesticide residues in leafy vegetables and culture solution, and HPLC-UV instrument was used for quantitative detection. This test method provides convenience for the follow-up work.

3.1.1 Chromatographic conditions and Chromatographs

Chromatographic column was Shim-Pack: VP-ODS; Mobile phase was acetonitrile and water, and the ratio of acetonitrile and water (V/V) was 30:70; The flow rate was 0.5 mL/min; The sample size was 10 μ L; The detection wavelength was 270; Quantitatively determined by calculating the peak areas.

Under the optimum Chromatographic conditions, a series of standard solutions with different concentrations of IMI were prepared for determination. The standard spectrum of IMI (concentration is 10 μ M) is shown in **Fig.3-1**. From the chromatogram, it can be seen that the retention time of IMI is 2.690 min, and the peak time of samples in the same batch is relatively consistent, while the peak time of imidacloprid in different batches is slightly different, and the IMI standard samples that respond at each injection are compared with them to correct the error.

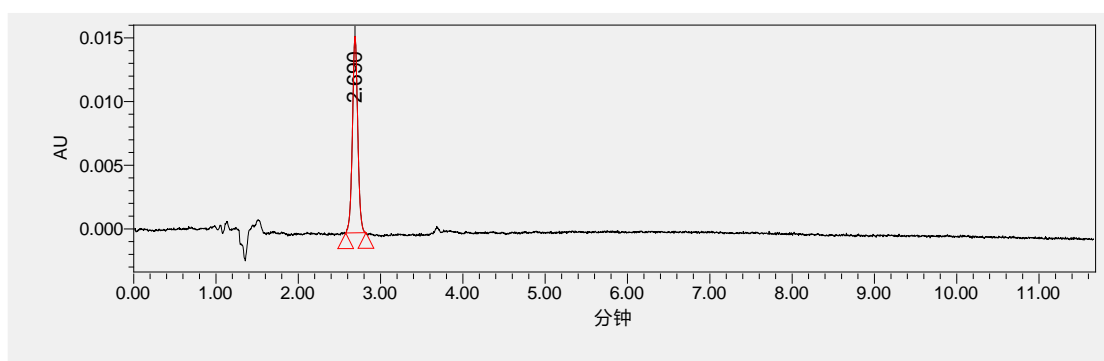


Fig. 3-1. HPLC chromatogram of IMI standard (10 μ M)

3.1.2 Standard curve

IMI pesticide stock solution is dissolved in acetonitrile to 100 μ M/L, stored at -18 $^{\circ}$ C for use. The standard reserve solution was diluted step by step to obtain

standard solutions with concentrations of 0.2 μM , 0.5 μM , 1 μM , 5 μM , 10 μM , 20 μM and 30 μM , respectively. Under chromatographic conditions, the standard curve was drawn with the concentration of IMI standard solution as abscissa and the response value of detection peak area as ordinate, and the linear regression equation was fitted. The results showed that the concentration of IMI was linear with the response value of peak area. The linear range of IMI was 0.2~30 μM , the standard curve equation was $y = 6265.4x + 1223.6$, and the correlation coefficient is 99.89%. It can meet the needs of quantitative analysis, and the curve of IMI standard under this condition is as shown in the **Fig 3-2**.

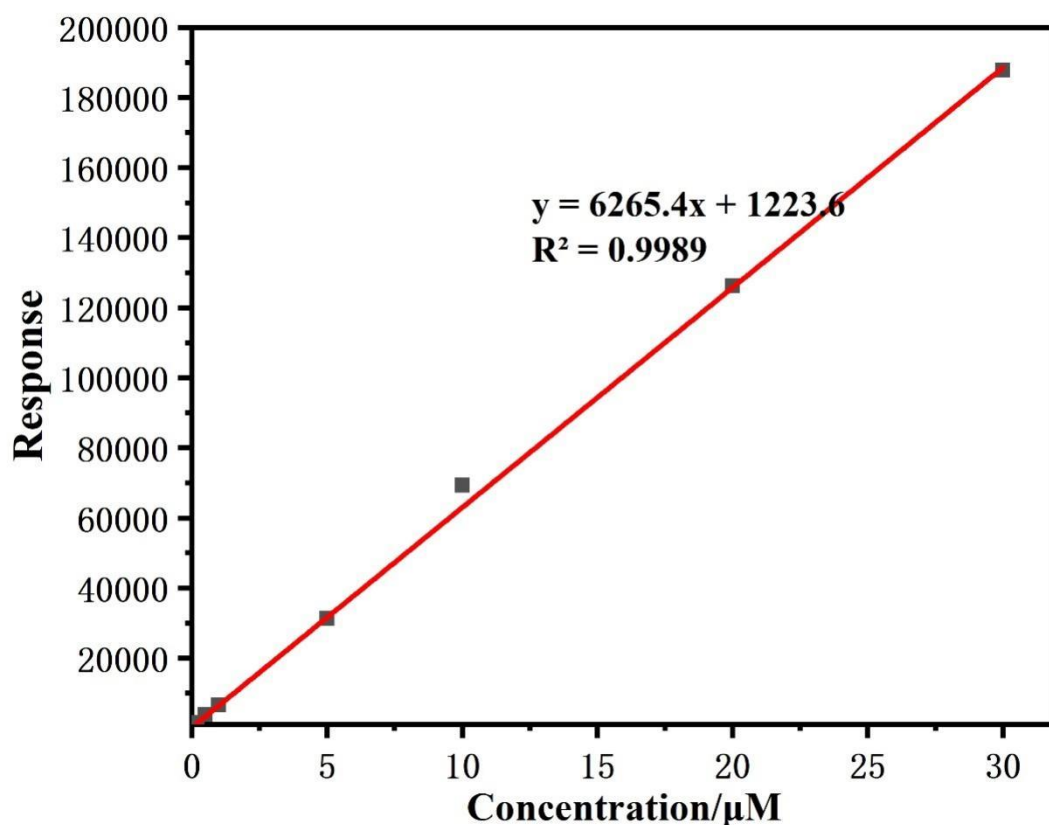


Fig. 3-2 Stander curve of Imidacloprid and Imidacloprid concentration are 0.2 μM , 0.5 μM , 1 μM , 5 μM , 10 μM , 20 μM , and 30 μM .

3.1.3 The results of spiked recovery

In this part, the samples of stem&leaf, root and culture solution of leafy vegetables without any pesticides were taken, a certain amount (0.5 μM , 2 μM , 5 μM)

of standard mixture was added, and the determination was repeated for 3 times according to the given chromatographic conditions. Using the sample pretreatment method and instrument detection method in 2.2.9, the residual amount of imidacloprid in each group of samples was quantitatively detected, and the recovery rate of IMI in three different leafy vegetables was calculated by using the peak area response value, which served as the theoretical basis for the feasibility and accuracy of the pretreatment method.

The relative standard deviation and spiked recovery results were shown in the **Table 3-1**. The recoveries rate and RSD were in the range of 81.47%~103.41% and 1.71~6.27. It can be seen that this method of pesticide pretreatment meets the requirements of analytical standards for pesticide residue experiments, so this experimental method is effective for the detection of IMI in leafy vegetables.

Table 3-1 Determination of spiked recovery rate of vegetable samples

Vegetable sample	Added(μM)	Found(μM)	Recovery (%)	RSD (%)
Stem&Leaf	0.5	0.40	81.47	5.45
	2	1.85	92.73	5.34
	5	4.48	89.61	1.71
Root	0.5	0.46	92.98	4.23
	2	1.94	97.24	5.46
	5	5.17	103.41	6.27
Culture solution	0.5	0.48	96.65	3.3
	2	1.83	91.41	4.81
	5	4.68	97.04	2.77

3.1.4 Sample collection

3.1.4.1 Samples collection of IMI absorbed and accumulated in different leafy vegetables

After the hydroponic vegetables grow stably, healthy plants with consistent growth are selected and moved into black opaque plastic fresh-keeping boxes, which contain 1.5L of culture solution with different concentrations of IMI ($2\mu\text{M}$ and $20\mu\text{M}$ respectively). 3 boxes of each kind of hydroponic leafy vegetables were

set at each concentration, and two leafy vegetables were transplanted in each box. At the same time, two control groups were set up, that is, a control group with two different concentrations without leafy vegetables and a control group with leafy vegetables without IMI. The black plastic fresh-keeping box was completely sealed, and the light management was carried out as usual. After 3 days, the leafy vegetables in each group were randomly collected, washed with clear water, grinded and crushed the roots, stems and leaves of each leafy vegetables with liquid nitrogen, and then the culture solution was evenly stirred to collect water samples.

3.1.4.2 Samples collection of IMI absorption and transfer in lettuce

After hydroponic lettuces grow stably, healthy plants with consistent growth are selected and moved into black opaque plastic fresh-keeping boxes, which contain 1.5L of culture solution with different concentrations of IMI (2 μ M and 20 μ M respectively).20 boxes of hydroponic lettuces were set at each concentration, and two lettuces were transplanted in each box. At the same time, two control groups were set up, that is, a control group with two different concentrations without lettuces and a control group with two lettuces without IMI. After 1 day, 3 days, 5 days, 7 days, 10 days, 15 days, and 20 days, the lettuces in each group were randomly collected (roots, stems, new leaves, and old leaves), washed with clear water, grinded and crushed the roots, stems and leaves of each leafy vegetables with liquid nitrogen. Lettuce culture solution was also sampled at the same time with lettuce plants after 1 day, 3 days, 5 days, 7 days, 10 days, 15 days and 20 days, sealed and protected from light.

All the collected samples were stored in a refrigerator at -20 for testing.

3.2 Experimental results and analysis

3.2.1 Variety differences of IMI absorbed and accumulated in different leafy vegetables

In this study, the distribution of IMI in leafy vegetables, roots and water environment (culture solution) was determined and studied through hydroponic

experiments of five kinds of leafy vegetables, in order to find out the absorption and accumulation law of IMI in leafy vegetables and their water environment.

Table 3-2 Residual concentration of IMI in culture solution after 3 days.

Vegetables	2 μ M		20 μ M	
	Experimental group	Control group	Experimental group	Control group
Lettuce	1.88 \pm 0.04	1.94 \pm 0.06	19.06 \pm 0.28	19.23 \pm 0.38
Pakchoi-SHQ	1.91 \pm 0.03	1.96 \pm 0.02	18.96 \pm 0.17	19.35 \pm 0.22
Pakchoi-JMC	1.93 \pm 0.06	1.95 \pm 0.04	19.17 \pm 0.33	19.41 \pm 0.32
GGC	1.87 \pm 0.04	1.92 \pm 0.05	18.98 \pm 0.53	19.28 \pm 0.36
Greengrocery	1.86 \pm 0.04	1.91 \pm 0.04	18.77 \pm 0.38	19.06 \pm 0.58

Note: **Pakchoi-SHQ:ShangHaiQing; Pakchoi-JMC:JiMaoCai;GaoGeng Cabbage:GGC.**

The above **Table 3-2** shows the concentration of IMI in the culture solution with leafy vegetables and the culture solution of the control group (without vegetables) after 72 hours. It can be seen that there is no obvious difference between the concentration of imidacloprid in the culture solution with leafy vegetables and the culture solution of the control group, indicating that the concentration of IMI has basically not changed before and after 3 days of culture in the culture solution containing leafy vegetables, which shows that leafy vegetables all absorb IMI pesticides from the nutrient solution through transpiration flow.

The residue detection results of IMI in hydroponic leafy vegetables are shown in Table 3-3, which showed that all the tested vegetables could quickly absorb and transfer IMI pesticide. When leafy vegetables were treated with high concentration (20 μ M), the residual concentration of IMI in roots, stems and leaves of plants was significantly higher than that of low concentration. Additionally, there are great differences in the absorption of IMI from stems and leaves by roots of different varieties of vegetables. The residue concentration of IMI in the root of Greengrocery is the highest, and the residue in the stem and leaf of Pakchoi-JMC is relatively

small.

Table 3-3 Residual concentration of IMI in different parts of different leafy vegetables

Vegetables	Root		Stem&Leafy	
	2 μ M	20 μ M	2 μ M	20 μ M
Lettuce	1.94 \pm 0.04	25.56 \pm 0.74	1.64 \pm 0.08	21.05 \pm 0.53
Pakchoi-SHQ	2.91 \pm 0.07	22.21 \pm 0.13	2.56 \pm 0.06	21.35 \pm 0.76
Pakchoi-JMC	1.85 \pm 0.06	18.25 \pm 0.13	1.84 \pm 0.08	19.15 \pm 0.12
GGC	2.31 \pm 0.04	20.12 \pm 0.05	1.84 \pm 0.05	17.93 \pm 0.11
Greengrocery	3.24 \pm 0.07	26.21 \pm 1.05	2.08 \pm 0.03	21.62 \pm 0.77

The residual concentrations in the roots of five leafy vegetables treated with low concentration of 2 μ M imidacloprid decreased in the order of Greengrocery (3.24 μ M), Pakchoi-SHQ(2.91 μ M),GGC(2.31 μ M), Pakchoi-JMC(1.95 μ M) and lettuce(1.94 μ M), and the residual concentration of IMI in the stem and leafy decreased in the following order: Pakchoi-SHQ(2.56 μ M),Greengrocery (2.08 μ M), GGC(1.84 μ M),lettuce(1.64 μ M) and Pakchoi-JMC(1.55 μ M). The residual concentrations in the roots of five leafy vegetables treated with 20 μ M imidacloprid decreased in the order of lettuce(26.09 μ M),Greengrocery (23.56 μ M), Pakchoi-SHQ(22.21 μ M),GGC(20.12 μ M) and Pakchoi-JMC(18.25 μ M), and the residual concentration of imidacloprid in the stem decreased in the following order:Greengrocery (21.62 μ M), lettuce(21.05 μ M), Pakchoi-JMC(19.15 μ M), Pakchoi-SHQ(19.02 μ M) and GGC(17.93 μ M).

3.2.2 Absorption and transfer dynamics of IMI in hydroponic lettuce.

In this study, the hydroponic lettuce experiments were carried out, and samples of different parts of lettuces and culture solution were randomly collected at regular intervals to quantitatively detect the IMI residual, and to study the dynamic law of distribution, transfer and accumulation of IMI in lettuce and its water environment (culture solution).

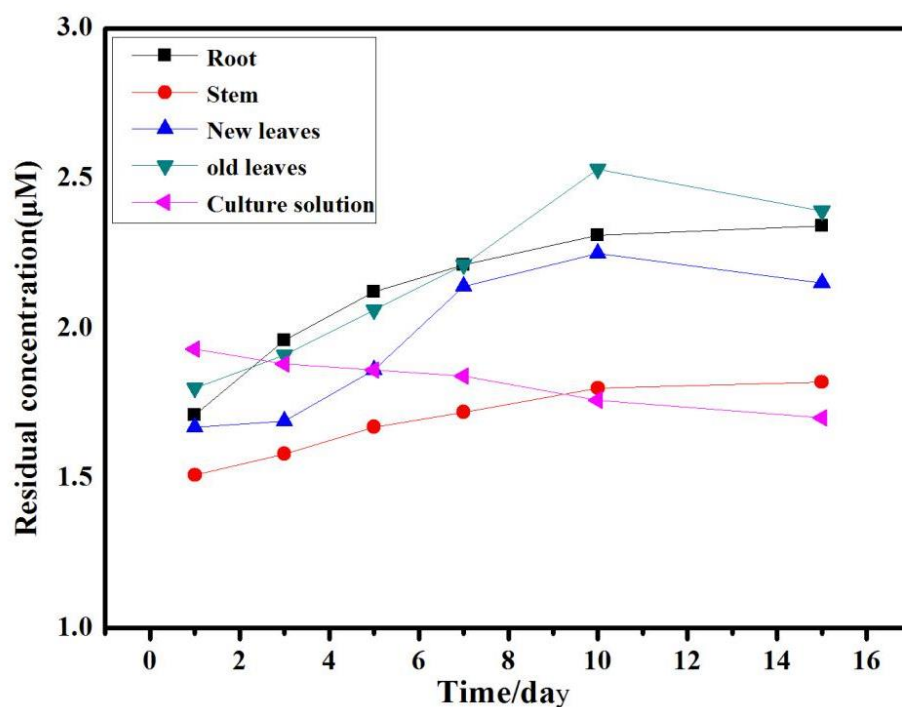


Fig.3-3 Concentration of Imidacloprid in different organs of lettuce for 2 μ M treatment

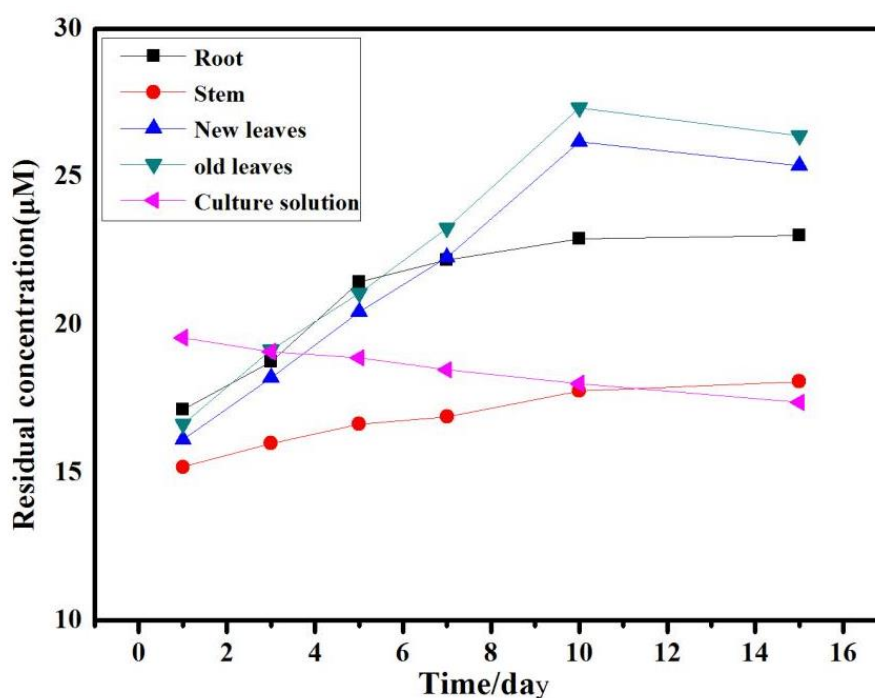


Fig.3-4 Concentration of Imidacloprid in different organs of lettuce for 20 μ M treatment

According to the above experiment results, after the lettuce roots were treated with a certain concentration of IMI culture solution, the IMI residues could be detected in all parts of the lettuce plants one day later, indicating that the lettuce

roots could quickly absorb IMI from the culture solution and conduct it in the lettuce plants. The detected concentration of IMI in different parts of lettuce plants was different, which indicates that IMI has the process of absorption and conduction in lettuce plants, and does not reach its functional parts quickly. The difference of IMI residues in different parts of lettuce plants was closely related to the physiological structure of lettuce plants and the physical and chemical properties of IMI.

As can be seen from the Fig3-3,3-4, the residual concentration of IMI in roots, stems, new leaves, old leaves and Culture solution of lettuce showed an upward trend during the detected period, while the residual concentration of IMI in water samples decreased slightly with time, which was in line with the degradation and decomposition law of IMI in water. At the same time, it also showed that the absorption of IMI by lettuce roots under the action of plant transpiration tension was proportional to the water content. As the transportation organization of plant materials, the residual concentration of IMI in the stem increased slightly with time, and was always lower than culture solution. The residual concentration of IMI in lettuce leaves reached the peak at 10 days, and decreased at 15 days compared with 10 days, which may be related to the degradation mechanism in plants and transpiration of leaves.

3.3 Conclusion in section 3

In this section, the distribution, dynamic transfer differences and rules of IMI in leafy vegetables-water system were preliminarily proved through hydroponic experiments, and leafy vegetables with high and low residues of imidacloprid were screened out, which provided scientific basis for guiding the rational and safe use of common pesticides such as imidacloprid. The conclusions drawn in this section are as follows:

(1) The extraction and detection method of IMI in leafy vegetables and culture solution were established. The extraction method was optimized on the basis of

QuEChERS method. Acetonitrile was used as extraction agents for leafy vegetables and culture solution, and anhydrous magnesium sulfate, PSA and GCB were used to eliminate impurity interference. Liquid chromatography was used to detect pesticide, the mobile phase is acetonitrile and water (30:70), the flow rate is 0.5mL/ min, and the detection wavelength is 270nm. Under the detecting condition, the correlation coefficient of the standard curve can reach 0.9989, with good linearity, good precision and high average recovery rate (> 80%). Therefore, this method has the characteristics of rapidity, simplicity, good repeatability, convenience and high accuracy, and is suitable for the analysis of pesticide residues. This detects method provides convenience for the subsequent test work.

(2) According to this experiment, there are variety differences of IMI pesticide residues in leafy vegetables, which are related to the physiological functions of plants (such as transpiration, transmembrane transport of substances, resistance physiology of plants, etc.), the growth environment of hydroponic vegetables and the properties of IMI itself (such as log k_{ow}, water solubility, molecular weight, etc.). The residue concentration of IMI in the root of Greengrocery was the highest, and the residue concentration of IMI in the root of Pakchoi-Jimaocai was the least. The residue concentration of IMI was the highest in the leaves of Pakchoi-Shanghaiqing, and relatively less in the leaves of Gaogenbai.

(3) The absorption, transport and accumulation of IMI pesticides in vegetables are related to the duration of IMI treatment. The results of this experiment showed that the residue of IMI could be detected in all parts of lettuce at 1 day after the root of lettuce was treated with a certain concentration of IMI culture solution; the concentration of IMI in old leaves was higher than that in any part of lettuce plants after 7 days; both new leaves and old leaves reached the peak after 10 days, and the content of IMI in new leaves was slightly lower than that in old leaves; after 15 days, the residual concentration of IMI in new leaves and old leaves of lettuce decreased compared with that in 10 days, which may be related to the degradation mechanism in plants, leaf surface area and transpiration of leaves. Therefore, there are great

differences in root absorption and stem-leaf transfer of IMI among different varieties of vegetables.

In this part, the distribution, dynamic transfer differences and rules of IMI in leafy vegetables-water system were preliminary proved through hydroponic experiments, and leafy vegetables with high and low residues of IMI were screened out, which provided scientific basis for guiding the rational and safe use of common pesticides such as IMI.

SECTION 4 DETERMINATION OF CARBENDAZIM IN VEGETABLES BY ELECTROCHEMICAL SENSOR BASED ON MWCNTS-COOH AND EVALUATED BY HIGH PERFORMANCE LIQUID CHROMATOGRAPHY

Carbendazim (CBZ), as a broad-spectrum fungicide, is widely used for preventing and controlling vegetable diseases and pests (Addrah et al., 2020; H. Ding et al., 2019; Z. Y. Liu et al., 2021; S. Singh et al., 2016). CBZ residues in agricultural products and the environment poses a serious threat to human health due to the stable structure and slow degradation rate of benzimidazole ring (Tao et al., 2020). Therefore, study accurate, rapid and convenient CBZ detection and analysis methods in agricultural products are very important to protect human health and environmental safety. At present, the commonly used methods for the detection of benzimidazole fungicides include high performance liquid chromatography (HPLC) (S. M. Huang, Hu, Chen, Li, & Xia, 2020; P. L. Li, Sun, Dong, & Li, 2020), liquid chromatography-mass spectrometry (LC-MS) (Chu et al., 2020; Y. H. Li, Hu, Yao, Wang, & Zhang, 2020), fluorescence spectrometry (Y. X. Yang et al., 2018; Q. W. Yu, Sun, Wang, He, & Feng, 2017; Yuan et al., 2020) and so on (L. T. Su et al., 2020; S. Y. Wang, Shi, Liu, & Laborda, 2020; Y. Zhai et al., 2021). These methods have high sensitivity and accurate results, but they have disadvantages such as complicated pretreatment, long time consuming, expensive equipment and professional operators. Electrochemical sensor detection method has the advantages of high sensitivity, simple operation, low cost and easy on-site inspection, etc., which has attracted extensive attention in the field of pesticide residue detection and analysis (Al-Hamry et al., 2019; Ghorbani, Ojani, Ganjali, & Raoof; Kumar, Kim, & Deep, 2015; Migliorini, Sanfelice, Mercante, Facure, & Correa, 2020; Noori, Mortensen, & Geto, 2021; Sakdarat et al., 2019; Tu et al., 2020; H. Y. Zhao et al., 2015).

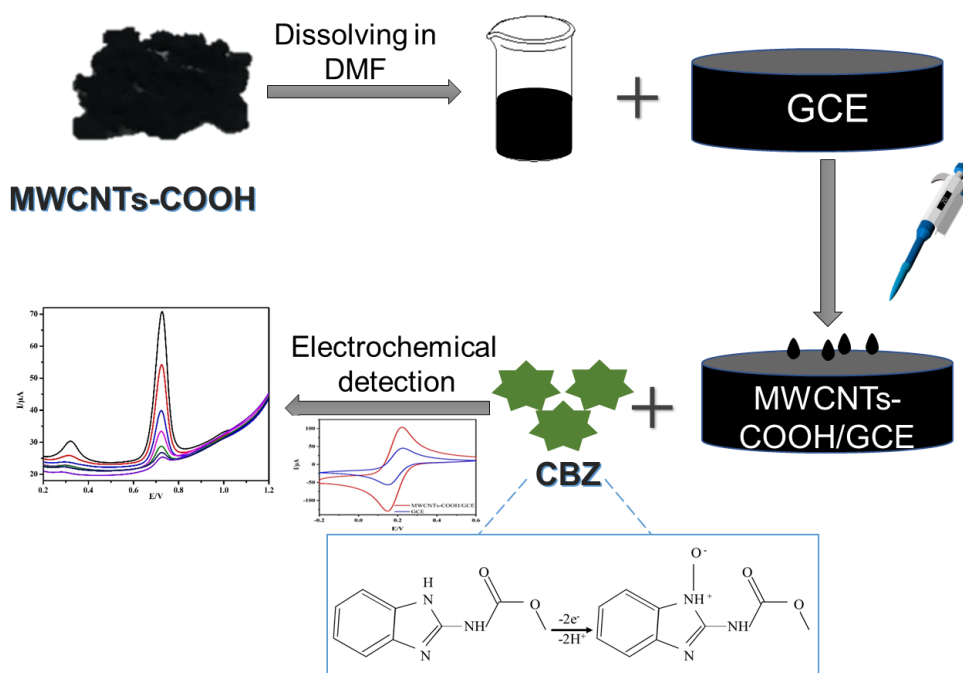
In this section, MWCNTs-COOH with special functional groups and large specific surface area were used to modify electrodes to improve the adsorption and

enrichment of CBZ on the electrode, and amplify the electrochemical signal, aiming to establish a highly sensitive electrochemical rapid detection technology for CBZ (Karimi-Takallo, Dianat, & Hatefi-Mehrjardi, 2021; Y. Liu et al., 2021; Zeng et al., 2021; Zou et al., 2016).

4.1 Materials and Preparation Methods for electrochemical sensor

4.1.1 Fabrication of MWCNTs-COOH/GCE sensor

10mg MWCNTS-COOH was dissolved in 5ml DMF and dispersed for 30min with the aid of ultrasonic instrument. A black uniform modified suspension is obtained. Then keep it at room temperature. After the suspension of 5 μ L MWCNTS-COOH was dropped on the surface of the dry bare electrode with a pipettor and baked with an infrared lamp, the MWCNTS-COOH /GCE sensor was prepared. The construction process of the electrochemical sensor is shown in the **Scheme 4-1**.



Scheme 4-1. The fabrication process of the MWCNTs-COOH/GCE sensor for the determination of CBZ.

4.1.2 Detection method of MWCNTS-COOH/GCE Sensor for CBZ

A three-electrode system was used to conduct electrochemical experiments in 0.1 M PBS solution pH=7.0. GCE was used as the working electrode, saturated calomel electrode as the reference electrode, and platinum wire electrode as the counter electrode. Cyclic voltammetry (CV) were performed at a potential range of -1.2 to 0.2 V with a scan rates of 50 mV s⁻¹. Electrochemical impedance spectroscopy (EIS) were performed in 5 mM K₃[Fe(CN)₆]/K₄[Fe(CN)₆] solutions containing 0.3M KCl at frequencies ranging from 0.1 to 100000 Hz. Differential pulse curves(DPV) method was used to study the linear relationship between peak current value and CBZ concentration. The potential range of DPV was 1.2-0.2V.

4.2 Experimental results and analysis of electrochemical sensor detection

4.2.1 Microstructure and morphology of MWCNTS-COOH

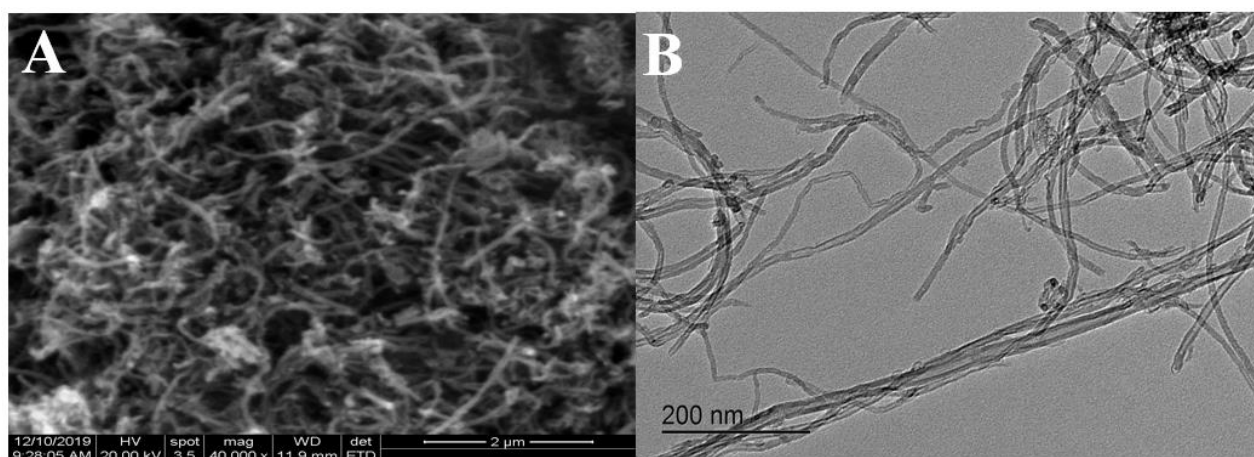


Fig. 4-1 (A) SEM image and (B) TEM image of MWCNTS-COOH

Fig. 4-1A shows the SEM image of the MWCNTS-COOH sample. It can be seen that the MWCNTS-COOH sample is composed of one-dimensional carbon nanotubes, which are closely intertwined without any dispersion rule. **Fig. 4-1B** shows the TEM image of the MWCNTS-COOH sample. The obvious one-dimensional hollow carbon nanostructure can be observed with interconnection status, which contributes to the interconnected conductive carbon channels. Such carbon structure contributes to the efficient charge transport on the sensing electrode surface, which could enhance the electrochemical response.

4.2.2 Electrochemical properties of MWCNTS-COOH /GCE

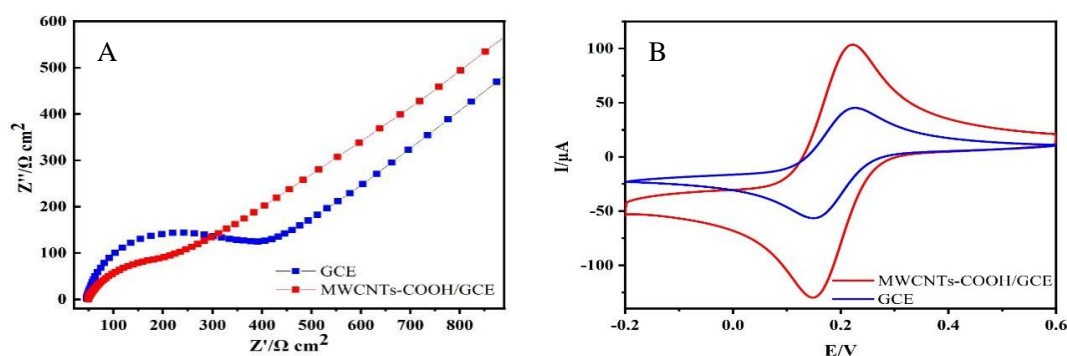


Fig. 4-2 (A) EIS and (B) CV measurement results of the bare GCE and MWCNTs-COOH/GCE sensor in 5.0 mM $\text{K}_3[\text{Fe}(\text{CN})_6]$ solution containing 0.3 M KCl, and Scan rate is 50 mvs^{-1} .

The 5.0 mM $\text{K}_3[\text{Fe}(\text{CN})_6]$ solution containing 0.3 M KCl was used as the electrolyte solution to test the alternating current impedance (IMP) in the frequency range of 1~105Hz. **Fig. 4-2A** shows the EIS measurement result of the bare GCE and MWCNTs-COOH/GCE sensor. The charge transfer resistance (R_{ct}) of the fabricated sensor can be estimated by using the diameter of the semi-circle. When MWCNTS-COOH was modified onto the GCE surface, the diameter of the semicircles was greatly reduced, indicating that the introduction of MWCNTS-COOH significantly improved the electrical conductivity property of sensing electrode surface. The MWCNT-COOH sample showed high electrical conductivity and good dispersing property due to the one-dimensional hollow conductive carbon structure and carboxyl functionalization. The presence of carboxyl group improved the dispersion degree of carbon nanotubes to a certain extent, which could realize the uniform distribution of carbon material, and the one-dimensional hollow conductive carbon structure contributes to the efficient charge transport on the sensing electrode surface, which could enhance the electrochemical response.

In order to further investigate the electrochemical performance of the modified electrode, CV measurements were carried out in a 5.0 mM $\text{K}_3[\text{Fe}(\text{CN})_6]$ solution containing 0.3 mM KCl. As shown in **Fig. 4-2B**, all the modified electrodes

have a good pair of reversible redox peaks. Compared with the bare electrode, the potential difference between oxidation peak and reduction peak on the MWCNTs-COOH/GCE sensor is reduced, and the response current is larger than that of the bare sensor, which may be due to the one-dimensional hollow conductive carbon structure and carboxyl functionalization of MWCNTs-COOH.

4.2.3 Electrochemical behavior of CBZ

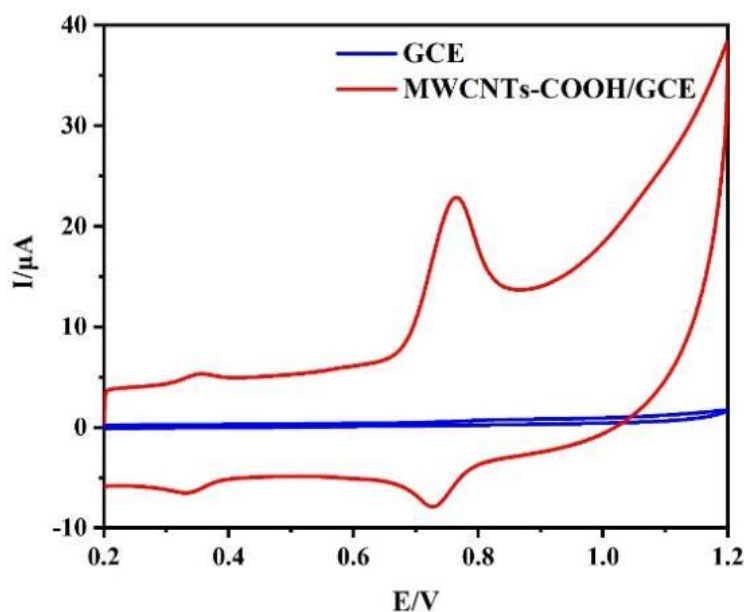


Fig. 4-3 CV curves of 50 μM CBZ at the bare GCE and MWCNTs-COOH/GCE sensor, Scan rate: 50mvs^{-1} .

Fig. 4-3 shows the CV curves of the bare GCE and MWCNTs-COOH/GCE sensor. It can be found that the electrochemical peak current response of the bare GCE sensor is not easy to observed in the CV curve. By contrast, the oxidation peak current of CBZ at the MWCNTs-COOH/GCE sensor can reach up to $15.92\ \mu\text{A}$, which was significantly higher than that of the bare GCE sensor, indicating that the introduction of MWCNTs-COOH significantly improved the electrochemical sensing analysis performance of CBZ, which has close association with the one-dimensional hollow conductive carbon structure and carboxyl functionalization of MWCNTs-COOH. The presence of carboxyl group improved the dispersion degree

of carbon nanotubes to a certain extent, which could realize the uniform distribution of carbon material, and the one-dimensional hollow conductive carbon structure contributes to the efficient charge transport on the sensing electrode surface. As a result, the MWCNTs-COOH/GCE sensor showed good CBZ detection performance.

4.2.4 Optimization of detection conditions

4.2.4.1 Influence of scan rate

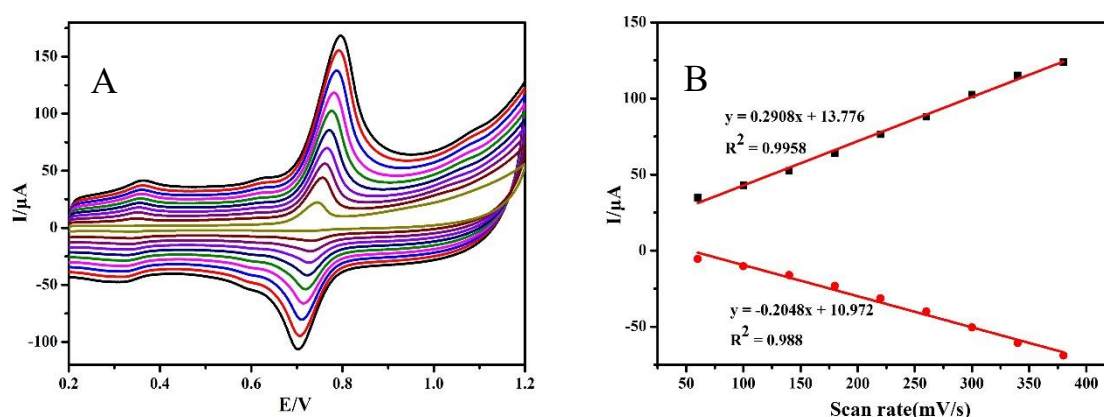


Fig. 4-4 (A) CV curves of 10 μM CBZ at the MWCNTs-COOH/GCE sensor at different scan rates of 60-380 mV s^{-1} and (B) relationship between peak current and scan rate.

The control type of electrochemical detection reaction at the fabricated sensor can be confirmed by the relationship between oxidation peak current and scan rate. **Fig. 4-4A** shows the influence of scan rate on the CV curves of 10 μM CBZ at the MWCNTs-COOH/GCE sensor (Scan rate: 60, 100, 140, 180, 220, 260, 300, 340, and 380). The results show that there is a good linear relationship between oxidation peak current and reduction peak current. The regression equations are described as $I_O = 0.2908x + 13.776$ ($R^2=0.9958$) and $I_R = -0.2048x + 10.972$ ($R^2=0.988$), respectively. The above good linear relationship suggests that the reversible redox reaction of 10 μM CBZ at the MWCNTs-COOH/GCE sensor has close association with the adsorption-controlled process.

4.2.4.1 Influence of pH

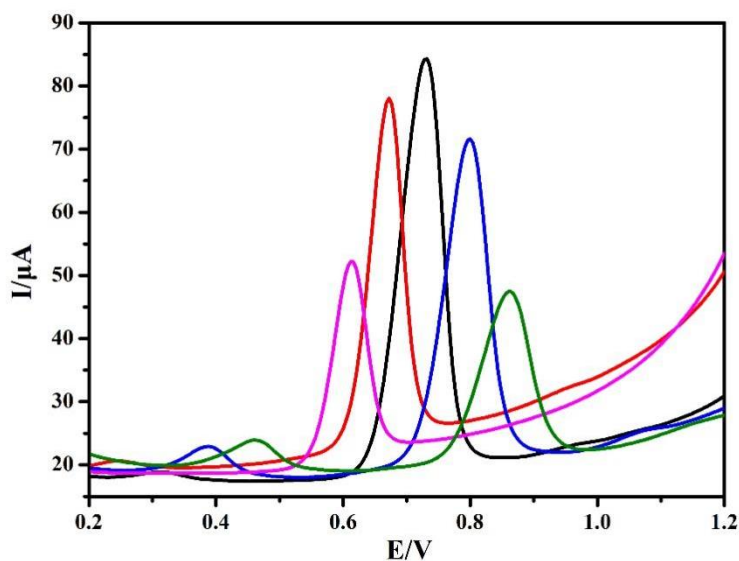


Fig. 4-5 Influence of pH value on the DPV curves of 10 μ M CBZ at the MWCNTs-COOH/GCE sensor.

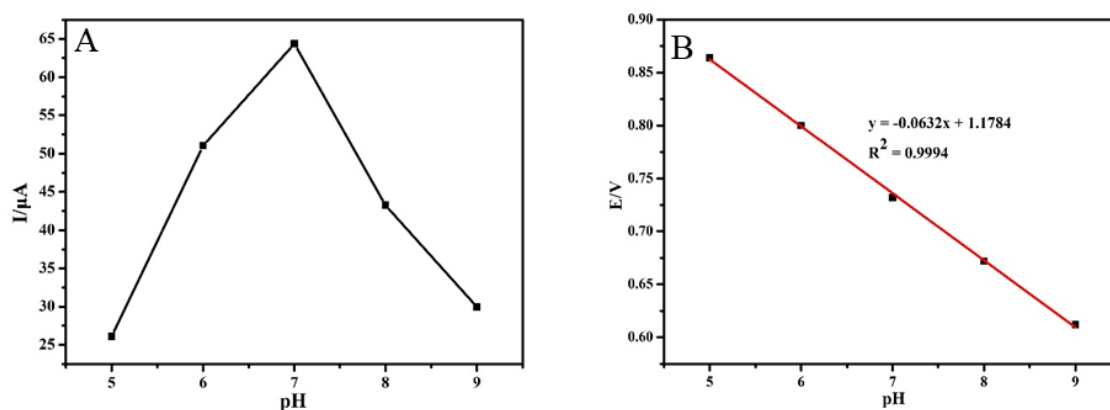


Fig. 4-6 (A) Relationship between oxidation peak current (I_p) and pH and (B) relationship between oxidation peak potential (E_p) and pH.

In this experiment, the influence of pH value on the CBZ detection property was investigated based on the DPV measurement. **Fig. 4-5** shows the influence of pH value on the DPV curves of 10 μ M CBZ at the MWCNTs-COOH/GCE sensor (pH: 5.0, 6.0, 7.0, 8.0, and 9.0). As can be seen, when the pH value is between 5 and 7, the peak current response increases positively with the constant increase of pH value. When pH is 7.0, the peak current response reaches up to the maximum peak

current value, and then the peak current response decreases with the further increase of pH value, which can be clearly observed in **Fig. 4-6A**. Therefore, pH=7.0 was selected as the optimized pH value for the CBZ detection at the MWCNTs-COOH/GCE sensor. The relation between oxidation peak current (I_p) and oxidation peak potential (E_p) is shown in **Fig. 4-6B**. The E_p value gradually decreases with the increase of pH value. The corresponding regression equation is expressed as $E_p(\text{V}) = -0.0632x + 1.1784$ ($R_2=0.9994$). The slope of the equation is 0.0632, which is close to the ideal value of 0.0585 V/ pH, indicating that the number of proton and electron transfer is equal in the oxidation process of CBZ on MWCNTs-COOH/GCE surface. It can be inferred that the possible oxidation mechanism of CBZ on MWCNTs-COOH/GCE surface is shown as in the **Fig.4-7**, in which CBZ loses two electrons and is oxidized.

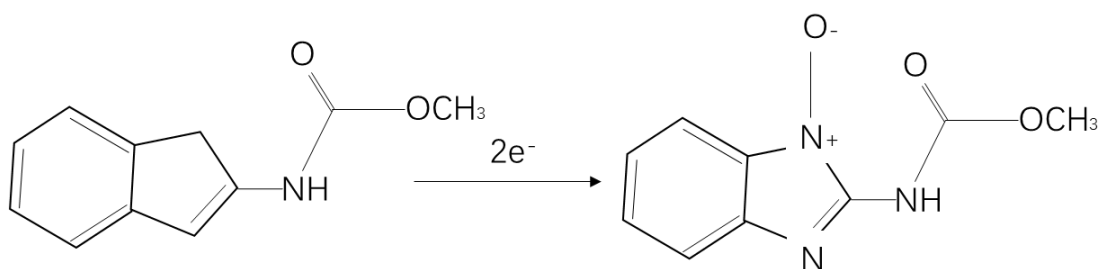


Fig.4-7 Oxidation mechanism of CBZ

4.2.4.2 Influence of accumulation time

The effect of accumulation time on the peak current signal of CBZ detection at the MWCNT-COOH/GCE sensor was studied by DPV method. **Fig. 4-8** shows the relationship between DPV peak current (I_p) and accumulation time. When the accumulation time increases from 0 to 60 s, the anode peak current also increases significantly. These results indicate that the adsorption capacity of CBZ molecules gradually increases on the electrode surface of the MWCNT-COOH/GCE sensor. When the accumulation time reaches up to 60s, the MWCNT-COOH/GCE sensor showed the largest peak current signal. With the further increase of accumulation

time, the peak current showed a basically unchanged trend without obvious change, which indicates that the adsorption of CBZ molecules on the electrode surface of the MWCNT-COOH/GCE sensor may reach up to a saturated state. Therefore, in order to improve detection efficiency, 60 s is selected as the appropriate accumulation time for the CBZ detection.

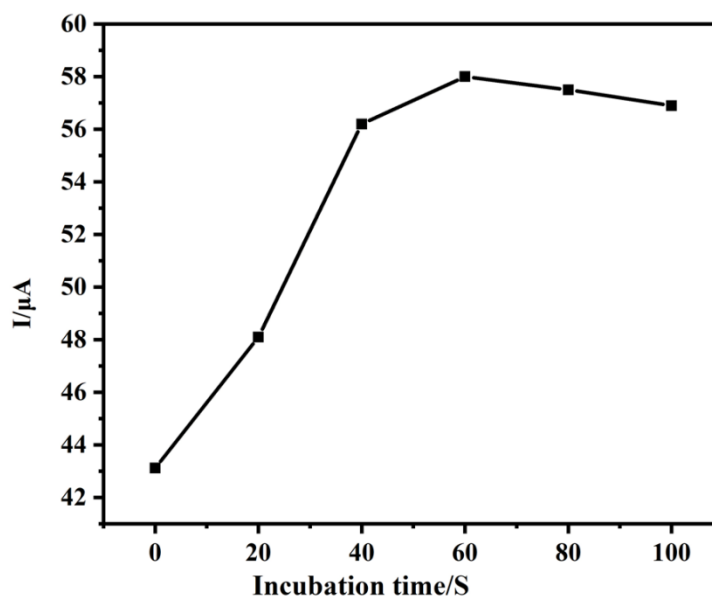


Fig. 4-8 Relationship between DPV peak current (I_p) and accumulation time

4.2.5 Analytical performance of MWCNTS-COOH /GCE sensor

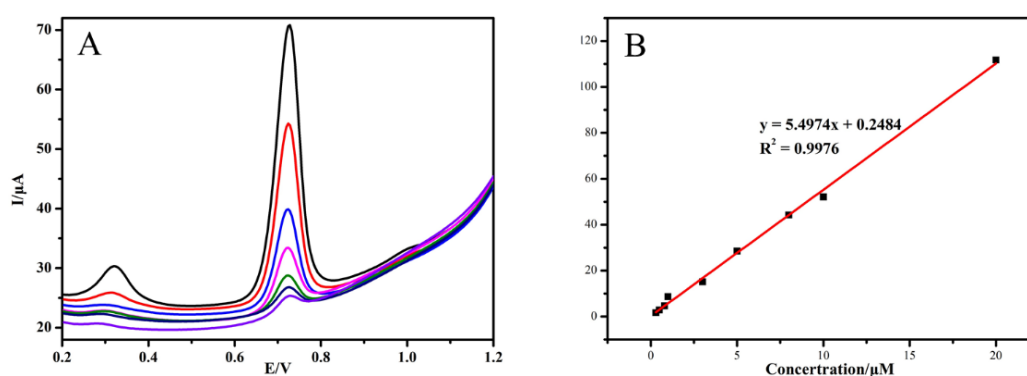


Fig. 4-9 (A) Effect of CBZ concentration on the DPV curves at the MWCNTS-COOH/GCE sensor and (B) relationship of peak current with CBZ concentration.

Fig. 4-9A shows the effect of CBZ concentration (Range: 0.3, 0.5, 0.8, 1.0, 3.0, 5.0, 8.0, 10, 20 μM) on the DPV curves at the MWCNTS-COOH/GCE sensor. In

certain concentration range of 0.03-20 μM , the electrochemical response of CBZ in the DPV curves increases gradually when the CBZ concentration increases. **Fig. 4-9B** exhibits the variation curve about these two parameters. There is a linear relationship between peak value of DPV curves and CBZ concentration with regression equation of $I(\mu\text{A}) = 5.4974C + 0.2484$ ($R^2=0.9976$). The analysis calculation result shows that the MWCNTS-COOH/GCE sensor presented a significantly lower limit of detection (6.7 nM).

4.2.6 Reproducibility, stability and anti-interference

Table 4-1 Reproducibility and repeatability of the MWCNT-COOH/GCE sensor

Electrode test	$I_1/\mu\text{A}$	$I_2/\mu\text{A}$	$I_3/\mu\text{A}$	$I_4/\mu\text{A}$	$I_5/\mu\text{A}$	RSD/%
The same electrode	9.134	8.432	8.934	8.298	8.189	4.81%
The different electrode	8.789	8.547	8.356	8.275	8.997	3.5%

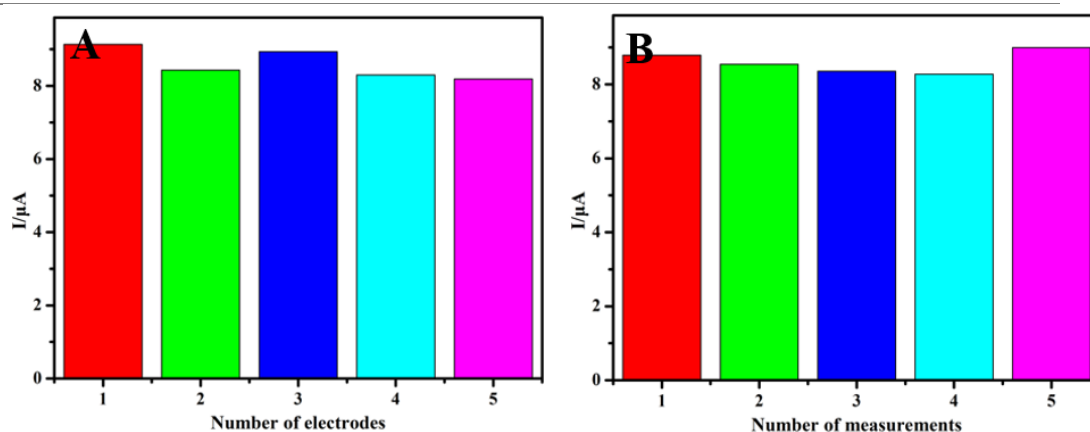


Fig. 4-10 (A) Reproducibility and (B) Stability of the MWCNT-COOH/GCE sensor.

Fig. 4-10A and B show the reproducibility and repeatability of the MWCNT-COOH/GCE sensor, and the corresponding peak current values were obtained from the DPV measurements of 1.0 μM CBZ at the MWCNT-COOH/GCE sensor. Five individual measurements with five different modified sensors and five repeatable measurements at one individual modified sensor were carried out in PBS solution containing 1.0 μM CBZ. The corresponding peak current values presented pretty good determination result with low relative standard deviation (RSD) values of

4.81%, which means the good reproducibility. Moreover, the stability results can be analyzed from the corresponding peak current values (**Fig. 4-10B** and **Table 4-1**) of one individual modified sensor. The consistent peak current response with low *RSD* values of 3.5% confirms the good stability of the MWCNT-COOH/GCE sensor.

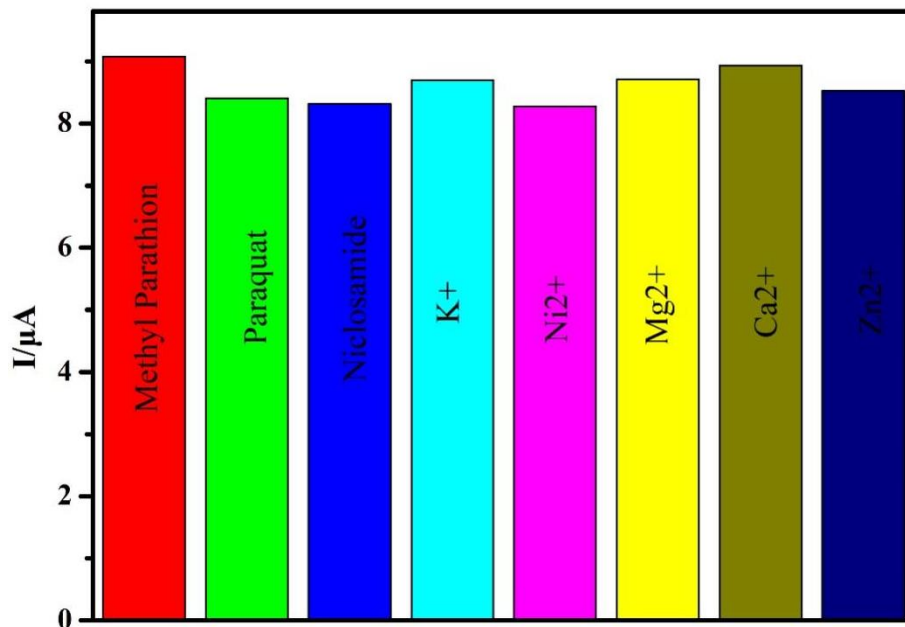


Fig. 4-11 Anti-interference of the MWCNT-COOH/GCE sensor

Fig. 4-11 shows the anti-interference of the fabricated MWCNT-COOH/GCE sensor based on the DPV measurement. The interference substances were methyl parathion, paraquat, niclosamide and other inorganic substances (K⁺, Ni²⁺, Mg²⁺, Ca²⁺, and Zn²⁺) with concentration of 0.1 mM. It can be found that the change of peak current of CBZ was less than 5%, indicating that the MWCNT-COOH/GCE sensor had good anti-interference for CBZ detection.

4.3 Detection of CBZ in vegetable samples and evaluated by HPLC

4.3.1 Detection of CBZ by electrochemical sensor based on MWCNT-COOH in vegetable samples

Table 4-2 provides the practicability of the MWCNT-COOH/GCE sensor, which was employed to detect the content of CBZ in vegetable samples. All these samples were divided into three parts. The practicability measurement of the fabricated sensor was performed by standard addition method. According to the repeatability measurements, the recoveries and its *RSD* values can be analyzed to

reflect the practical feasibility of the present sensor. It can be seen that the MWCNT-COOH/GCE sensor presented a satisfactory CBZ detection result with low RSD from 1.95% to 4.78% and good recoveries from 93.6 to 104.4%. The above result confirms the good practical feasibility of the MWCNT-COOH/GCE sensor.

Table 4-2 Practical feasibility of the MWCNT-COOH/GCE sensor for the detection of CBZ in vegetable samples.

Vegetable sample	Added(μM)	Found(μM)	Recovery (%)	RSD (%)
Cabbage	1	1.039	103.9	4.46
	5	5.18	103.6	2.99
	10	9.54	95.4	1.95
Cucumber	1	0.968	96.8	4.78
	5	4.72	94.4	3.21
	10	9.36	93.6	2.39
Potato	1	0.95	95	2.1
	5	5.11	102.2	4.44
	10	10.44	104.4	2.05

4.3.2 Determination of CBZ by HPLC in vegetable samples

A method for determination of CBZ residues in vegetables by HPLC was established, and the chromatographic conditions for sample extraction, purification and detection were optimized. As we known, the matrix is complex in vegetables, and there are many interference factors compared with low pesticide residue. In this part, the chromatographic conditions of acetonitrile as extractant, methanol: water (85:15) as mobile phase and ultraviolet detection wavelength of 274 nm were finally determined after lots of experimental exploration.

Under the optimum Chromatographic conditions, a series of standard solutions with different concentrations of CBZ were prepared for determination. Then draw the standard curve of mass concentration according to the peak area of each component. The results show that the linear range of CBZ was 0.03~10 μM , the

standard curve equation was $y = 5632.38x - 32.6$, and the correlation coefficient is 99.42%. It can meet the needs of quantitative analysis.

QuEChERS (Quick, Easy, Cheap, Effective, Rugged and Safe) was applied to the pretreatment of the vegetables to be tested, and PSA and GCB were finally selected as the purifying agents for sample pretreatment. **Fig. 4-12** and **Fig. 4-13** were respectively the control check chromatogram and spiked chromatogram of cucumber sample. The relative standard deviation and spiked recovery results were shown in the **Table 4-3**. The recoveries rate cucumber, lettuce and Potato were in the range of 91%~104.7%, and RSD was below 5%.

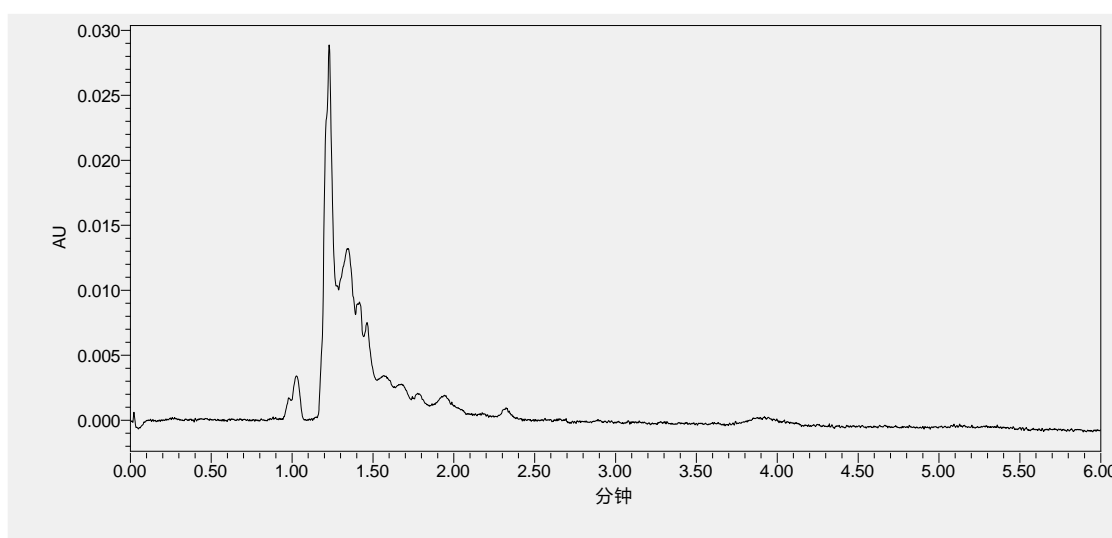


Fig.4-12. The control check Chromatogram of cucumber sample

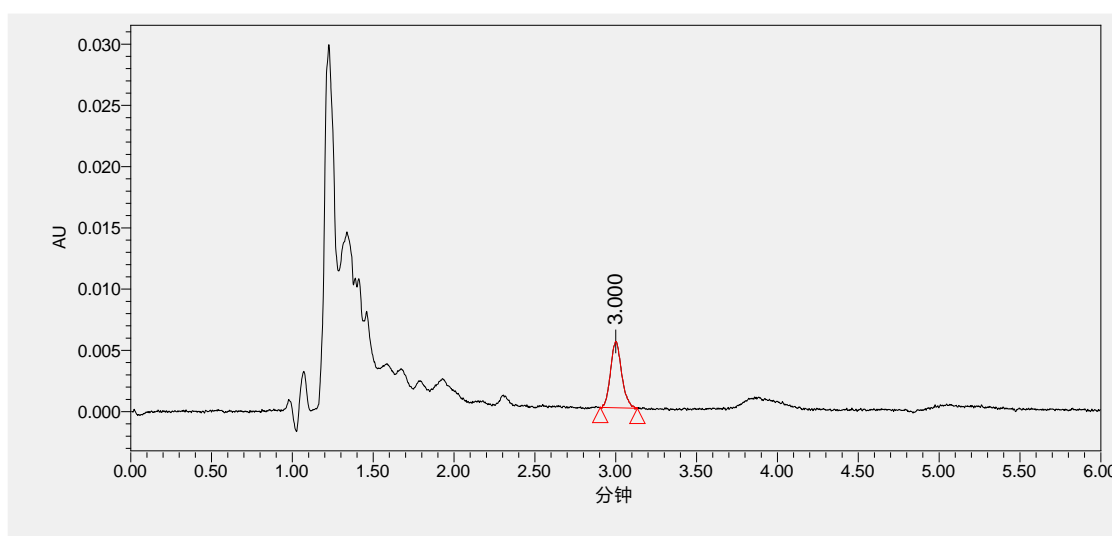


Fig. 4-13. The spiked chromatogram of cucumber sample

Table 4.3 Determination of spiked recovery rate of vegetable samples

Vegetable sample	Added(μM)	Found(μM)	Recovery (%)	RSD (%)
Cabbage	1	0.95	95	2.11
	5	5.14	102.87	4.61
	10	9.4	94.03	2.53
Cucumber	1	0.91	91	2.76
	5	4.73	94.6	4.02
	10	9.36	93.6	2.39
Potato	1	0.94	94	2.13
	5	4.92	98.4	3.8
	10	10.47	104.7	4.28

4.3.3 Comparative evaluation on electrochemical sensor based on MWCNTs-COOH and HPLC for CBZ detection in Vegetables

As can be seen from the experimental results in the above two parts, the recovery rate of electrochemical sensor for CBZ detection is between 93.6% and 104.4%, compared with the recovery rate of 91%~104.7% obtained by HPTC method, both of them can meet the detection requirements. The detection of CBZ residue results by electrochemical sensor based on MWCNT-COOH/GCE is basically consistent with HPTC, indicating that the electrochemical sensor method is relatively accurate and reliable, and can be used as an alternative method for the detection of CBZ residue in vegetables.

4.4 Conclusion in section 4

In this section, we reported the MWCNT-COOH/GCE sensor for the detection of CBZ. MWCNT-COOH showed high electrical conductivity and good dispersing property due to the one-dimensional hollow conductive carbon structure and carboxyl functionalization. The presence of carboxyl group improved the dispersion degree of carbon nanotubes to a certain extent, which could realize the uniform distribution of carbon material, and the one-dimensional hollow conductive carbon structure contributes to the efficient charge transport on the sensing electrode surface, which could enhance the electrochemical response. The electrochemical

sensing test results showed that the MWCNT-COOH/GCE sensor presented a low LOD value of 6.7 nM within an acceptable linear CBZ concentration range of 0.03-20 μ M. In addition, the fabricated sensor possessed good reproducibility (*RSD*: 4.81%) and repeatability (*RSD*: 3.5%). For the anti-interference of the MWCNT-COOH/GCE sensor, the change of peak current of CBZ was less than 5%, suggesting the good anti-interference. Moreover, In order to compare the performance in actual sample detection about CBZ residue, the classical method based on HPLC was studied, and then the experimental results were compared. After a series of sample pretreatment, the CBZ residues in three kinds of vegetables (Cabbage, Cucumber and Potato) were determined by HPLC method under optimal chromatographic conditions.

The comparison between the experimental results and the commonly used HPLC method's results showed that the detection of CBZ concentration based on the electrochemical sensor method was basically consistent with HPTC method, indicating that the new electrochemical sensor method was relatively accurate and reliable. In addition, the electrochemical sensor method was simple and fast to operate, providing the possibility of realizing the convenient field detection of pesticide residues.

SECTION 5 DETERMINATION OF IMIDACLOPRID IN VEGETABLES BY ELECTROCHEMICAL SENSOR BASED ON SOYBEAN-DERIVED POROUS CARBON AND EVALUATED BY HIGH PERFORMANCE LIQUID CHROMATOGRAPHY

Imidacloprid (IMI), as a widely used nicotinoid insecticide, can effectively control pests by directly acting on the central nervous system of pests (Brandt, Gorenflo, Siede, Meixner, & Buchler, 2016), and has become one of the largest selling insecticides in the world (Vijver & van den Brink, 2014). However, IMI does not decompose easily, which poses a great threat to human health and poses a serious risk of contamination to the environment and food. Therefore, it is of great significance to develop a simple, sensitive, and efficient IMI detection method for human health and ecological environment. The commonly used detection methods of IMI include: high performance liquid chromatography (Samnani, Vishwakarma, & Pandey, 2011), gas chromatography (Ko et al., 2014), spectrophotometry (Guzsvany et al., 2009), fluorescence spectrophotometry (M. L. Chen et al., 2015; W. Li et al., 2015), etc.. Although the above detection methods have high sensitivity and stability, they are expensive, time-consuming, and costly to analyze. In contrast, the electrochemical sensor detection method has attracted extensive attention in the detection of IMI due to its high sensitivity, short reaction time and easy miniaturization (L. Liu, J. W. Guo, & L. H. Ding, 2021; Oliveira, Bettio, & Pereira, 2018; Paula et al., 2020; X. C. Zhai et al., 2020).

Electrode modification material determines the performance of electrochemical sensor to a great extent. As we known, bare electrode has poor electrocatalytic performance for IMI, some modification materials can be introduced to the surface of the sensor electrode to modify it. Because of their excellent electrochemical properties, carbon nanomaterials show good electrochemical performance, sensitivity, and anti-interference for the detection of various organic and inorganic molecules. However, at present, most of the carbon-based materials are synthesized

using fossil fuels as raw materials, and the preparation process is complicated, the experimental conditions are harsh, and the environmental pollution is caused by shortcomings (Kalinke, Mangrich, Marcolino, & Bergamini, 2016), which limit the wide application of carbon materials. Therefore, it is particularly important to find a carbon material with a wide range of sources, low cost, simple preparation process and no pollution to the environment.

As a renewable resource, biomass has the advantages of low price, abundant storage, and environmental friendliness (Lu & Zhao, 2017; Lyu et al., 2019; B. Zhang, Jiang, & Balasubramanian, 2021). In recent years, high performance carbon materials made from biomass have attracted more and more attention. Biomass carbon materials not only have the advantages of extensive sources, low cost, and high yield, but also show the advantages of large specific surface area, high electrical conductivity and strong chemical stability (B. Zhang et al., 2021). Using biomass raw materials to produce a variety of carbon materials, not only can reduce the production cost, but also can realize the sustainable development of carbon materials. Wang et al. (C. Wang, Xiong, Wang, & Sun, 2018) prepared the monolithic porous carbon by one-step carbonization of orange peel, and further synthesized another composite electrode by simple hydrothermal process. The above porous carbon has a high specific surface area of 860 m²/g and naturally doped nitrogen. The synergistic effect of orange peel porous carbon and MnO₂ significantly improved the electrochemical performance of the composite electrode. In addition, the flexibility of orange peel is utilized to achieve custom-shaped monolithic porous carbon electrodes and devices, further expanding the dimension of biomass for supercapacitors.

Biomass-derived porous carbon has abundant pore structure and interconnected electron conduction network, which is beneficial to enhance the adsorption and electrical conductivity of carbon materials. In this section, the soybean-derived porous carbon (SDPC) with three-dimensional (3D) interconnected porous structure was prepared by using the expired soybean as carbon source through a high-

temperature carbonization process. SDPC was used to modify the glassy carbon electrode (GCE) for the fabrication of SDPC/GCE sensor towards IMI. The 3D interconnected porous structure of SDPC significantly improved the electrical conductivity and good absorption capability for IMI due to the interconnected carbon conductive network and large specific surface area. The fabricated SDPC/GCE sensor was successfully constructed for the highly sensitive detection of IMI.

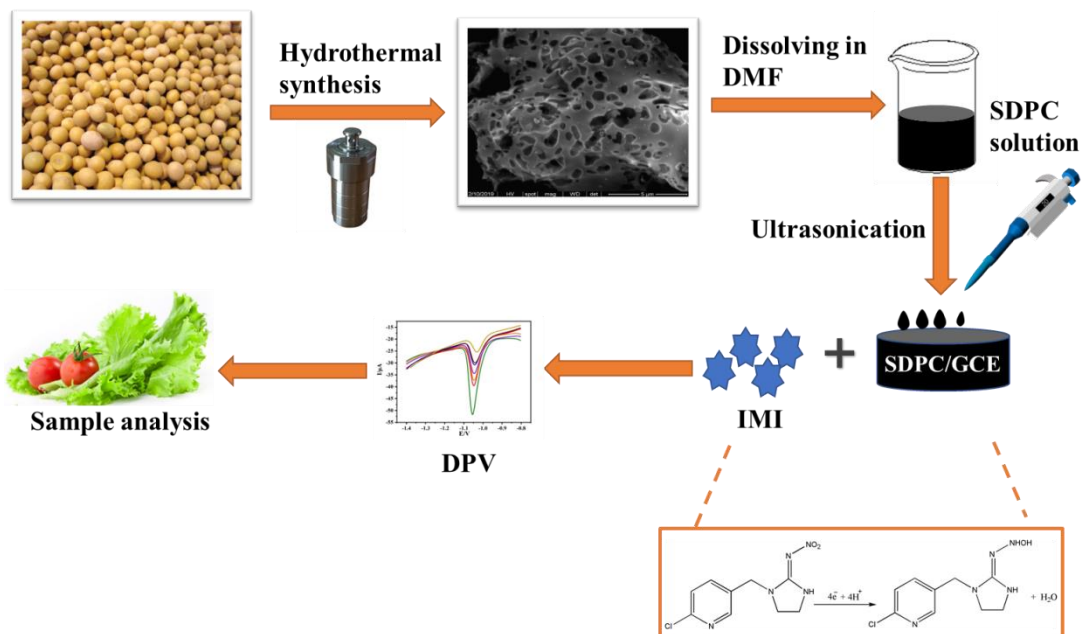
5.1 Materials and Preparation Methods for electrochemical sensor

5.1.1 Preparation of nanocomposites SDPC

40 g soybeans were sealed in a 100 mL hydrothermal reactor and heated at 180 °C for 22 hours. After cooling, 20 g soybean carbon paste was evenly mixed with KOH at a mass ratio of 1:1, then added to 25 mL deionized water and fully stirred to form a uniform slurry. The resulting slurry was dried under vacuum at 105°C to obtain a well-mixed soybean and KOH. The mixture was then placed in a tubular furnace and carbonized under argon at 800 °C for 2 hours at a heating rate of 3 °C per minute. After the completion of high temperature pyrolysis, the mixture was first cleaned with dilute hydrochloric acid for several times, and then washed with deionized water for several times to eliminate the impurities. Finally, the SDPC sample was obtained by drying the washed product under the vacuum condition of 105 °C.

5.1.2 Fabrication of SDPC/GCE sensor

20 mg SDPC was ultrasonically dispersed in 10 mL DMF for 30 mins to prepare the SDPC dispersion solution (2.0 mg/ml). Before the preparation of sensing electrode, the bare GCE surface was carefully polished by using aluminum oxide powders with different particle sizes. And then, the surface impurities were removed by ultrasonic cleaning with ethanol and deionized water for 3 minutes. Finally, the obtained SDPC suspension (5 µL) was measured out by a micropipettor to modify the surface of GCE by a drop-coating technology. **Scheme 5-1** shows the fabrication process of the SDPC/GCE sensor for the determination of IMI.



Scheme 5-1 Fabrication of the SDPC/GCE sensor for the determination of IMI.

5.2 Experimental results and analysis of electrochemical sensor detection

5.2.1 Microstructure and morphology of SDPC

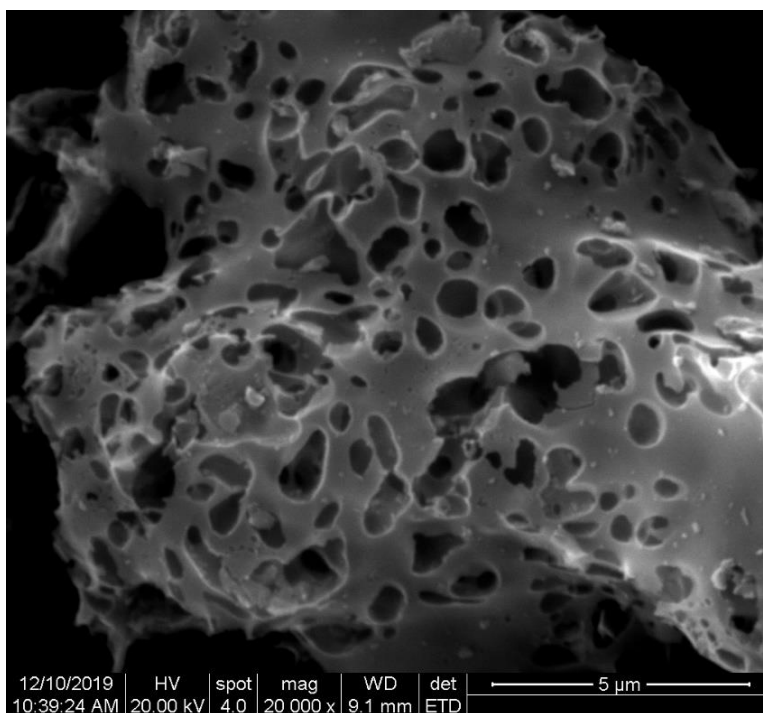


Fig. 5-1 SEM images of of the SDPC sample

SEM characterization was used to study the surface morphology of the SDPC sample. **Fig. 5-1** shows the SEM image of of the SDPC sample. It can be found that

this porous carbon materials has a three-dimensional porous structure with interconnected large pores and carbon walls. The 3D interconnected porous structure of SDPC significantly improved the electrical conductivity and good absorption capability for IMI due to the interconnected carbon conductive network and large specific surface area, which may improve the detection performance of IMI (N. Wang et al., 2019).

5.2.2 Electrochemical characterization

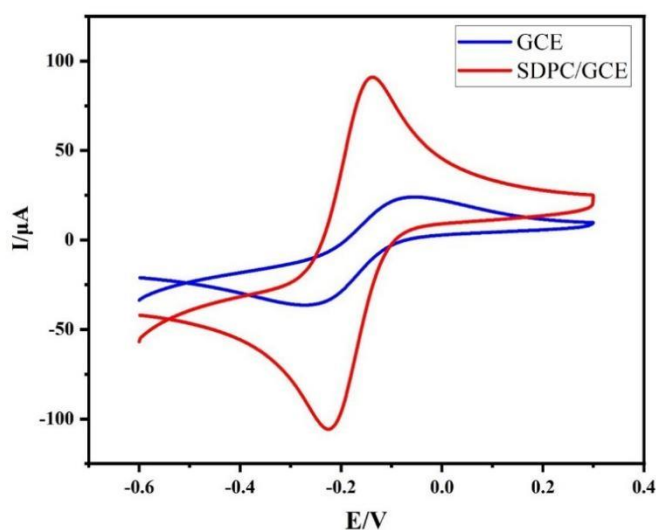


Fig. 5-2 CV curves of the bare GCE and SDPC/GCE sensors in 5 mM $K_3[Fe(CN)_6]$ solution containing 0.3M KCl at a scan rate of 50 mV/s

In order to study the electrochemical performance of the modified electrode, the assembled sensors were performed based on the CV experiments in 5.0 mM $K_3[Fe(CN)_6]$ solution containing 0.3M KCl. **Fig. 5-2** shows the CV curves of the bare GCE and SDPC/GCE sensors. As shown here, both the bare GCE and SDPC/GCE sensors showed a pair of reversible redox peaks. For the bare GCE sensor, the CV curve presents small redox peaks ($I_{pa}=22.95 \mu A$, $I_{pc}=-31.4 \mu A$). By contrast, the SDPC/GCE sensor presents much higher peak current response ($I_{pa}=106.7 \mu A$, $I_{pc}=-109.7 \mu A$) than that of the bare GCE sensor, which has

close association with the 3D interconnected porous structure of SDPC with high electrical conductivity and large specific surface area.

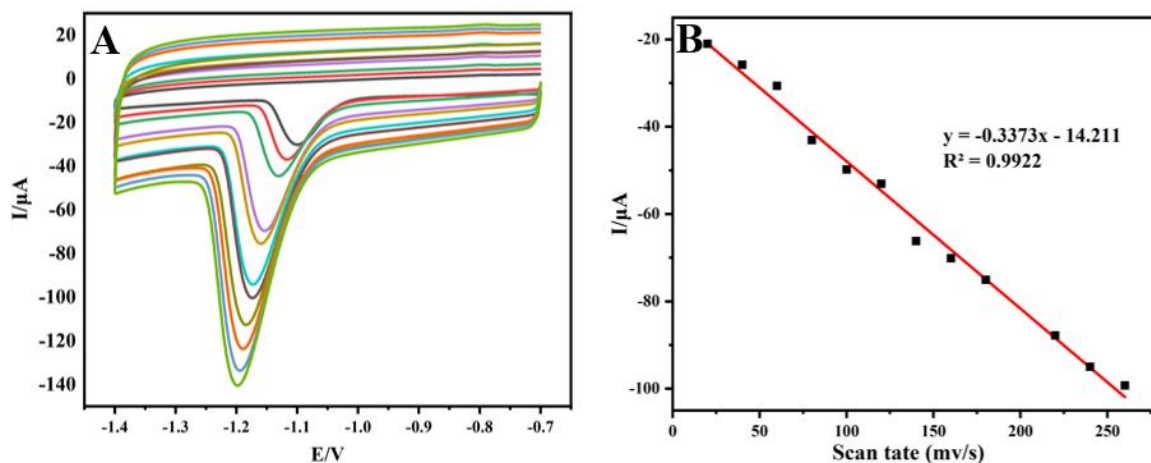


Fig. 5-3 (A) CVs of 100 μM IMI detection of the SDPC/GCE sensor at different scan rates (20, 40, 60, 80, 100, 140, 160, 180, 220, 240, and 260 mV s^{-1}) and (B) relationship between peak current and scan rate.

Fig. 5-3 shows the CV curves of the SDPC/GCE sensor with different scan rates (20,40,60,80,100,140,160,180,220, 240 and 260 mVs^{-1}) in 5 mM $\text{K}_3[\text{Fe}(\text{CN})_6]$ solution containing 0.3 M KCl. It can be seen from the **Fig. 5-3(A)** that the SDPC/GCE sensor has a great influence on the change of peak current of IMI under different scan rates, and the response of peak current shows a trend of gradual increase with the increase of scan rate. As can be seen from **Fig. 5-3(B)**, there is a linear relationship between the scan rate and the peak current of IMI. The relationship between peak current and scan rate can be obtained by theoretical calculation as follows : the reduction peak current response of IMI is linearly related to the scan rate, and the corresponding linear equation is $y = -0.3373x - 14.211$ ($R^2 = 0.9922$), which indicates that the reaction of IMI is a process controlled by adsorption.

5.2.3 Electrochemical behavior of IMI

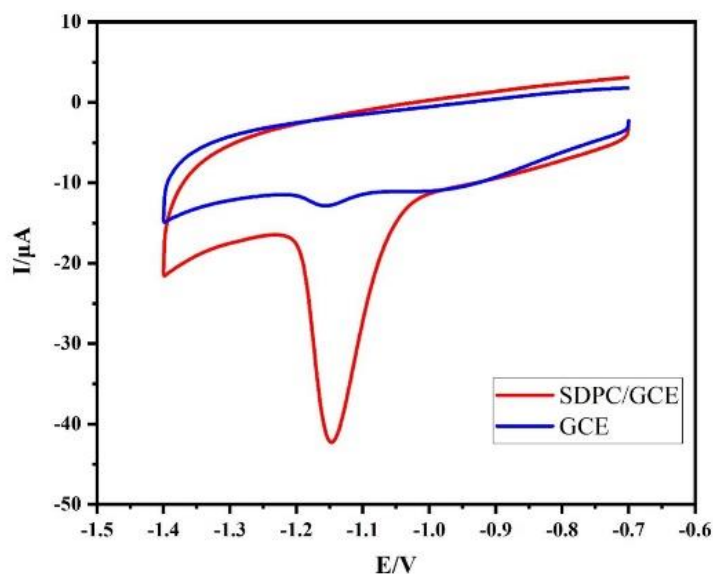


Fig. 5-4 CV curves of GCE, SDPC/GCE in the presence of 30 μM IMI (pH 7.0)

Fig. 5-4 shows the CV curves of 30 μM IMI detected by GCE and SDPC/GCE sensors. As can be seen, there is only one irreversible reduction peak in the CV curves of the two electrodes, and no oxidation peak. The reduction peak is caused by the reduction of nitro group to hydroxylamine, indicating that the nitro group of IMI exhibits a completely irreversible reduction process on the electrode(Si et al., 2016),and the reaction mechanism is shown in **Fig.5-5**. Clearly, the reduction peak current of IMI is weak on the CV curve of the unmodified GCE sensor. The CV curve corresponding to the SDPC/GCE sensor shows a slightly larger reduction peak current, which is mainly because that SDPC has a rich porous structure, which can provide abundant active sites and electrolyte transfer channels to promote the transfer rate of electrons between the electrode interface. Therefore, the prepared SDPC/GCE sensor has been used as the electrochemical sensor with the best performance to detect IMI.

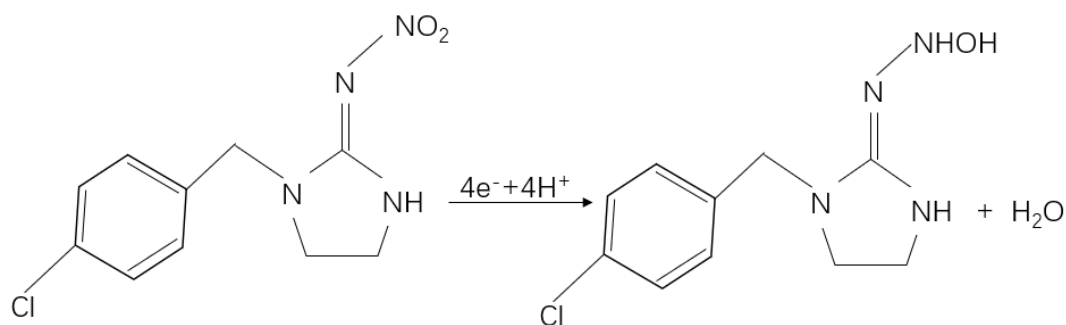


Fig. 5-5 The mechanism of IMI reduction

5.2.4 Optimization of detection conditions

In order to obtain more excellent IMI detection performance, the influencing factors such as accumulation time, drip-coating amount and pH were optimized.

5.2.4.1 Accumulation time

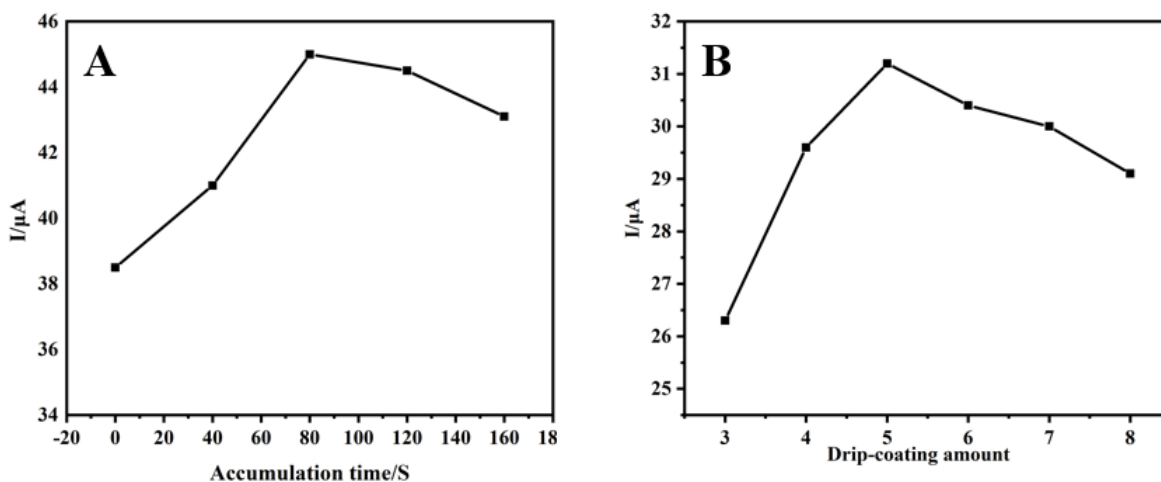


Fig.5-6 (A)Effect of accumulation time on the peak current value,(B). Effect of Drip-coating amount on the peak current value.

Fig.5-6(A) shows the influence of accumulation time on the peak current response of IMI detected by the SDPC/GCE sensor. The SDPC/GCE sensors were immersed in IMI solution with a concentration of $50\mu M$ and enriched for 0, 40, 80, 120 and 160s, respectively. As can be seen, the peak current response gradually increases with the increase of accumulation time. When the accumulation time reaches 80s, the peak current response reaches the maximum value. With the further increase of enrichment time, the peak current response doesn't continue to

increase, only remained in a relatively stable state, indicating that the adsorption capacity of IMI on the surface of SDPC/GCE electrode reached saturation. Therefore, 80s was chosen as the accumulation time.

5.2.4.2 Material drip-coating amount

It has been reported that the electrochemical detection performance is significantly related to the thickness of the electrode surface modification material(Shams et al., 2016; Ying Zhou et al., 2020). Therefore, it is necessary to study the effect of the drip-coating amount on the electrochemical performance of IMI on the constructed sensor. As shown in **Fig.5-6B**, with the modifier dosage increasing from 3 μ L to 5 μ L, the peak current of IMI anode also increased significantly. However, with the increase of modifier dosage, the peak current decreased significantly. This may be due to the formation of a thick film layer on the surface of GCE by the overmodified SDPC nanocomplex, which significantly limits the electrode conductivity [78]. Therefore, 5 μ L was chosen as the optimal amount of modifier to modify GCE in the experiments in this chapter.

5.2.4.3 pH

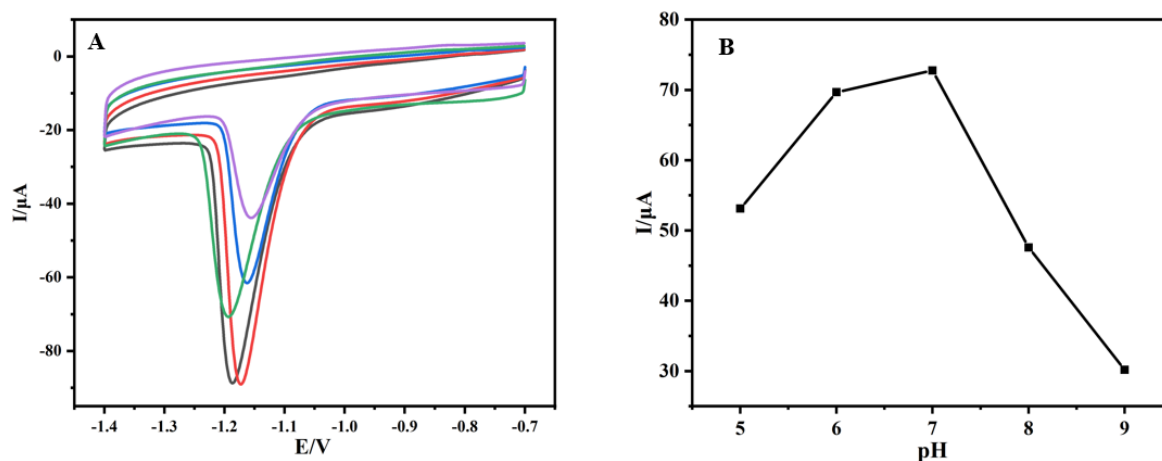


Fig. 5-7 CV curves of 100 μ M IMI at different pH.

CV was used to optimize the pH value in PBS buffer solution, and the influence of pH value on IMI detection performance is systematically studied. As shown in **Fig.5-7(B)**, when pH value is between 5 and 7, the peak current response value increases with the pH value increasing. When pH is 7, the peak current response reaches the maximum value, and then the peak current response decreases with the increase of pH, which because H^+ participates in the irreversible reduction reaction of IMI and the degradation of IMI can be accelerated in alkaline environment. Based on the above analysis, the optimal pH value of this experiment is 7.

5.2.5 Analytical performance of SDPC /GCE sensor

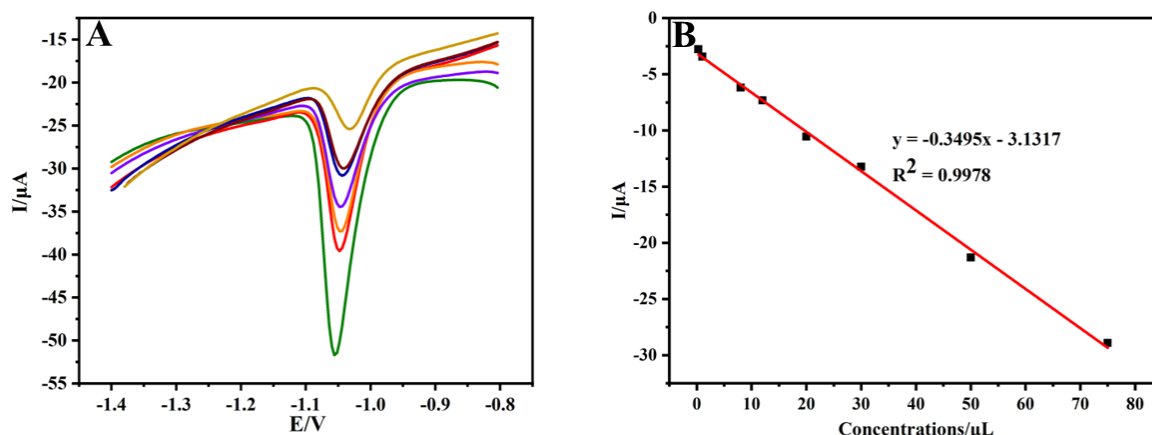


Fig. 5-8 (A) DPVs for determination of IMI at SDPC/GCE. IMI with different concentrations. (B) Linear relationship between peak current and IMI concentration.

In this experiment, DPV method was used to explore the efficient and sensitive detection effect of SDPC/GCE sensor on IMI detection. **Fig. 5-8A** shows the peak current response of the SDPC/GCE sensor to different concentrations of IMI under optimal experimental conditions. As can be seen from the **Fig.5-8B**, when the concentration range of IMI is between 0.3-75 μM , the peak current response and the concentration of IMI show a good linear relationship. The corresponding linear equation is: $I(\mu A) = -0.3495x - 3.1317$ ($R^2=0.9978$), and the corresponding limit of detection (LOD) is 5.18 μM ($S/N=3$). **Table 5-1** lists the

results of the comparison between this work and published studies. Compared with published studies, the SDPC/GCE sensor assembled in this work can show a more sensitive detection performance to IMI, mainly in the low LOD and high sensitivity. The excellent IMI detection performance can be attributed to the 3D layered porous structure of SDPC, rich pore size distribution, large specific surface area, good adsorption and excellent electrical conductivity. The SDPC/GCE sensor based on SDPC shows excellent IMI detection performance, and has a good application prospect for the analysis and detection of IMI residues.

Table 5-1. Comparison the performance of different IMI electrochemical sensors

Electrode	Analytical method	LOD (μM)	Linear range (μM)	References
Bismuth film electrode	DPV	2.9	9.5-200	(Guzsvány et al., 2008)
CPE	DPV	2.04	6.7-117.4	(Papp, Švancara, Guzsvány, Vytrás, & Gaál, 2009)
GO/GCE	SWV	7.9	10–200	(Urbanova, Bakandritsos, Jakubec, Szambo, & Zboril, 2017)
Boron-doped diamond electrode	SWV	8.60	30–200	(Ben Brahim, Belhadj Ammar, Abdelhédi, & Samet, 2016)
SPDC/GCE	DPV	5.18	0.3-75	This work

5.2.6 Reproducibility, repeatability, and anti-interference

Table 5-2 Reproducibility and repeatability of the SDPC/GCE sensor

Electrode test	$I_1/\mu\text{A}$	$I_2/\mu\text{A}$	$I_3/\mu\text{A}$	$I_4/\mu\text{A}$	$I_5/\mu\text{A}$	RSD/%
The same electrode	6.215	6.1	6.306	6.145	6.52	2.65%
The different electrode	6.203	6.098	6.201	6.705	6.18	3.86%

In order to verify the practicability and accuracy of this method, the reproducibility, repeatability, and anti-interference of the constructed sensor are further studied. **Table 5-2** shows the reproducibility and repeatability of the SDPC/GCE sensor in PBS solution containing 10 μM IMI (0.1 M, pH 7.0). The results showed that the RSD of the same electrode for five consecutive measurements was 2.96%, and the RSD of the five different electrodes was 2.98%. The above results showed that the constructed SDPC/GCE sensor had good reproducibility and repeatability.

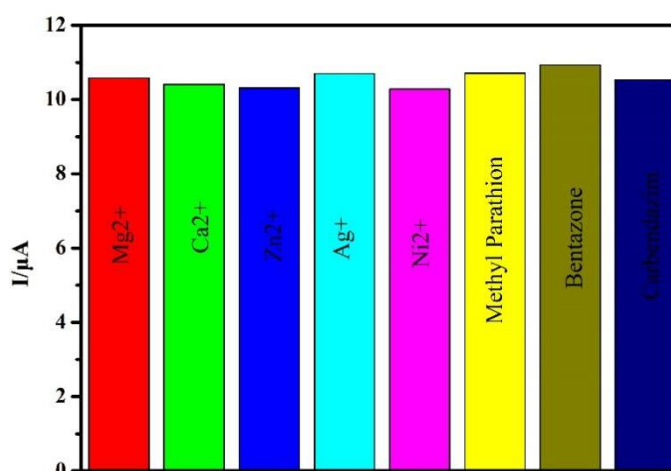


Fig. 5-9 Anti-interference of the proposed SDPC/GCE sensor

Anti-interference has an important influence on the detection performance of the sensor. In this part, some common inorganic ions and pesticides with similar structure are selected as interferers, that is, interfering ions (Mg^{2+} , Ca^{2+} , Zn^{2+} , Ag^+ and Ni^{2+}) and 20 μM pesticides (Methyl Parathion, bentazone and carbendazim), were mixed with 20 μM IMI, respectively. The results showed that

the influence of interfering ions and pesticides on IMI detection is negligible. Therefore, the prepared SDPC/GCE sensor has a strong anti-interference to IMI detection.

5.3 Detection of IMI in vegetable samples and evaluated by HPLC

5.3.1 Determination of IMI by electrochemical sensor based on SDPC in vegetable samples

In order to investigate the practicability of the SDPC/GCE sensor, the standard addition method was used to quickly detect IMI in tomato and cucumber sample(Zambianco, Silva, Zanin, Fatibello-Filho, & Janegitz, 2019). Three different concentrations of standard IMI solutions were added to the actual samples (tomato and cucumber). As can be seen from **Table 5-3**, the recovery rates of the two actual samples are between **92.6% and 108%**, and the **RSD is between 1.67% and 4.63%**, showing strong practicability.

Table 5-3 Recovery measurements of IMI in actual samples (n = 3)

Actual samples	IMI spiked (μM)	IMI found (μM)	Recovery (%)	RSD (%)
Tomato	0.5	0.47	94	2.46
	2	1.95	97.5	4.2
	5	4.94	98.8	3.95
lettuce	0.5	0.48	96	4.45
	2	2.16	108	1.67
	5	4.63	92.6	4.63

5.3.2 Determination of IMI by HPLC in vegetable samples

A method for determination of IMI residues in vegetables by HPLC was established, and the chromatographic conditions for sample extraction, purification and detection were optimized. As we known, the matrix is complex in vegetables, and there are many interference factors compared with low pesticide residue. In this part, the chromatographic conditions of acetonitrile as extractant, acetonitrile: water

(90:10) as mobile phase and ultraviolet detection wavelength of 270 nm were finally determined after lots of experimental exploration.

Under the optimum Chromatographic conditions, a series of standard solutions with different concentrations of IMI were prepared for determination. The standard spectrum of IMI (concentration is 10 μ M) is shown in **Fig. 5-10**. Then draw the standard curve of mass concentration according to the peak area of each component. The results show that the linear range of IMI was 0.2~30 μ M, the standard curve equation was $y = 6281x + 94.003$, and the correlation coefficient is 99.97%. It can meet the needs of quantitative analysis.

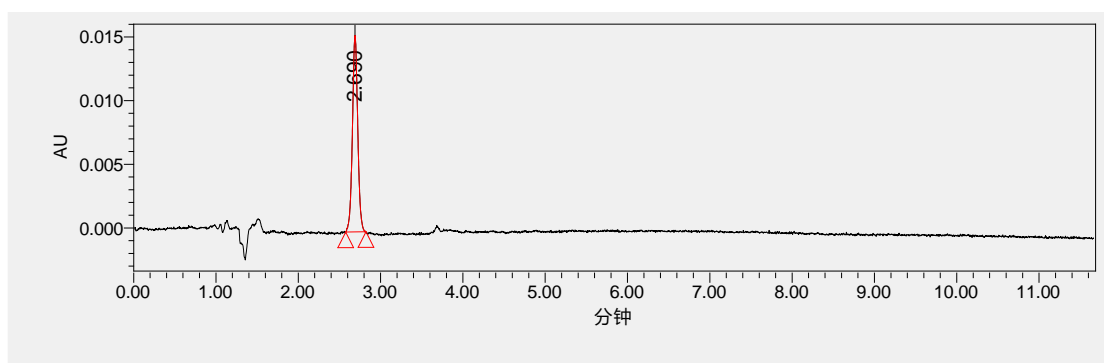


Fig. 5-10. HPLC chromatogram of IMI standard (10 μ M)

Quechers (Quick, Easy, Cheap, Effective, Rugged and Safe) was applied to the pretreatment of two kinds of vegetables, and PSA and GCB were finally selected as the purifying agents for sample pretreatment. **Fig. 5-11** and **Fig. 5-12** were respectively the control check chromatogram and spiked chromatogram of tomato sample. The relative standard deviation and spiked recovery results were shown in the **Table 5-4**. The recoveries rate and RSD of tomato and lettuce were in the range of 87.38%~114.12% and 1.38~2.62 respectively.

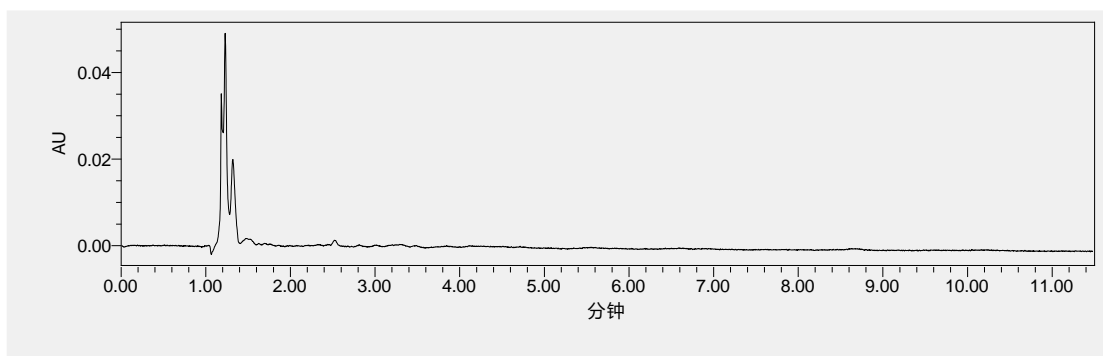


Fig. 5-11. The control check Chromatogram of tomato sample

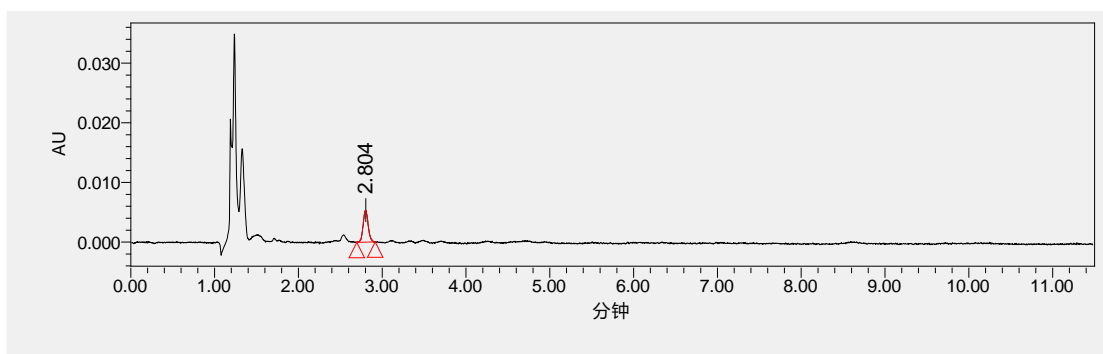


Fig. 5-12. The spiked chromatogram of tomato sample

Table 5.4 Determination of spiked recovery rate of vegetable samples

Vegetable sample	Added(μM)	Found(μM)	Recovery (%)	RSD (%)
Tomato	0.5	0.46	91.67	2.42
	2	1.73	86.48	2.61
	5	4.18	83.59	2.33
lettuce	0.5	0.46	91.67	2.42
	2	1.73	86.48	2.62
	5	45.82	91.64	1.38

5.3.3 Comparative evaluation on electrochemical sensor based on SDPC and HPLC for IMI detection in Vegetables

According to the above experimental results, both the electrochemical sensor detection method based on SDPC and the HPLC method realized the actual detection of IMI residue in vegetable samples, and the recovery rates were 92.6%~108% and 83.59~91.67 respectively. On one hand, the latter recovery rate is slightly lower, indicating that matrix effect of vegetable pretreatment still interferes

with HPTC experiment, but there are less effect in sensor detection. On the other hand, the RSD of HPTC method are all low then 3%, showing HPLC is relatively stable. Therefore, the electrochemical sensor detection method based on SDPC is a feasible tool for the IMI residues detection in vegetables, and provides the possibility for the realization of on-site detection of plant products due to its simple and fast operations.

5.4 Conclusion in section 5

Biomass-derived porous carbon possessed abundant low-cost biomass carbon source. Soybean-derived porous carbon (SDPC) with three-dimensional (3D) interconnected porous structure was prepared by using the expired soybean as carbon source through a high-temperature carbonization process. SDPC was used to modify the glassy carbon electrode (GCE) for the fabrication of SDPC/GCE sensor towards imidacloprid (IMI). The 3D interconnected porous structure of SDPC significantly improved the electrical conductivity and good absorption capability for IMI due to the interconnected carbon conductive network and large specific surface area. Under the optimal conditions, the fabricated SDPC/GCE sensor exhibited a low LOD value (5.18 μM) in wide IMI linear concentration range of 0.5-50 μM . The good practical feasibility can be obtained at the fabricated sensor for the detection of IMI in tomato and cucumber samples.

From the comparison of two sets of experiments results, the detection of IMI residues based on SDPC/GCE sensor was basically consistent with the HPTC method, and the recovery rate is even higher than HPTC method, indicating that the new electrochemical sensor method was relatively accurate. In addition, the sensor method was simple and fast to operate, providing the possibility of realizing the convenient field detection of pesticide residues.

SECTION 6 DETERMINATION OF METHYL PARATHION IN VEGETABLES BY ELECTROCHEMICAL SENSOR BASED ON SUPERCONDUCTIVE CARBON BLACK@ ZIRCONIA AND EVALUATED BY HIGH PERFORMANCE LIQUID CHROMATOGRAPHY

Excessive pesticides residues of agricultural products usually produce serious negative impact on food safety. It is of great significance to detect the pesticide residues in agricultural products, fruits, and vegetables to ensure the food safety and good health (Castilla-Fernandez, Moreno-Gonzalez, Gilbert-Lopez, Garcia-Reyes, & Molina-Diaz, 2021; H. Zhao, B. Li, et al., 2021; H. Y. Zhao et al., 2021). Methyl parathion (MP) is an organic pesticide with molecular formula of $C_8H_{10}O_5NPS$. As an organic phosphorus insecticide, MP can inhibit the activity of cholinesterase in the nervous system of pests, which promotes the wide application of this pesticide in agricultural production activities (H. Zhao, Liu, et al., 2020; H. Zhao, H. Ma, et al., 2021). However, MP is one kind of highly toxic organic phosphorus insecticide (Acute toxicity LD50 value: 14-24 mg/kg for rats; 300-400 mg/kg for rabbits). The great toxicity of MP residue seriously endangers food safety and human health. Therefore, MP is prohibited in the plantation and production of vegetables and fruits. Unfortunately, some farmers illegally use this pesticide to achieve a good harvest due to the excellent insecticidal effect. Thus, in order to protect food safety and human health, it is essential to achieve the efficient and sensitive detection of MP residue.

Compared with traditional technologies, electrochemical sensor has attracted more and more attention because of its advantages of high detection efficiency, low detection cost and real-time monitoring. Among them, Sensor electrode modification materials play an important role in improving sensor detection performance (Ye, Gu, & Wang, 2012). Superconductive carbon black (SCB) has high conductivity and can accelerate electron transfer on the electrode surface (J. Yang & Liang, 2011). Zhou et al. (X. F. Zhou, He, Wang, Zheng, & Suye, 2015)

prepared a novel composite membrane modified electrode by electropolymerization of poly (3, 4-ethylenedioxythiophene) (PEDOT) and superconducting carbon black (SCB) on a gold electrode. Pedot-scb /Au electrode has excellent electrocatalytic oxidation ability for ascorbic acid. Under optimal conditions, the current detection of ascorbic acid showed a good linear relationship in the range of 1.0×10^{-7} to 8.0×10^{-4} M, with a detection limit of 5.0×10^{-8} M (S/N = 2).

In addition, zirconia (ZrO_2) nanoparticles are also widely used in electrochemical sensors. ZrO_2 has strong adsorption capacity for phosphate groups, which makes the electrochemical sensor constructed based on ZrO_2 have good molecular recognition and adsorption performance for MP (Y. Dai et al., 2017; N. Gao et al., 2019; H. Y. Zhao et al., 2015). In particular, nano-structured ZrO_2 material has a large specific surface area, which is conducive to further improve the adsorption performance of the material. ZrO_2 has high chemical stability and non-toxicity, which is also the reason for its wide application. According to research reports, the synergistic effect of carbon material and ZrO_2 nanoparticles can significantly improve the detection performance of MP (H. B. Wang et al., 2015; H. Zhao, B. Li, et al., 2021; H. H. Zhou et al., 2019). Wang et al. (H. B. Wang et al., 2015) developed a sensitive electrochemical sensor based on zirconia (ZrO_2) nanoparticle modified electrode for the detection of organic phosphoric pesticides. Organophosphorus Pesticides can strongly bind to the surface of ZrO_2 nanoparticles (ZrO_2 NPs) due to the strong affinity between ZrO_2 and phosphate groups. Omethoate (an OP compounds) was detected under optimized operating conditions at an absorbance of 5 minutes, which showed a wide detection range from 98.5 pM/L to 985nM /L, and the detection limit is 52.5 pM /L. Dai et al.(Y. Dai et al., 2017) successfully synthesized an electrochemical sensor embedded with ZrO_2 nanoparticles and Carbon nanofibers. The sensor makes full use of the molecular recognition and enrichment ability of ZrO_2 nanoparticles for phosphate groups, as well as the advantages of graphene's high conductivity and large specific surface area, and significantly improves the detection performance of MP. These results

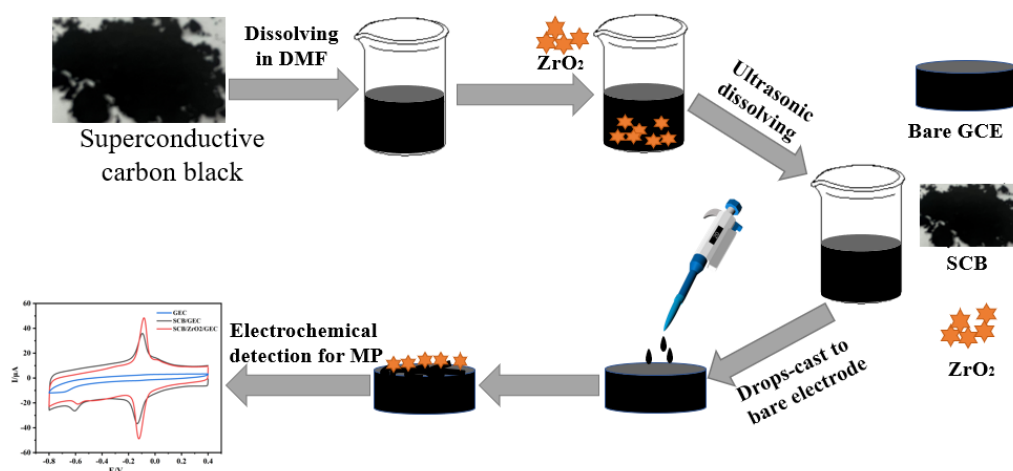
indicate that the combination of carbon materials and ZrO_2 nanoparticles has synergistic effect and can give full play to the advantages of both. Carbon materials with nano structure have a large specific surface area, showing good adsorption, which is conducive to further improve the electrochemical performance of the sensor.

In this section, the $\text{SCB@ZrO}_2/\text{GCE}$ electrochemical sensor is constructed to modify glassy carbon electrode, and the synergistic effect of SCB and ZrO_2 combination is fully utilized to improve the detection performance of the sensor, providing a new method for efficient and sensitive detection of MP.

6.1 Materials and Preparation Methods for electrochemical sensor

6.1.1 Fabrication of $\text{SCB@ZrO}_2/\text{GCE}$ sensor

A certain amount of SCB was weighed and dispersed in DMF, and the concentration of 0.5 mg/ml SCB dispersion was obtained by ultrasonic for 15 minutes. By taking 5 μL of SCB dispersed droplets and coating them on the pretreated glassy carbon electrode with a pipette, the SCB/GCE electrode was prepared. Then, 120mg nanometer zirconia particles were weighed and added to the SCB dispersion. SCB@ZrO_2 suspension was obtained by ultrasonic for 30 minutes. The $\text{SCB@ZrO}_2/\text{GCE}$ electrochemical sensor was obtained under the drying condition of the infrared lamp. The preparation process is shown in **Scheme 6-1**.



Scheme 6-1 The preparation process of $\text{SCB}/\text{ZrO}_2/\text{GCE}$ and MP determination

6.2.2 Detection method of SCB@ZrO₂/GCE Sensor for MP

An electrolytic cell was selected, with 10 mL PBS solution with pH 7.0 into it, and then add a certain amount of MP solution with the help of pipette. Before MP electrochemical detection, the composite electrode should be concentrated in PBS solution for a certain time. MP was measured by CV and DPV.

6.2 Experimental results and analysis of electrochemical sensor detection

6.2.1 Microstructure and morphology of SCB@ZrO₂

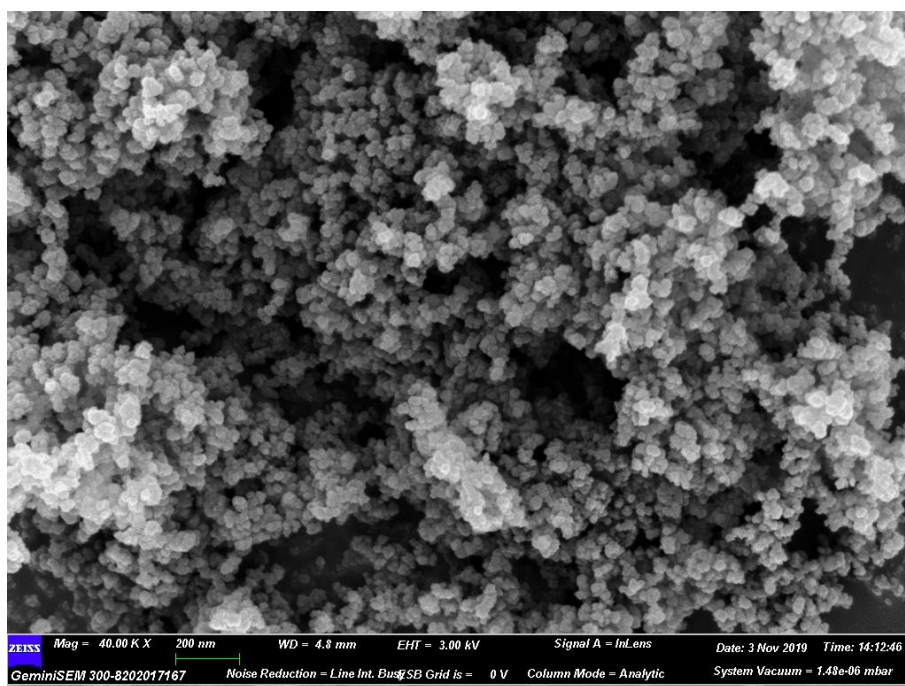


Fig. 6-1 SEM image of the SCB@ZrO₂ nanocomposite.

Fig. 6-1 shows the SEM images of the SCB@ZrO₂ nanocomposite. As can be seen, the SCB@ZrO₂ nanocomposite presents uniform particle size distribution. Since SCB nanoparticles and ZrO₂ nanoparticles have similar particle sizes, no obvious difference can be observed in the SEM image. The uniform distribution of SCB nanoparticles and ZrO₂ nanoparticles can help to achieve the functional combination of their respective advantages. SCB nanoparticles present good conductivity property based on the point-point contact of conductive carbon nanoparticles, and ZrO₂ nanoparticles present good recognition and enrichment ability towards MP due to the high affinity of ZrO₂ nanoparticles for the phosphate

groups on MP molecules. The modification of the SCB@ZrO₂ nanocomposite on GCE surface may improve the MP detection performance.

6.2.2 Electrochemical characterization

To investigate the electrochemical performance of SCB@ZrO₂, the assembled sensor was subjected to CV in a solution containing 5 mM [Fe(CN)₆]^{3-/4-} of 0.3 mM KCl. As shown in Fig.6-2, a pair of reversible REDOX peaks appeared on the unmodified electrode, which was consistent with the research results(Runqiang Liu et al., 2019). The SCB/GCE sensor also showed an obvious pair of reversible REDOX peaks, mainly due to the high conductivity of SCB(Jia et al., 2020). In addition, the electrode modified by SCB and ZrO₂ also showed obvious REDOX peak and high response current, which is due to the large specific surface area and fast electron transfer rate of SCB and ZrO₂ composites. This indicates that the SCB@ZrO₂/GCE sensor has excellent electrochemical performance.

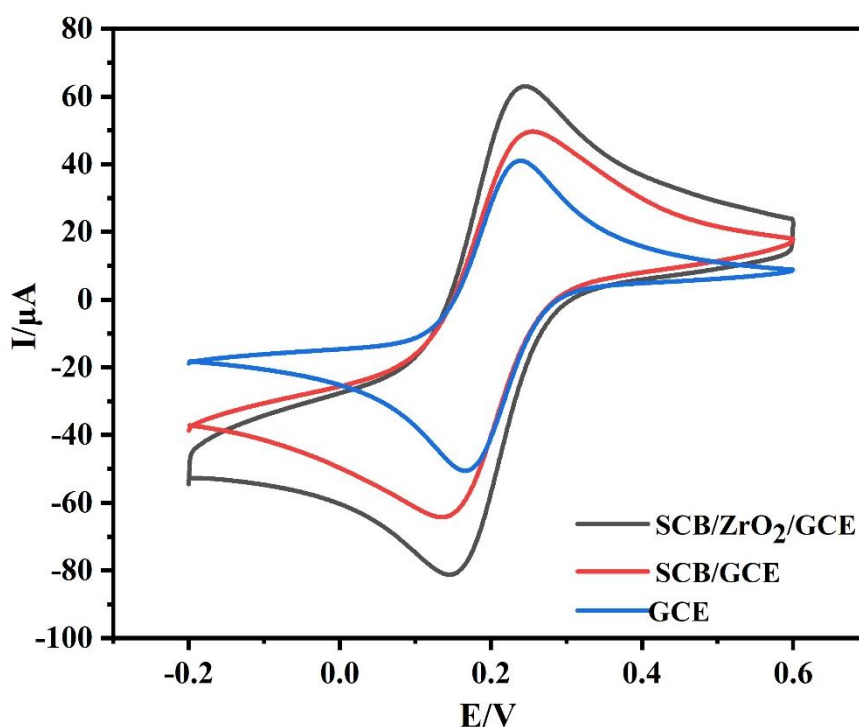


Fig.6-2 CV curves of GCE, SCB/GCE and SCB/ZrO₂/GCE in 5 mM K₃[Fe(CN)₆]/K₄[Fe(CN)₆] solution containing 0.3 M KCl at a scan rate of 20 mV s⁻¹

6.2.3 Electrochemical behavior of MP

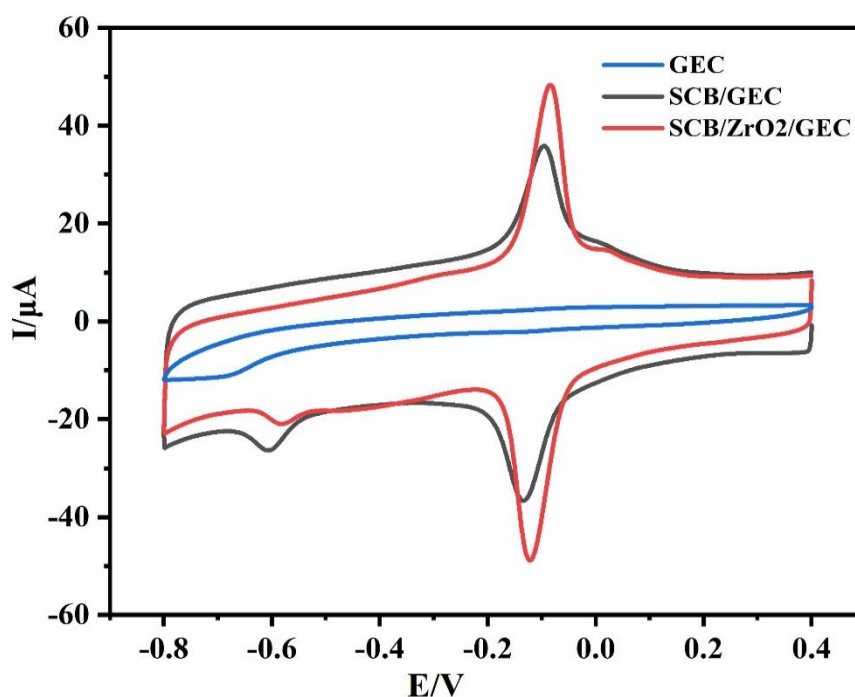


Fig. 6-3 CV curves of GCE, SCB/ GCE and SCB/ZrO₂/GCE in the presence of 50 μM MP in 0.1 M PBS (pH =7.0)

As shown in **Fig.6-3**, the detection results of the GCE sensor don't show an obvious REDOX peak, which means that the bare GCE sensor has certain deficiencies in detecting MP. In contrast, there is an irreversible reduction peak and a pair of reversible REDOX peaks on the CV of SCB/GCE sensor and SCB@ZrO₂/GCE sensor. The irreversible reduction peak is mainly attributed to the reduction of nitro group to hydroxylamine (Thota & Ganesh, 2016), while the REDOX peak in pairs corresponds to the reversible REDOX reaction between nitro group and hydroxylamine (B. A. Huang, Zhang, Chen, & Yu, 2010). The reaction mechanism is shown in **Fig.6-4**. It can also be seen from **Fig.6-3** that the peak current corresponding to the SCB/GCE sensor is significantly improved, which mainly benefits from the high conductivity of SCB. When SCB and ZrO₂ are co-modified on the surface of glassy carbon electrode, the assembled SCB @ZrO₂/GCE sensor shows better electrochemical response, mainly because SCB has high conductivity and large specific surface area, and ZrO₂ has strong adsorption of

phosphate groups(Z. H. Bi et al., 2019; J. X. Li et al., 2019; X. L. Niu et al., 2021). The co-modification of SCB and ZrO₂ resulted in synergistic effect, which resulted in better MP detection performance of the assembled electrochemical sensor.

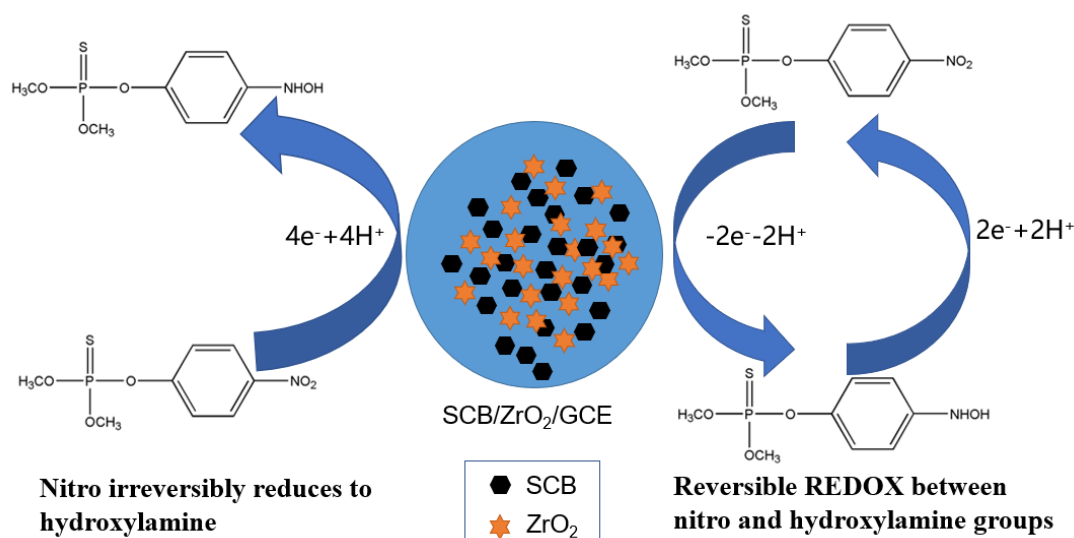


Fig.6-4 The redox reaction mechanism of MP at SCB/ZrO₂/GCE sensor

6.2.4 Optimization of detection conditions

In order to obtain more excellent MP detection performance, the experimental conditions were optimized, including material drip-coating amount, scan rate, accumulation time, pH of buffer solution(F. Li et al., 2022b).

6.2.4.1 The material drip-coating amount

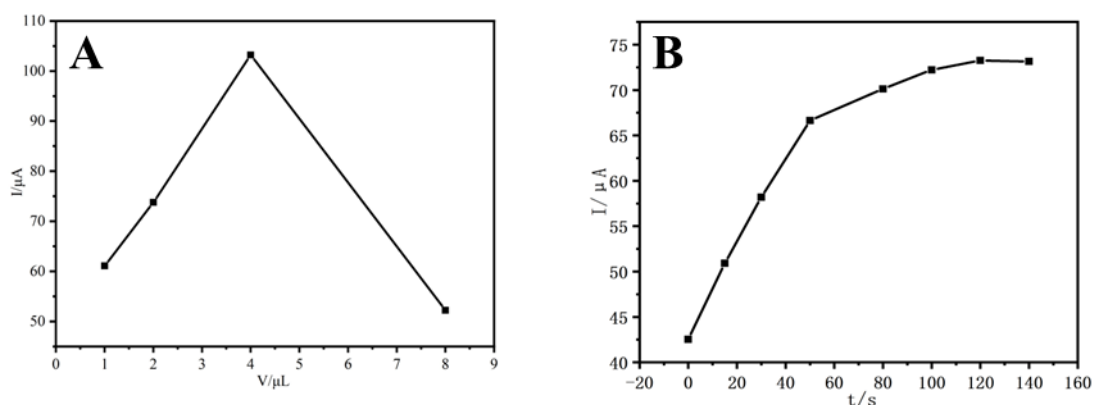


Fig.6-5 (A)Effect of drip-coating amount; (B) Effect of accumulation time on anodic peak current

The drip-coating amount of SCB@ZrO₂ on the electrode is directly related to the adsorption capacity of MP on the electrode surface and the rate of electron transfer. Therefore, the electrode surface was dripped with 1,2,4,8uL composite materials in MP with a concentration of 20μM/L. As shown in **Fig.6-5(A)**, the electrochemical signal increased with the increase of the dosage, but when the amount of modified material is too much, the modified film is easy to fall off from the electrode surface, thus affecting the stability of the electrode. Therefore, the electrode surface was modified with 4μL SCB@ZrO₂ in the experiment.

6.2.4.2 Scan rate

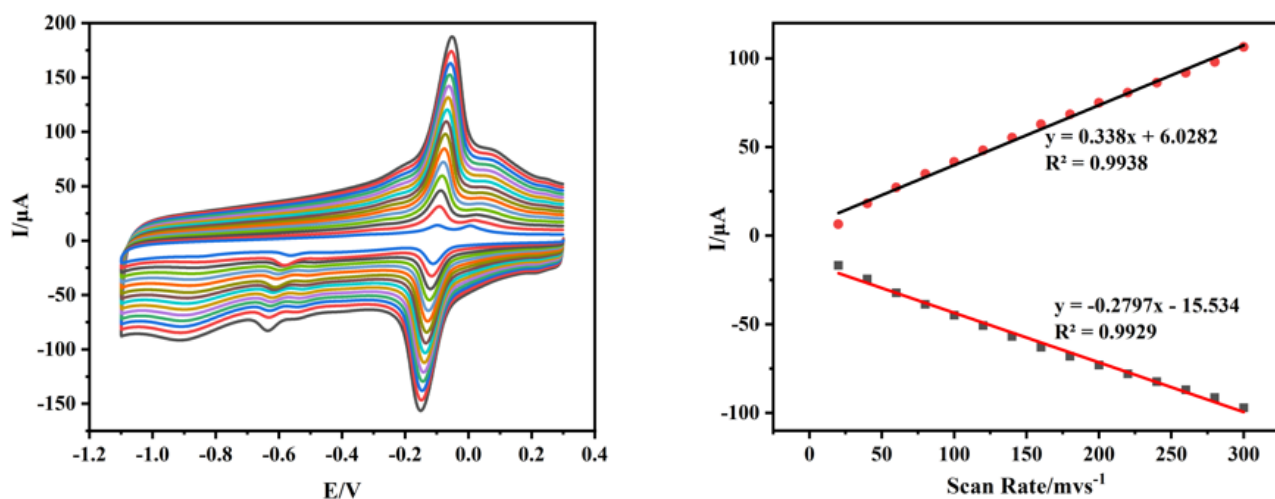


Fig.6-6 Influence of scan rate on the electrochemical behavior of MP at the SCB@ZrO₂/GCE sensor (scan rates range: 20-300 mV s⁻¹). (B) the linear relationship between scan rate and oxidation peak current value

In order to investigate the electrochemical behavior of MP molecules on the modified electrode surface, CV tests were carried out at different scan rates. As shown in the **Fig.6-6**, when the scan rate increases from 20mV/s to 300mV/s, the REDOX peak currents gradually increase, and the spike potential almost remain unchanged. Oxidation peak current (I_{pc}) and reduction peak current (I_{rc}) were plotted with scan rate respectively, and the linear fitting curves were obtained as shown in **Fig 6-6(B)**. The linear regression equations are: $I_{pc} = 0.338x +$

$6.0282(R^2 = 0.9938)$ and $I_{rc} = -0.2797x - 15.534(R^2 = 0.9929)$, and peak current I and scan rate x (mV/s) can present a good linear relationship in the range. This indicates that the reaction of MP on the electrode surface is a surface adsorption control process.

6.2.4.3 Accumulation time

Fig.6-5(B) shows the influence of accumulation time on the peak current response of MP detected by SCB@ZrO₂/GCE sensor. The SCB@ZrO₂/GCE sensors were immersed in a solution of 20 μM MP and accumulated for 15, 30, 50, 80, 100, 120 and 140 s, respectively. As can be seen from **Fig.6-5(B)**, with the increase of accumulation time, the peak current response gradually increased, then peak current response reached the maximum when accumulation time at 120s. Finally, As the accumulation time increases, the response peak current remain stable. Therefore, 120s was chosen as the best accumulation time.

6.2.4.4 pH

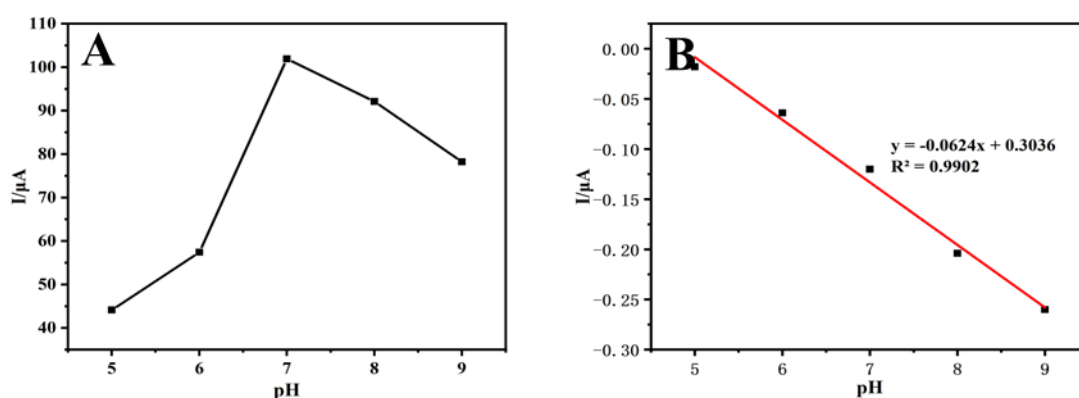


Fig.6-7(A) Effect of pH value on the peak current;(B). Effect of pH value on the peak potential.

Under the above optimal conditions, DPV was used to study the pH systematically, and pH range was set from 5 to 9. As shown in **Fig.6-7(A)**, when pH is between 5 and 7, the peak current response gradually increases with the increase of pH. When pH is 7, the peak current reached the maximum, and then the peak

current response decreases when pH continues to increase, which may be due to the accelerated degradation of MP in alkaline environment. Therefore, the optimal pH of this experiment is 7. In addition, the anode peak potential (E_{pa}) is linearly proportional to pH value (**Fig.6-7(B)**). The corresponding linear regression equation is $E_{pa} = -0.0624pH + 0.3036 (R^2 = 0.9902)$, and the absolute value of the slope is 62.4 mVpH^{-1} , which is very close to the theoretical value of 58.5 mVpH^{-1} . This indicates that the number of proton and electron transfers during the oxidation reaction of MP is equal.

6.2.5 Analytical performance of SCB@ZrO₂/GCE sensor

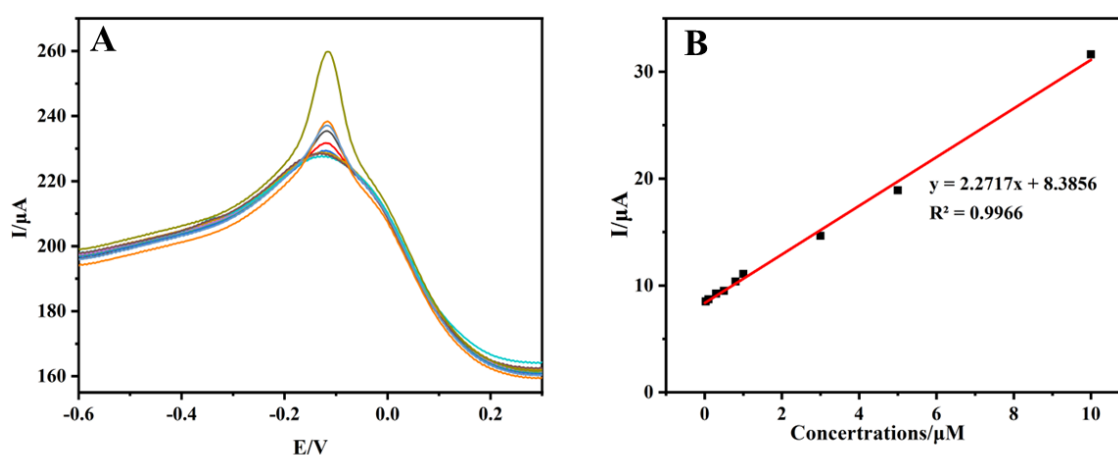


Fig. 6-8 (A) DPVs for determination different concentrations of MP (0.03, 0.1, 0.3, 0.5, 0.8, 1, 3, 5, 10 μM) at SCB@ZrO₂/GCE. (B) Linear relationship between peak current and MP concentration.

In this experiment, DPV method was used to explore the quantitative detection of MP by SCB@ZrO₂/GCE sensor. **Fig. 6-8(A)** showed the peak current response of different concentrations of MP on the SCB@ZrO₂/GCE sensor under optimal conditions. When the concentration of methyl parathion is between 0.03 and 10 μM , the peak current response has a good linear relationship with the concentration of MP, and the corresponding linear equation is: $y = 2.2717x + 8.3856 (R^2 = 0.9966)$. and the LOD is 0.016 μM (S/N=3). Compared with the sensors that have been reported publicly, as show as **Table 6-1**, the SCB@ZrO₂/GCE sensor

assembled in this work shows good MP detection performance, this is mainly due to the good adhesion, high conductivity and large specific surface area of SCB@ZrO₂ nanocomposites to organophosphorus pesticides, which play an important role in the efficient and sensitive detection of MP.

Table 6-1. Comparison the performance of different MP electrochemical sensors

Electrode	Analytical method	LOD (μM)	Linear range (μM)	References
Hal-WCNTs/GCE	DPV	0.034	0.5–11	(H. Zhao, H. Ma, et al., 2021)
ZrO ₂ NPs/Au	DPV	11.4	0.076-0.532	(M. Wang & Li, 2008)
SCB@ZrO ₂ /GCE	DPV	0.016	0.03-10	This work

6.2.6 Reproducibility, repeatability, and anti-interference

In order to improve the practicability of SCB@ZrO₂/GCE sensor, the reproducibility, stability and anti-interference of SCB@ZrO₂/GCE sensor are further discussed by using DPV method. In order to reduce the detection error, five identical SCB@ZrO₂/GCE sensors were fabricated by the same method, and the reproducibility and repeatability was investigated by the continuous detection of 1 μM MP. **Table 6-2** shows the relative standard deviation (RSD) of 3.69% for five independent measurements of SCB@ZrO₂/GCE sensors and 4.51% for five consecutive measurements using the same SCB@ZrO₂/GCE sensor. The low RSDS confirmed the excellent reproducibility and repeatability of the prepared SCB@ZrO₂/GCE sensor.

Table 6-2 The reproducibility of the SCB/ZrO₂/GCE sensor for MP detection.

	I ₁ / μA	I ₂ / μA	I ₃ / μA	I ₄ / μA	I ₅ / μA	RSD/%
The five sensors	10.66	11.76	11.18	11.31	11.09	3.69
The same sensor	11.19	12.21	11.45	11.98	12.13	4.51

The anti-interference has an important influence on the detection performance of the

constructed sensor. In this section, some common inorganic ions and pesticides with similar structure were selected as disruptors, i.e., interfering ions (Ag^+ , Ca^{2+} , Ni^{2+} and Zn^{2+}) with concentrations of $100 \mu\text{M}$ and pesticides (imidacloprid, diachronium, paraquat and niclosamide) with concentrations of $10 \mu\text{M}$ were mixed with $10 \mu\text{M}$ MP, respectively. The results showed that the influence of interfering ions and pesticides on MP detection was negligible, as **Fig.6-9**. Therefore, the prepared $\text{SCB@ZrO}_2/\text{GCE}$ sensor has strong anti-interference for MP detection.

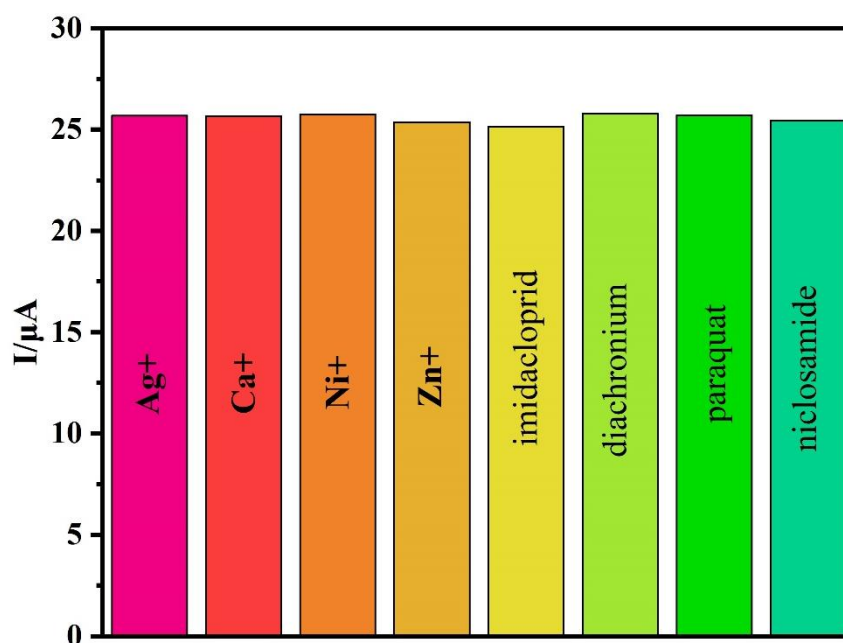


Fig.6-9 Anti-interference of the proposed the $\text{SCB@ZrO}_2/\text{GCE}$ sensor

6.3 Detection of MP in vegetable samples and evaluated by High Performance Liquid Chromatography

6.3.1 Determination of MP by electrochemical sensor based on SCB@ZrO_2 in vegetable samples

The application performance of $\text{SCB@ZrO}_2/\text{GCE}$ sensor to detect MP in lettuce and tomato samples was studied. Firstly, a certain amount of lettuce and tomato were washed, weighed, juiced and centrifuged, then the supernatant was extracted. The collected supernatant was diluted with PBS solution. Then, the MP standard solution was added into lettuce and tomato samples by standard addition method, and the recovery amount of each sample was measured three times to get its

average value. As shown in **Table 6-3**, the recoveries of MP in lettuce samples ranged from 95.33%-103.5% with lower RSDS of 3.2%-5.37%, while those of cucumber sample's recovery rates ranged from 102.67%-104.33%,with RSDS of 1.12%-3.88%. The results show that the proposed SCB@ZrO₂/GCE sensor can be used for the accurate determination of MP in real samples.

Table 6-3 The SCB/ZrO₂/GCE sensor for the detection of MP in lettuce and tomato samples.

Vegetable sample	Added(μM)	Recovery (%)	RSD (%)
lettuce	0.5	95.33%	3.2
	1	103.5%	3.83
	2	96.58%	5.37
Cucumber	0.5	102.67%	1.12
	1	103.50%	3.17
	2	104.33%	3.88
Tomato	0.5	104.67%	2.92
	1	106.83%	1.18
	2	105.17%	5.32

6.3.2 Determination of MP by HPLC

A method for determination of MP residues in vegetables by HPLC was established, and the chromatographic conditions for sample extraction, purification and detection were optimized. As we known, the matrix is complex in vegetables, and there are many interference factors compared with low pesticide residue. In this part, the chromatographic conditions of acetonitrile as extractant, methanol: water (73:27) as mobile phase and ultraviolet detection wavelength of 270 nm were finally determined after lots of experimental exploration.

Under the optimum Chromatographic conditions, a series of standard solutions with different concentrations of MP were prepared for determination. The standard spectrum of MP(concentration is 10μM) is shown in **Fig. 6-10**. Then draw the standard curve of mass concentration according to the peak area of each component.

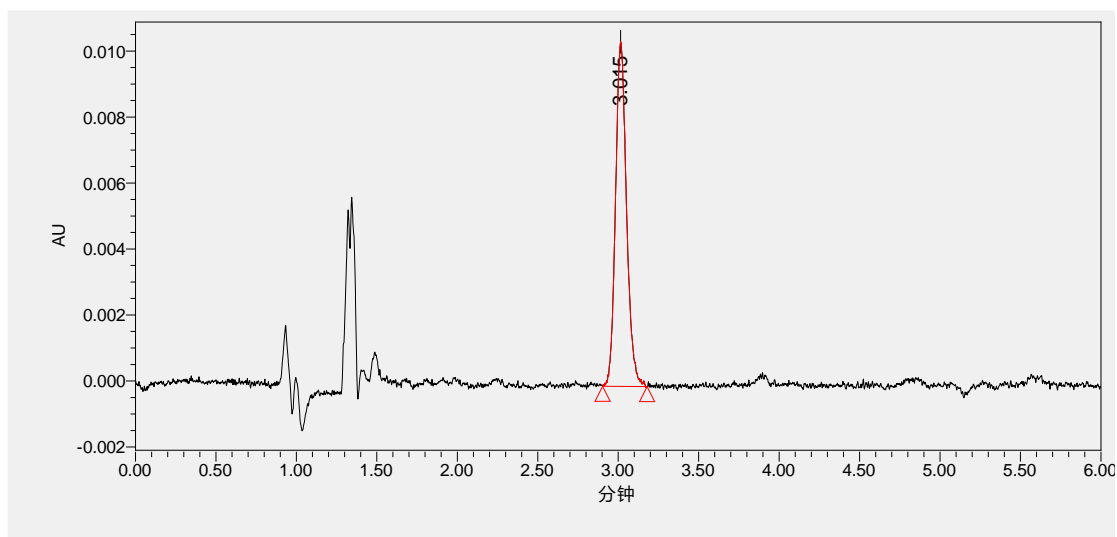


Fig. 6-10. HPLC chromatogram of MP standard (10 μ M)

Quechers (Quick, Easy, Cheap, Effective, Rugged and Safe), a new technology developed internationally in recent years, was applied to the pretreatment of two kinds of vegetables, and PSA and GCB were finally selected as the purifying agents for sample pretreatment. **Fig. 6-11** and **Fig. 6-12** were respectively the control check chromatogram and spiked chromatogram of cucumber sample. The relative standard deviation and spiked recovery results were shown in the **Table 6-4**. The recoveries rate and RSD of cucumber, lettuce and Potato were in the range of 87.38%~114.12%.

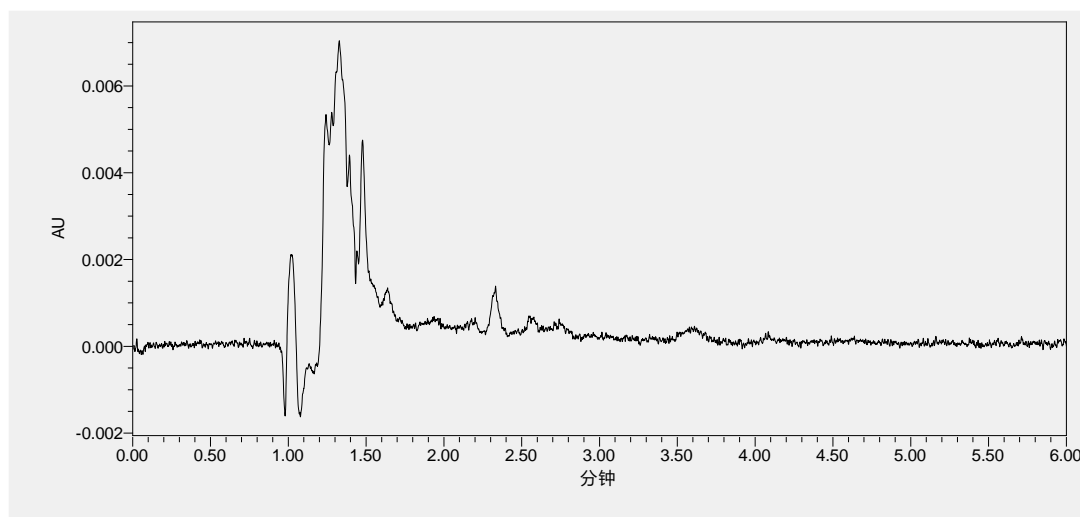


Fig. 6-11. The control check Chromatogram of cucumber sample

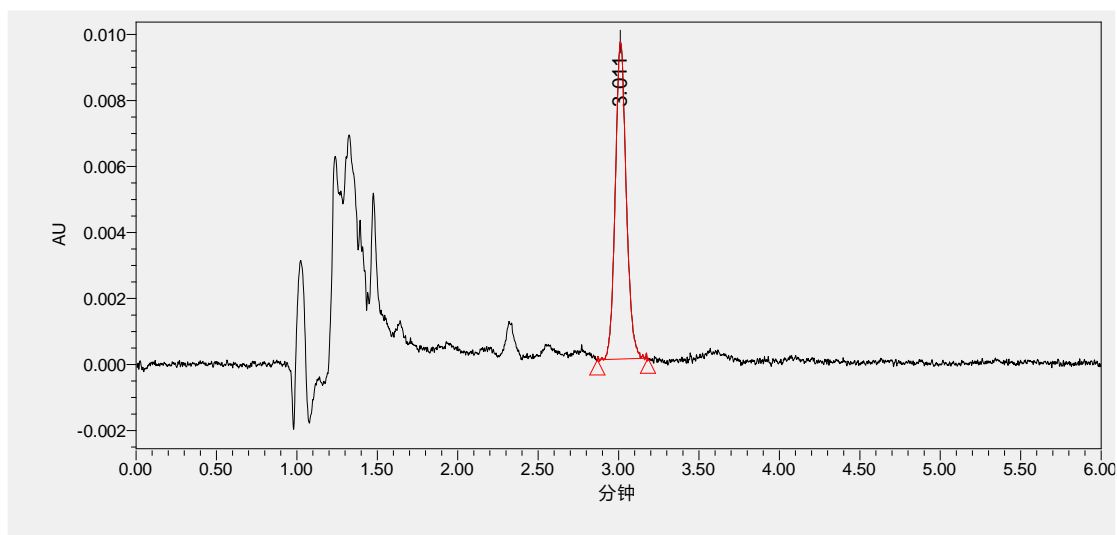


Fig. 6-12. The spiked chromatogram of cucumber sample

Table 6-4 Determination of spiked recovery rate of vegetable samples

Vegetable sample	Added(μM)	Recovery (%)	RSD (%)
lettuce	0.5	109.84%	2.61
	2	114.11%	4.2
	8	103.3%	1.72
Cucumber	0.5	102.23%	6.2
	2	108.58%	3.51
	8	104.82%	2.89
Tomato	0.5	89.67%	2.47
	2	87.38%	4.86
	8	90.31%	5.83

6.3.3 Comparative evaluation on electrochemical sensor based on SCB@ZrO₂ and HPLC for MP detection in Vegetables

According to the above experimental results, both the electrochemical sensor detection method based on SCB@ZrO₂ and the HPLC detection method realized the actual detection of MP residue in vegetable samples, and the recovery rates were 95.33%~106.83% and 87.38%~109.84% respectively. This indicates that the new electrochemical sensor method is relatively accurate and reliable, and can be used as an alternative method for detecting MP residues in vegetable samples. In addition, the electrochemical sensor is simple and fast to operate, which provides the possibility for the realization of on-site detection of plant products.

6.4 Conclusion in selection 6

The pesticide electrochemical detection performance can be improved based on the synergistic effect of nanocomposite sensitizer. The multifunctional nanocomposite of superconductive carbon black (SCB) and ZrO_2 was prepared by a simple and efficient ultrasound-assisted strategy. The SCB@ZrO_2 nanocomposite was used to modify the glassy carbon electrode (GCE) for the fabrication of $\text{SCB@ZrO}_2/\text{GCE}$ sensor towards methyl parathion (MP). SCB nanoparticles showed high electrical conductivity, which promoted the efficient charge transport, and ZrO_2 nanoparticles possessed strong affinity towards the phosphorus groups of MP, which enhanced the accumulation ability of MP. Under the optimal conditions, the fabricated $\text{SCB@ZrO}_2/\text{GCE}$ sensor exhibited a low LOD value ($0.016 \mu\text{M}$) in MP linear concentration range of $0.03\text{-}10.0 \mu\text{M}$. The good practical feasibility can be obtained at the fabricated sensor for the detection of MP in vegetable samples (lettuce, Cucumber and Tomato). The experimental results comparison between electrochemical sensor method and HPLC method showed that the detection of MP residue based on the electrochemical sensor method was basically consistent with the HPTC method, indicating that the new electrochemical sensor method was relatively accurate and reliable. In addition, the sensor method was simple and fast to operate, providing the possibility of realizing the convenient field detection of pesticide residues.

SECTION 7 DETERMINATION OF METHYL PARATHION IN VEGETABLES BY ELECTROCHEMICAL SENSOR FABRICATED FROM BIOMASS-DERIVED AND B-CYCLODEXTRIN FUNCTIONALIZED POROUS CARBON SPHERES AND EVALUATED BY HIGH PERFORMANCE LIQUID CHROMATOGRAPHY

Methyl parathion (MP) residues will cause serious damage to human life and health and ecological environment. Therefore, it is of great practical significance to increase the research on MP detection technology and develop a simple, low-cost, and efficient MP detection technology.

Nowadays, several traditional analysis methods (HPLC, LC-MS, GC/MS) play an important role in analyzing the MP residue, but these approaches have unavoidable weaknesses, which include the complicated measurement operation, lengthy analysis period, and expensive analysis cost (Azzouz, Colon, Souhail, & Ballesteros, 2019; L. Chen, Dang, Ai, & Chen, 2018; Mouskeftara, Virgiliou, Iakovakis, Raikos, & Gika, 2021). By contrast, electrochemical sensors have received increasing attention due to the simple professional operation, cheap analysis cost, and high detection efficiency (F. Li et al., 2022a; H. Zhao, Ran, et al., 2020). In order to rigorously analyze the MP residue, many efforts were devoted to design the novel sensing electrodes and optimize the modification sensing materials (Govindasamy, Mani, Chen, Chen, & Sundramoorthy, 2017b; Y. Li et al., 2021; H. Zhao, H. Ma, et al., 2021). According to the existing literature (Silva Junior et al., 2021; Tian et al., 2018; Yue, Han, Zhu, Wang, & Zhang, 2016; H. Zhou et al., 2019), the MP detection performance of electrochemical sensors can be optimized by means of modification materials such as carbon materials, conducting polymer, metallic oxides, noble metals, etc. Yue et al. successfully prepared the carbon nanotube/carbon paper composite by chemical vapor deposition (CVD) method (Yue et al., 2016). The modified GCE sensor showed satisfactory limit of detection (LOD) of 3.9 ng mL⁻¹. Pan et al. reported the fabrication of ordered mesoporous

carbon modified glassy carbon electrode, which achieved the good electrochemical determination of MP by linear sweep voltammetry (LSV) with a low LOD value of 7.6 nM in the MP concentration range of 0.09-61 μM (Pan, Ma, Bo, & Guo, 2011). Xue et al. fabricated a MIP-based sensor by using nitrogen doped graphene sheets, which presented good MP determination performance (Xue et al., 2014). Based on these analyses, carbon materials are hypothesized to have significant role in the improvement of MP detection performance. It is important to note, however, that the above-mentioned carbon materials usually possess complex synthesis process and high production cost. Therefore, it is definitely necessary to develop the low-cost carbon materials with simple preparation technology and good electrochemical performance.

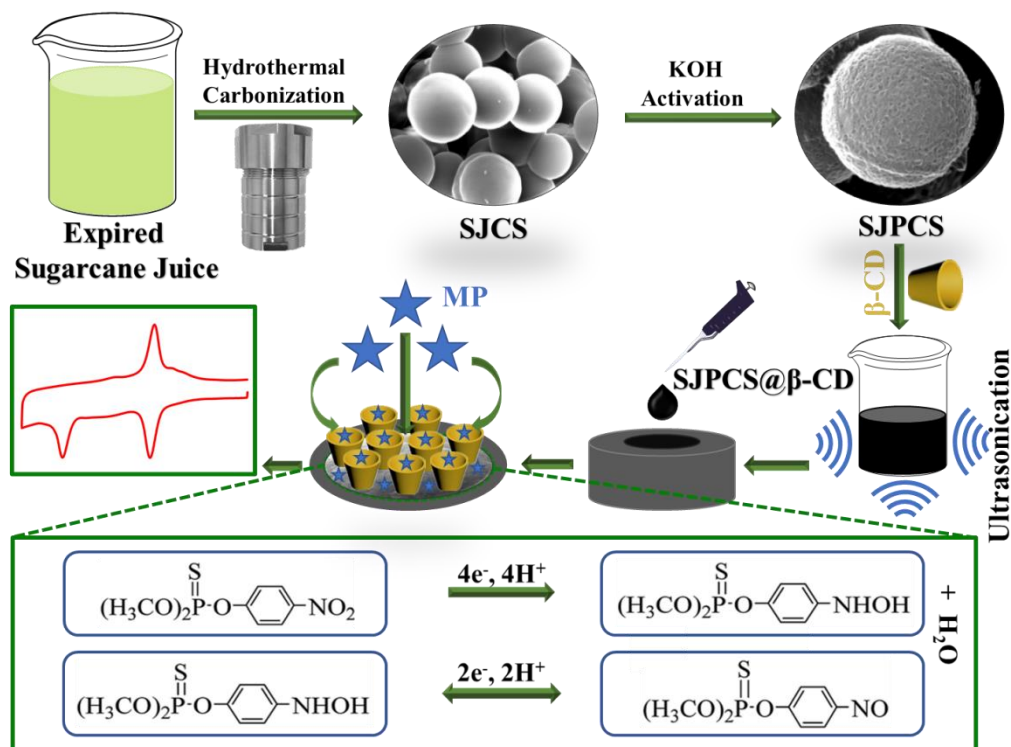
In recent years, biomass-derived porous carbon materials have attracted extensive interest because of abundant carbon source and low production cost. This type of porous carbon materials with interconnected carbon skeleton structure have been widely used in the fields of adsorption, catalysis, electrochemical sensors, and energy storage (Z. Bi et al., 2019; D. Chen et al., 2017; J. Li et al., 2019; F. Tang, Wang, & Liu, 2019). Chen et al. successfully prepared the nitrogen doped hierarchical porous carbon through the carbonization process with pig lung as carbon source (D. Chen et al., 2017). The modified GCE sensor has wide linear ranges (0.5-320, 0.5-340 and 1-360 μM) and low detection limits (0.078, 0.057 and 0.371 μM) for the catechol, resorcinol and hydroquinone, respectively. Mahmood et al. reported the synthesis of porous graphene based on the biomass precursor of kraft lignin and cellulose nanofibers, which achieved the good electrochemical determination of dopamine with a LOD value of 3.4 μM (F. Tang et al., 2019). Niu et al. fabricated the Au nanoflakes decorated porous carbon with three-dimensional interconnected frameworks by using banyan leaves as carbon source. The prepared sensor presented good luteolin determination performance with a LOD value of 0.07 μM (3S0/S) in the linear luteolin concentration ranges of 0.15-1.8 μM and 1.8-10.0 μM based on the differential pulse voltammetry (DPV) (X. Niu et al., 2021). Zhang

et al. synthesized the biomass-derived microporous carbons by high-temperature activation technology with kiwi skin as carbon source (W. Zhang et al., 2018). When used for the determination of ascorbic acid, the constructed sensing platform showed good electrochemical sensing performance (LOD: 0.02 μM). These results demonstrate that biomass-derived porous carbon materials may have very important value and potential for the MP electrochemical detection.

According to the existing works (R. Liu et al., 2019; Yao et al., 2014), β -cyclodextrin (β -CD) with seven glucose units present hydrophilic external cavity and hydrophobic inner cavity. The former can promote the uniform dispersion of carbon materials due to the good hydrophilic properties of the primary hydroxyl group of C_6 , and the latter possesses good molecular recognition ability, which can promote the recognition and adsorption of MP molecule. Yao et al. constructed an carbon matrix composite sensor by using the β -CD modified single-walled carbon nanotubes, which realized very high sensitive detection of MP (Yao et al., 2014). Furthermore, it has been reported that the β -CD dispersed graphene modified electrochemical sensor showed very low detection limit for the determination of MP due to the strong π - π interaction, rapid accumulation, and high electrical conductivity (Wu et al., 2011). These results suggest the constructive role of β -CD in the design of high-performance MP electrochemical sensor.

In this work, we synthesized the expired sugarcane juice-derived three-dimensional porous carbon spheres (SJPCS) based on the combination strategy of hydrothermal method and high-temperature KOH activation. The β -cyclodextrin (β -CD) functionalized SJPCS were employed to fabricate the SJPCS@ β -CD/GCE sensor towards the MP determination (**Scheme 7-1**). For the SJPCS@ β -CD composite, SJPCS with interconnected porous structure exhibits excellent electrical conductivity, strong adsorption property, and high specific surface area, while β -CD with molecular recognition property achieves the uniform dispersion of SJPCS and promotes the recognition and adsorption of MP molecules at the 3DSJPCS@ β -

CD/GCE sensor. Thanks to the synergistic combination of SJPCS and β -CD, the SJPCS@ β -CD/GCE sensor presented good MP determination performance.



Scheme 7-1. Preparation of the SJPCS@ β -CD composite and schematic of the SJPCS@ β -CD/GCE sensor for the determination of MP.

7.1 Materials and Preparation Methods for electrochemical sensor

7.1.1. Preparation of nanocomposites SJCS

All the chemical reagents and materials were used directly without further purification treatment. The expired sugarcane juice-derived carbon spheres (SJCS) were prepared via a hydrothermal synthesis process. One hundred and fifteen ml of expired sugarcane juice was directly added into hydrothermal synthesis reactor (150 ml), which was then sealed and maintained at 160 °C for 20 h. After cooling the reactor to ambient temperature, the obtained carbonaceous material was washed by filtration with deionized water and absolute ethanol to obtain the SJCS sample. To achieve the three-dimensional porous structure, both the SJCS sample and KOH activator were mixed uniformly in the mass proportion of $m_{\text{KOH}}:m_{\text{C}}=6:1$. The mixed powder was maintained at 800 °C in tubular furnace with argon atmosphere, and the

high-temperature activation time was 2 h. After 3M HCl acidification and thorough water washing treatment, the expired sugarcane juice-derived three-dimensional porous carbon spheres (SJPCS) was obtained by drying the activated carbon material at 105 °C for 10 h in air.

7.1.2. Fabrication of SJPCS@ β -CD sensor

The as-synthesized SJPCS (15 mg) was firstly dispersed in the dimethylformamide solvent (mSJPCS:Vdimethylformamide=3/4) under ultrasonic treatment. After 60 mins of ultrasonication, β -CD (10 mg) was added into the above SJPCS dispersion. After 30 mins of ultrasonication, the obtained homogeneous suspension was filtered and washed by deionized water to obtain the SJPCS@ β -CD composite. The bare GCE was polished with alumina powders followed by ultrasonic cleaning treatment. To prepare the SJPCS@ β -CD/GCE sensor, the as-synthesized SJPCS@ β -CD composite (10 mg) was uniformly re-dispersed in the dimethylformamide solvent. After ultrasonic dispersion for 30 mins, the obtained SJPCS@ β -CD suspension (5 μ L) was measured out by micro pipette and further dropped on the surface of the polished GCE. After drying for 15 mins with the aid of infrared lamp, the SJPCS@ β -CD/GCE sensor was obtained for the electrochemical measurements.

7.2. Experimental results and analysis of electrochemical sensor detection

7.2.1. Microstructure and morphology of SJPCS

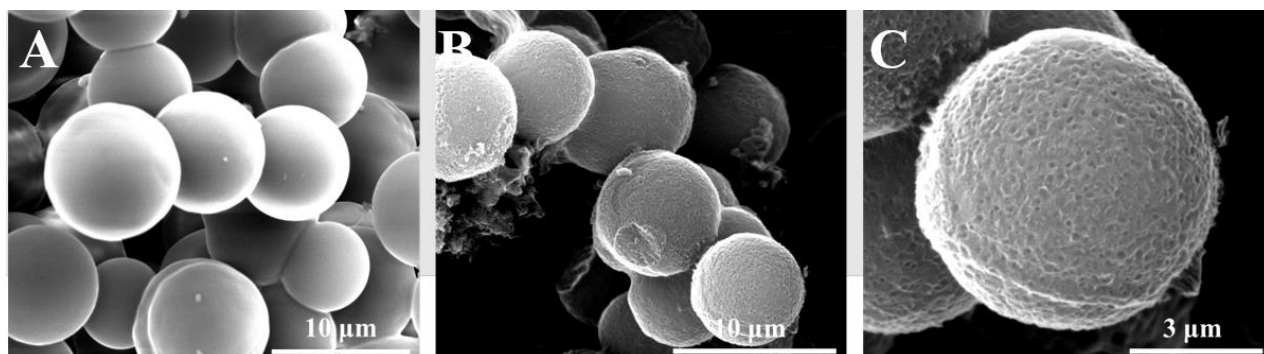


Fig. 7-1. (A) SEM image of SJCS synthesized by hydrothermal method, (B-C) SEM image.

The surface morphologies of the as-synthesized SJCS and SJPCS samples were characterized by SEM technique. **Fig.7-1(A)** displays the SEM image of the SJCS sample prepared by hydrothermal carbonization. The SJCS sample consists of many carbon spheres, which show very obvious three-dimensional spherical structure with relatively smooth surface. For the SJPCS sample shown in **Fig. 7-1(B-C)**, the surface morphology presents obvious difference compared to that of the SJCS sample, which has close association with high-temperature KOH activation treatment (Z. Bi et al., 2019; D. Chen et al., 2017). It can be seen that the SJPCS sample shows three-dimensional porous spherical structure. Compared with the SJCS sample, there are a great many of interconnected porous channels on the surface of the SJPCS sample. This porous structure effectively increases the specific surface area of carbon spheres, which can improve the adsorption property and surface accessibility towards the electrolyte (F. Li et al., 2022a; Y. Zhang et al., 2020; H. Zhao, Ran, et al., 2020). Moreover, the interconnected porous structure contributes to the efficient transport of ions and electrons, which can enhance the electrical conductivity (D. Chen et al., 2017; Z. Chen et al., 2021; X. Niu et al., 2021).

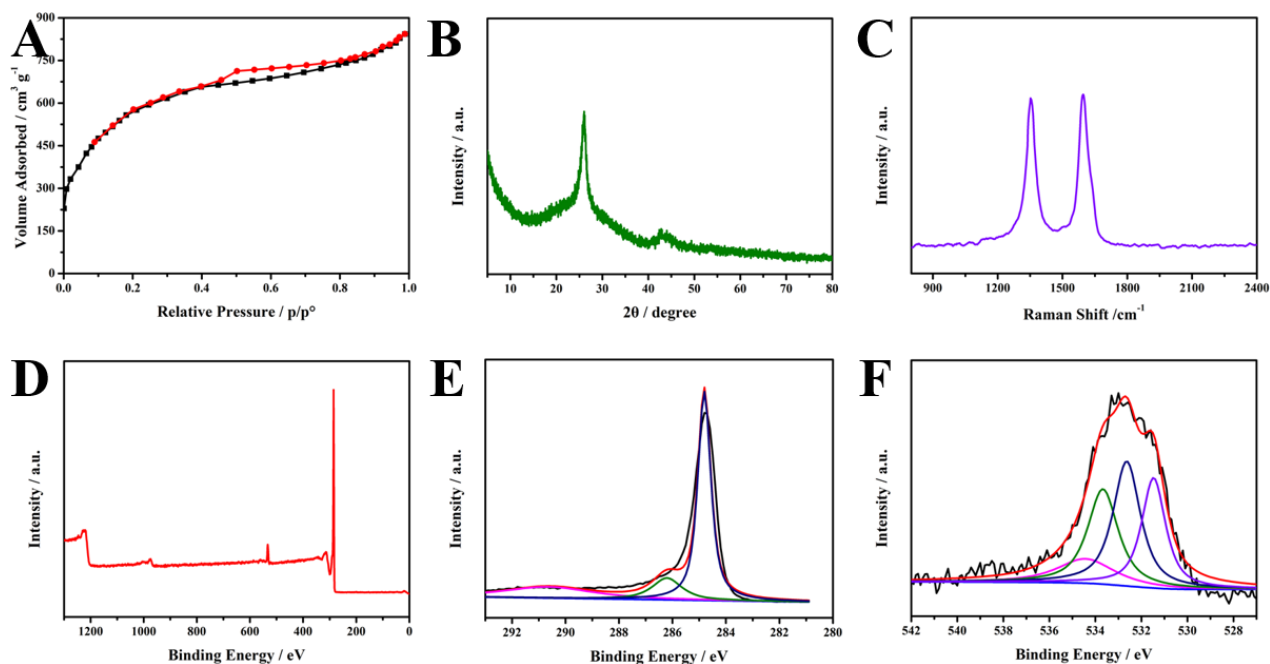


Fig. 7-2. (A) N₂ adsorption-desorption isotherms, (B) XRD pattern, (C) Raman spectrum, and (D-F) XPS result of SJPCS with porous structure after KOH activation ;

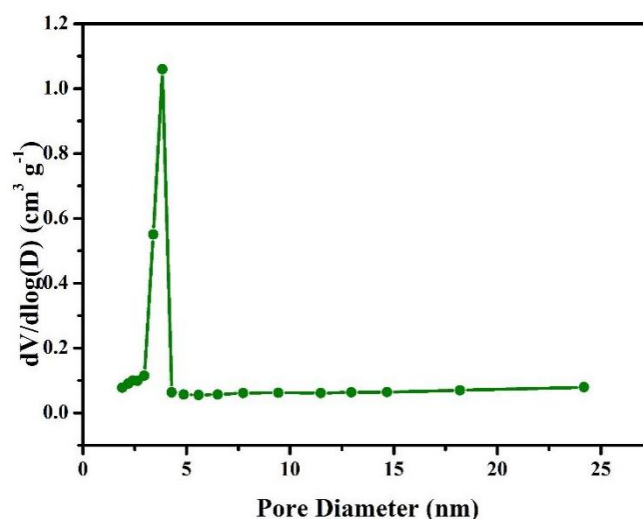


Fig. 7-3. Pore size distribution profile of the SJPCS sample.

Fig. 7-2A exhibits the nitrogen adsorption-desorption isotherms of the SJPCS sample. It can be found that the SJPCS sample presents a typical characteristic of type I isotherm with H4-type hysteresis loop (Marichi et al., 2020). The analysis result indicates that the SJPCS sample shows a very large BET surface area of $1365 \text{ m}^2 \text{ g}^{-1}$ with numerous mesopores in the structure, which can be observed in the pore size distribution profile shown in **Fig. 7-3**. This porous structure with large surface area and abundant mesopores is closely related to the activation effect and pore-forming function of KOH (Z. Bi et al., 2019; D. Chen et al., 2017; Shijie Wang, Wang, Zhang, Jin, & Zhang, 2018). **Fig. 7-2B** shows the XRD pattern of the SJPCS sample. After high-temperature KOH activation treatment, the obtained SJPCS sample presents obvious characteristic diffraction peaks of carbon materials. The diffraction peak corresponding to the (002) plane of the SJPCS sample appearing at a high diffraction angle because of the reduction of various functionalities in the KOH activation process. On the basis of the existing works (Marichi et al., 2020; S. Wang et al., 2018), the above diffraction peak at high diffraction angle suggests the high graphitization degree of carbon materials, which suggests a high electrical conductivity for SJPCS.

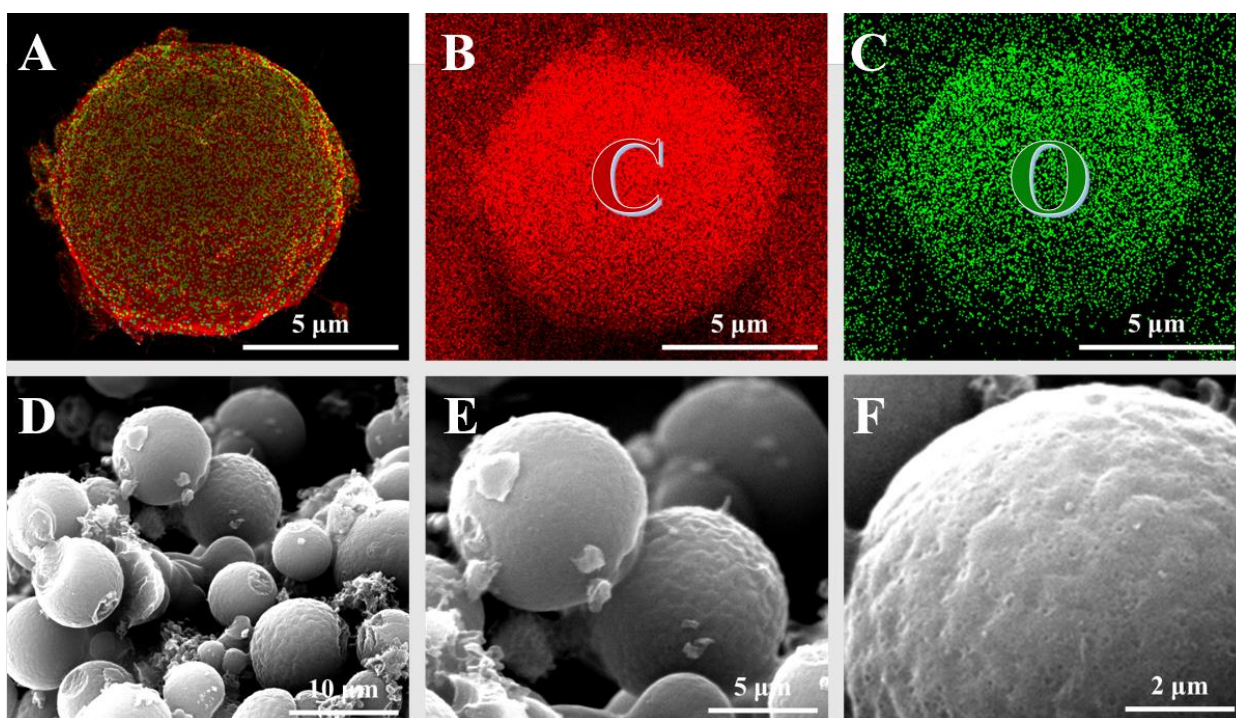


Fig. 7-4. (A-C) SEM mapping results and (D-F) SEM images of SJPCS@ β -CD obtained by ultrasound strategy.

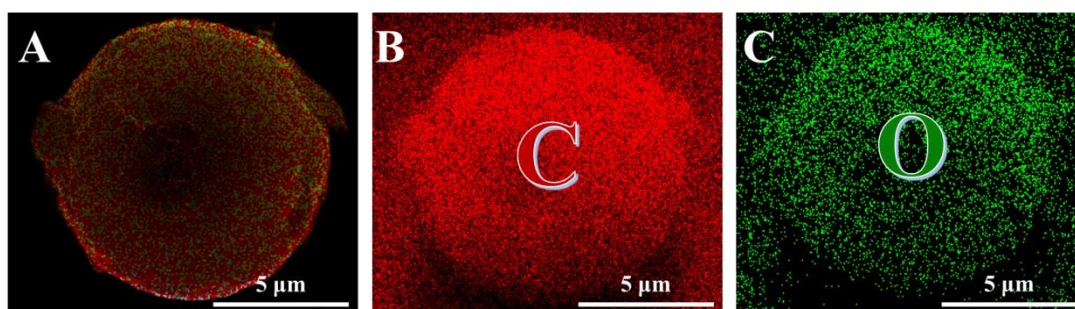


Fig. 7-5. SEM mapping results of SJPCS prepared by hydrothermal carbonization.

Table 7-1 Content ratio of O and C elements in the SJPCS and SJPCS@ β -CD samples.

Element	SJPCS		SJPCS@ β -CD	
	Wt%	At%	Wt%	At%
C	86.55	89.55	85.72	88.89
O	13.45	10.45	14.28	11.11
Sum	100.00	100.00	100.00	100.00

Fig. 7-2C shows the Raman spectroscopy of the SJPCS sample, which can be used to confirm the electronic properties of carbon-based materials. As shown here, the SJPCS sample presents two characteristic peaks at about 1352 cm^{-1} and 1596 cm^{-1} , which can be indexed as D-band and G-bands (F. Li et al., 2022a; H. Zhao, Liu, et al., 2020). It has been reported that D-band represents the presence of defective graphitic carbon with the vibration of sp^3 domains and G-band represents the graphitic carbon layers with the vibration of sp^2 -hybridized carbon atoms in carbon ring or hexagonal crystal (F. Li et al., 2022a; Marichi et al., 2020). These two characteristic peaks have close association with the disordered carbon and graphitic carbon. The $I_{\text{D}}/I_{\text{G}}$ value can reflect the defect degree of carbon-based materials. The high $I_{\text{D}}/I_{\text{G}}$ value of SJPCS indicates that there are more defects in the obtained porous carbon spheres with highly disordered carbon structure (Z. Chen et al., 2021; F. Li et al., 2022a). **Fig. 7-2D** shows the XPS survey spectrum of the SJPCS sample. It can be found that there are two obvious signature peaks in the XPS spectrum, which corresponds to the C1s and O1s, respectively. As shown in **Fig. 7-2E**, the C1s survey spectrum possesses three main characteristic peaks at 284.7, 286.2, and 290.6 eV, which represent C=C, C-C, and O-C=O groups (Marichi et al., 2020; S. Wang et al., 2018). For the O1s survey spectrum shown in **Fig. 7-2F**, the main characteristic peaks at 531.4, 532.6, 533.7, and 534.5 eV correspond to the O=C, C-O, C-O-C and O-C groups (Marichi et al., 2020; W. Zhou et al., 2014). **Fig. 7-4A, 4B and 4C** show the SEM mapping result of C and O in SJPCS@ β -CD, which can be used to further confirm the element distribution. The hybrid electronic image (**Fig. 7-4A**) presents the existence of C and O elements, which are completely in accord with the designed element composition. It can be observed from **Fig. 7-4(B and C)** that both C and O elements are evenly distributed in the SJPCS@ β -CD composite, which confirms the uniform decoration of β -CD on the surface of SJPCS. It is important to note that the content ratio of O and C elements in the SJPCS@ β -CD sample (O:C=11.11At%:88.89At%) was higher than that of the SPCS sample (O:C=10.45At%:89.55At%, **Fig. 7-5.** and **Table 7-1**),

which can be attributed to the oxygen-dominant β -CD (Balasubramanian, Annalakshmi, Chen, Sathesh, & Balamurugan, 2019; Xianlu Feng, Qiu, Dang, & Sun, 2021). This result can be further confirmed by the surface morphology of the SJPCS@ β -CD sample, as shown in **Fig. 7-4(D to F)**. It can be found that the surface of the SJPCS@ β -CD sample is a little bit different from that of the SJPCS sample (**Fig. 7-1C**), which is closely relevant to the decoration of β -CD. This phenomenon further suggests the successful formation of the SJPCS@ β -CD composite (F. Li et al., 2022a; H. Zhao, H. Ma, et al., 2021). For this composite, the decoration of β -CD helps achieve the uniform dispersion of SJPCS and promote the recognition and adsorption of MP molecule due to the good hydrophilic property and molecular recognition performance.

7.2.2. Electrochemical characterization

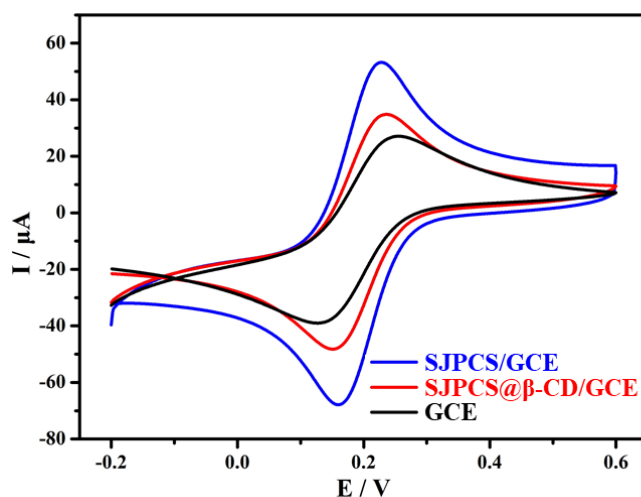


Fig. 7-6. CV measurement results of the unmodified GCE, SJPCS/GCE, SJPCS@ β -CD/GCE sensors.

Fig. 7-6 shows the CV measurement results of the unmodified GCE, SJPCS/GCE, SJPCS@ β -CD/GCE sensors, which was performed at the scan rate of 50 mV s^{-1} . It can be found that the unmodified GCE presents a relatively low peak current ($I_{\text{pa}}=27.1 \mu\text{A}$, $I_{\text{pc}}=-38.5 \mu\text{A}$). After the decoration of SJPCS on the surface of GCE, the obtained SJPCS/GCE sensor presents very obvious CV measurement result ($I_{\text{pa}}=53.2 \mu\text{A}$, $I_{\text{pc}}=-67.7 \mu\text{A}$), which can be attributed to the excellent electrical

conductivity of SJPCS with interconnected porous carbon structure that helps to promote the charge transport efficiency (Marichi et al., 2020; S. Wang et al., 2018). Moreover, the porous carbon structure of SJPCS provides large surface area, which contributes to the increased interfacial surface of electrolyte with GCE surface (Z. Bi et al., 2019; F. Li et al., 2022a). For the SJPCS@ β -CD/GCE sensor, the peak intensity of CV (I_{pa} =34.9 μ A, I_{pc} =-48.3 μ A) shows a slightly reduced CV characteristic, which has close association with the decoration of β -CD on the surface of SJPCS. The poor electrical conductivity of β -CD slightly weakened the charge transfer efficiency to a certain extent (Wu et al., 2011; Yao et al., 2014). However, it is important to note that both SJPCS/GCE and SJPCS@ β -CD/GCE sensors can lead to better electrochemical performance than that of the unmodified GCE sensor.

7.2.3. Electrochemical behavior of MP

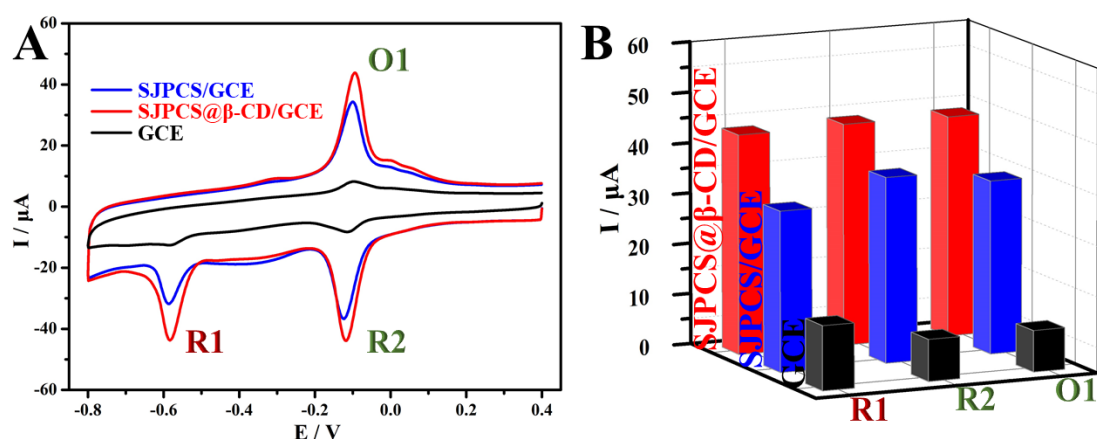


Fig. 7-7. (A) CV curves and (B) peak current bar charts of 50 μ M MP at the unmodified GCE, SJPCS/GCE, SJPCS@ β -CD/GCE sensors (pH of PBS solution is 7.0).

Fig.7-7A shows the CV measurement of 50 μ M MP at the unmodified GCE, SJPCS/GCE, SJPCS@ β -CD/GCE sensors, and the pH of the corresponding PBS solution is 7.0. These three sensors present quite obvious differences in terms of the peak current response, which is clearly reflected by the peak current bar charts (**Fig. 7-7B**). For the CV measurement results of MP, these three sensors show similar

peak characteristics with a pair of reduction-oxidation peaks and an individual reduction peak. According to the previously published results (H. Zhao, H. Ma, et al., 2021), the electrochemical conversion between nitro group and hydroxylamine group belongs to a four-electron irreversible reaction, which generated an irreversible reduction peak. For the subsequent reaction of hydroxylamine group, the two-electron electrochemical conversion is reversibly achieved between hydroxylamine group and nitroso group, which generated a pair of reduction-oxidation peaks. The peak current response has close association with the MP concentration. The unmodified GCE displays a relatively low peak current ($I_{O1-pa}=8.2 \mu A$, $I_{R2-pc}=-8.3 \mu A$, $I_{R1-pc}=-12.8 \mu A$), which suggests the poor MP determination performance. By contrast, the SJPCS/GCE sensor possesses a satisfactory CV measurement result with significantly enhanced peak current ($I_{O1-pa}=34.3 \mu A$, $I_{R2-pc}=-36.7 \mu A$, $I_{R1-pc}=-31.8 \mu A$), which mainly benefitted from the excellent electrical conductivity of SJPCS with interconnected porous carbon structure that helps to promote the charge transport efficiency (Marichi et al., 2020; S. Wang et al., 2018). Moreover, the porous carbon structure of SJPCS provides large surface area, which contributes to the increased interfacial surface of electrolyte with GCE surface (Z. Bi et al., 2019; F. Li et al., 2022a). These positive factors can effectively optimize the detection performance of MP. For the SJPCS@ β -CD/GCE sensor, the CV measurement result shows the highest peak current value ($I_{O1-pa}=43.7 \mu A$, $I_{R2-pc}=-43.9 \mu A$, $I_{R1-pc}=-43.5 \mu A$) compared to that of the unmodified GCE and SJPCS/GCE sensors, which is not synchronized with the sensing performance change shown in **Fig. 7-7**. According to the existing literature, β -CD possesses good molecular recognition ability, which can promote the recognition and adsorption of MP molecules at the fabricated sensors, and β -CD effectively contributes to the homogeneous dispersion of SJPCS with high electrical conductivity and high surface area (R. Liu et al., 2019; Yao et al., 2014). These functions are helpful to improve the enrichment ability of MP on the SJPCS@ β -CD/GCE electrode surface, which can compensate for the disadvantage of poor

electrical conductivity. Based on the above analysis, the fabricated SJPCS@ β -CD/GCE sensor is expected to show excellent MP determination performance, which is due to the synergistic combination of SJPCS and β -CD.

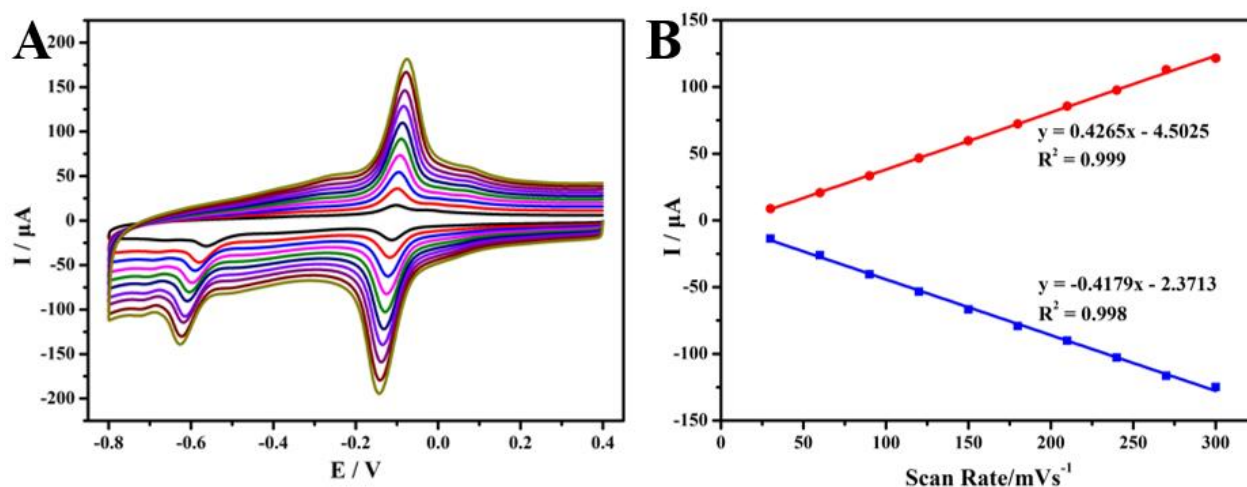


Fig. 7-8. (A) Effect of scanning rate on the CV curve of 50 μ M MP at the SJPCS@ β -CD/GCE sensor (Scanning rate: 30, 60, 120, 150, 180, 210, 240, 270, and 300 mV s^{-1}), and (B) fitting function relationship between peak current value and scanning rate.

Fig.7-8A shows the CV results of 50 μ M MP at the SJPCS@ β -CD/GCE sensor with the scan rates varied from 30 to 300 mV s^{-1} . The peak current value of the CV curve is related closely with the scan rate for the determination of MP. As the scan rate increased, the peak current value showed an increasing trend gradually. Based on the calculated results, the fitting function relationship of peak current value and scan rate is shown in **Fig. 7-8B**. The peak current value correlated linearly with the scan rate. In order to specifically describe this linear relationship, the fitting regression equations between peak current value and scan rate are calculated to be as follows: $I_{O1-pa}(\mu\text{A})=0.4265v-4.5025$ ($R^2=0.999$) and $I_{R2-pc}(\mu\text{A})=-0.4179v-2.3713$ ($R^2=0.998$). These values suggest an adsorption-controlled process of MP determination at the SJPCS@ β -CD/GCE sensor, which is completely in accordance with the previously reported research results (Govindasamy et al., 2017b; H. Zhao, H. Ma, et al., 2021).

7.3.5. The optimization of detection conditions

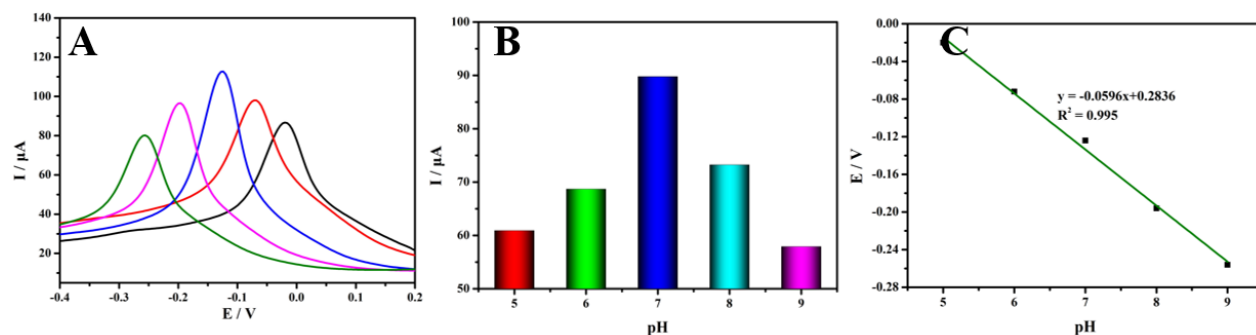


Fig. 7-9. (A) Effect of pH value of PBS solution on the DPV curve of 50 μM MP at the SJPCS@β-CD/GCE sensor (pH value: 5, 6, 7, 8, and 9), (B) effect of pH value on the peak current, and (C) fitting function relationship between pH value and peak potential.

Fig. 7-9A exhibits the DPV measurement results of 50 μM MP at the SJPCS@β-CD/GCE sensor in the PBS solution with different pH values. The anodic peak was trending to move towards the negative voltage as the pH value increased. Moreover, the corresponding peak current response was greatly affected by the pH value of PBS solution. When the pH value increased, the peak current response showed an increasing trend first and then a decreasing trend. The corresponding maximum peak current response can be obtained when the pH value is adjusted to 7.0. This phenomenon can be attributed to the fact that the acidity/alkalinity of PBS solution has a rather large influence on the electrochemical redox reaction. The strong acidic environment ($\text{pH} \leq 7.0$) can provide more H^+ ions, which severely restricted the reversible reaction from $-\text{NHOH}$ to $-\text{NO}$, while the strong alkaline environment ($\text{pH} > 7.0$) with only tiny amounts of H^+ ions causes much negative impact on the subsequent redox reaction of MP (H. Zhao, H. Ma, et al., 2021). The influence of pH value on the peak potential (E_p) can be further reflected by the fitting function relationship (**Fig. 7-9B**). As shown here in **Fig. 7-9C**, E_p is linearly correlated with the pH value. The corresponding mathematical relationship is $E_{\text{pa}} = -0.0596\text{pH} + 0.2836$ ($R^2 = 0.995$). The corresponding slope absolute value of 59.6 mV pH^{-1} is in good agreement with the theoretical absolute value of 58.5 mV pH^{-1} , which means the same amounts of electrons and protons in

the electrochemical conversion process of MP at the SJPCS@ β -CD/GCE sensor (Y. Li et al., 2021; Tian et al., 2018). The above analysis indicates that the electrochemical sensing determination of MP was deeply affected by the pH value of PBS solution.

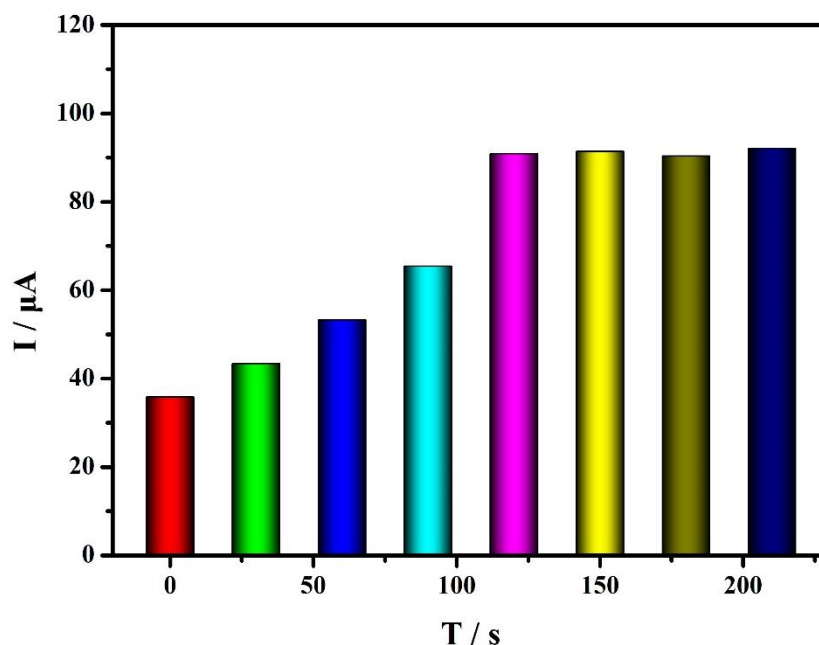


Fig. 7-10. Effect of accumulation time on the peak current value.

Fig. 7-10 shows the peak current responses of DPV measurement results of MP at the SJPCS@ β -CD/GCE sensor for different accumulation times. It can be found that the accumulation time presents a great influence on the determination performance of MP. When the accumulation time reached up to 120 s, the SJPCS@ β -CD/GCE sensor showed a higher peak current response. It is important to note that the corresponding peak current response remain stable without obvious change with the increasing of accumulation time. It is clear that there was not linearity correlation between peak current response and accumulation time, which is consistent with the existing literature (Xue et al., 2014; Yao et al., 2014; Hongyuan Zhao, Huina Ma, et al., 2021). According to the reported research results, the gradually increasing peak current response is closely associated with the adsorption quantity of MP at the SJPCS@ β -CD/GCE electrode surface with the increasing of the accumulation time. As the accumulation time increases further, the adsorption

quantity of MP reaches the saturation state, which can lead to the fact that the corresponding peak current response remain stable without obvious change. The above analysis indicates that the accumulation time of 120 s can be selected for the subsequent efficient electrochemical detection of MP at the SJPCS@ β -CD/GCE sensor.

7.3.6. Analytical performance of SJPCS@ β -CD/GCE

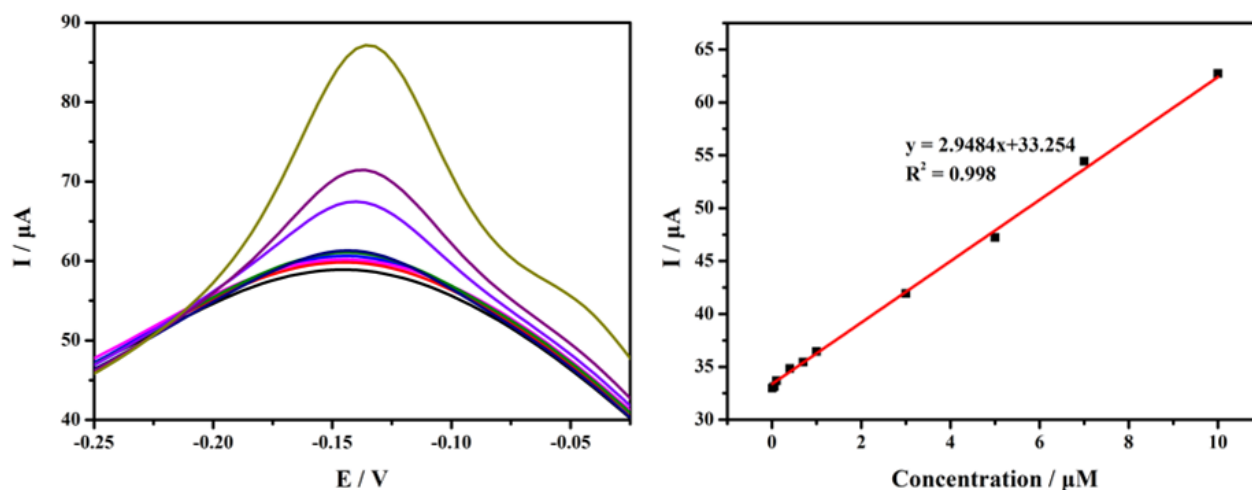


Fig. 7-11. Effect of MP concentration on the DPV curve (MP concentration: 0.01, 0.05, 0.1, 0.4, 0.7, 1.0, 3.0, 5.0, 7.0, and 10 μ M), and (H) fitting function relationship between peak current and MP concentration.

Fig. 7-11A shows the DPV measurement result of the SJPCS@ β -CD/GCE sensor towards the electrochemical determination of MP at different concentrations, which can be used to investigate the sensitivity of the fabricated sensor. With the increasing MP concentration (0.01-10 μ M), the peak current responses of DPV resulted in a gradual increasing trend. The influence of MP concentration on the peak intensity can be further reflected by the fitting function relationship (**Fig. 7-11B**). The fitting result indicates that the peak current response is linearly and positively correlated to the MP concentration with the corresponding equation of $I(\mu\text{A})=2.9484C+33.254$ ($R^2=0.998$). It has been reported that the limit of detection (LOD) can be calculated using the following equation of $\text{LOD}=3S/q$ (Yue et al., 2016; H. Zhao et al., 2021). For this calculation equation, “S” corresponds to the

standard deviation of the blank signal, and the corresponding denominator value “q” corresponds to the slope from the calibration plot. Based on the above experimental data and calculation formula, the calculation result shows that the limit of detection of MP at the SJPCS@ β -CD/GCE sensor can reach up to 5.87 nM in the linear concentration range of 0.01-10 μ M. **Table 7-2** shows the comparison of MP at the SJPCS@ β -CD/GCE sensor and other reported MP sensors. The fabricated SJPCS@ β -CD/GCE sensor shows a relatively low LOD compared to other reported MP sensors. Such excellent MP determination performance was mainly benefitted from the synergistic combination of SJPCS and β -CD. SJPCS with interconnected porous carbon structure helps to promote the charge transport efficiency (Marichi et al., 2020; S. Wang et al., 2018). Moreover, the porous carbon structure of SJPCS provides large surface area, which contributes to the increased interfacial surface of electrolyte with GCE surface (Z. Bi et al., 2019; F. Li et al., 2022a). These positive factors can effectively enhance the electron/ion transport efficiency in electrochemical sensing determination process. Apart from the advantages mentioned above, β -CD possesses good molecular recognition ability, which can promote the recognition and adsorption of MP molecules at the fabricated sensors, and β -CD with molecular recognition property achieves the uniform dispersion of SJPCS and promotes the recognition and adsorption of MP molecules at the 3DSJPCS@ β -CD/GCE sensor (R. Liu et al., 2019; Wu et al., 2011; Yao et al., 2014). These functions are helpful to improve the enrichment ability of MP on the SJPCS@ β -CD/GCE electrode surface. Thanks to the synergistic combination of SJPCS and β -CD, the fabricated SJPCS@ β -CD/GCE sensor realizes the highly sensitive determination of MP as reported here.

Table 7-2 Determination performance comparison of different MP sensors.

Electrode	Detection limit (nM)	Linear range (μM)	Reference
AuNPs/Nafion/GCE	100	0.5-120	(Kang, Wang, Lu, Zhang, & Liu, 2010)
Hal-MWCNTs/GCE	34	0.5–11	(H. Zhao, H. Ma, et al., 2021)
ZrO ₂ NPs/Au	11.4	0.076-0.532	(M. Wang & Li, 2008)
β -CD/MWCNTs/CP	9.12	0.037-53.2	(R. Liu et al., 2019)
Hal/ZrO ₂ /CB/GCE	5.23	0.01-10	(H. Zhao, H. Ma, et al., 2021)
SJPCS@ β -CD/GCE	5.87	0.01-10	This work

7.3.7. Reproducibility, repeatability, and anti-interference

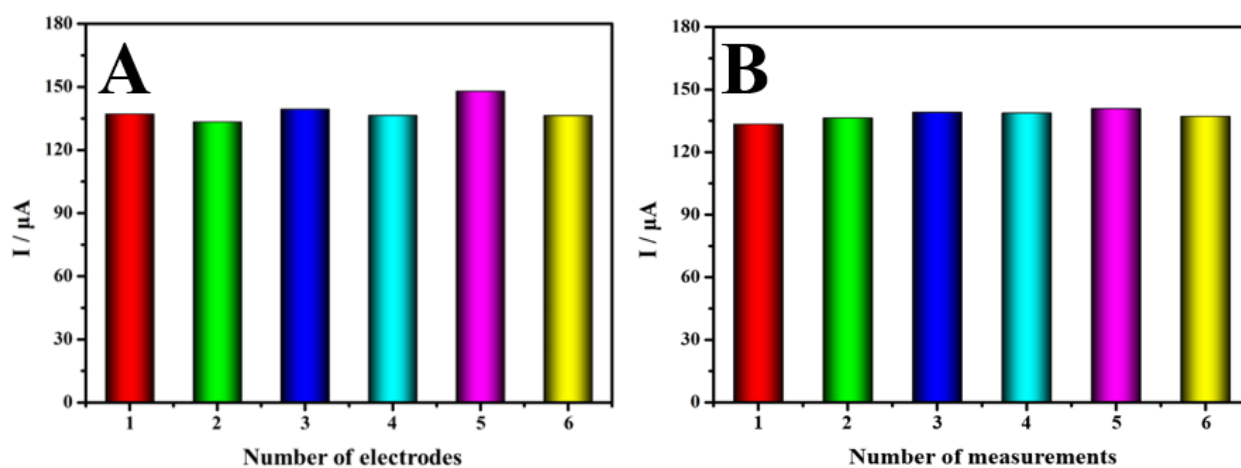


Fig. 7-12. (A) Reproducibility measurement of the SJPCS@ β -CD/GCE sensor; (B) Repeatability measurement of the SJPCS@ β -CD/GCE sensor.

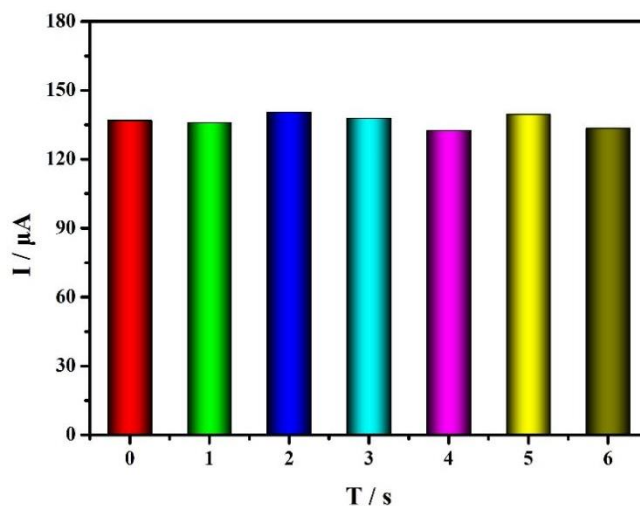


Fig. 7-13. Anti-interference measurement of the SJPCS@ β -CD/GCE sensor.

The reproducibility and repeatability are very important factors for the application of the SJPCS@ β -CD/GCE sensor. For the reproducibility measurement (**Fig. 7-12A**), there is not much difference between the peak current values of MP using different SJPCS@ β -CD/GCE sensors. The low relative standard deviation (RSD, 3.64%) suggests that a satisfactory reproducibility of the SJPCS@ β -CD/GCE sensor was achieved. In order to analyze the repeatability, one individual MP sensor was applied for the determination of peak current response of MP. **Fig. 7-12B** presents the repeatability of the SJPCS@ β -CD/GCE sensor. The peak value shows good consistency with desirable *RSD* of 1.89%, which indicates the satisfactory repeatability of the SJPCS@ β -CD/GCE sensor. **Fig. 7-13** exhibits the peak current responses of the DPV measurement result of MP at the SJPCS@ β -CD/GCE sensor toward the anti-interference measurement. The electrochemical determination performance of MP was not severely influenced after the introduction of other potential interfering ions (0.1 M PO_4^{3-} , 0.1 M SO_4^{2-} , 0.1 M $\text{C}_6\text{H}_7\text{O}_6^-$, 0.1 M K^+ , 0.1 M Ca^{2+} , 0.1 M Al^{3+}) and molecules (4-nitrophenol, methyl viologen, sucrose, glucose, polyphenol, and dichlorvos). The change of peak current response was less than 5% with no obvious influence, which suggests that a satisfactory Anti-interference of the SJPCS@ β -CD/GCE sensor was attained.

7.3 Detection of MP in vegetable samples and evaluated by High Performance Liquid Chromatography

7.3.1 Determination of MP by electrochemical sensor based on SJPCS@ β -CD in vegetable samples

Table 7-3 Practical feasibility of the SJPCS@ β -CD/GCE sensor.

Sample	MP spiked (μ M)	MP found (μ M)	Recovery (%)	RSD (%)
Onion	0.5	0.483	96.5	4.25
	2.0	2.003	100.2	2.09
	8.0	7.860	98.3	3.14
Cabbage	0.5	0.493	98.6	2.43
	2.0	1.963	98.2	4.12
	8.0	8.040	100.5	1.06
Spinach	0.5	0.496	99.3	1.37
	2.0	2.007	100.3	3.54
	8.0	7.930	99.1	2.52

Table 7-3 presents the practical measurement results of the SJPCS@ β -CD/GCE sensor with different vegetables (onion, cabbage, and spinach). It has been previously reported that the practical feasibility can be reflected by means of the recoveries and RSD values of the peak current responses of MP. As shown here, the SJPCS@ β -CD/GCE sensor shows an excellent MP detection performance of MP with desirable RSD of 1.06%-4.25% and high recoveries of 96.5-100.5%, which indicates the good practical properties of the SJPCS@ β -CD/GCE sensor for the MP determination in vegetables.

7.3.2 Determination of MP by HPLC

A method for determination of MP residues in vegetables by HPLC was established, and the chromatographic conditions for sample extraction, purification and detection were optimized as section 5. MP residues in three kinds of vegetables (onion, cabbage, and spinach) was detected, and the spiked concentration were

0.5 μ M 2.0 μ M 8.0 μ M respectively. The relative standard deviation and spiked recovery results were shown in the **Table 7-4**. The recoveries rate and RSD of onion, cabbage and spinach were in the range of 87.38%~114.12%.

Table 7-4 Determination of spiked recovery rate of vegetable samples.

Sample	MP spiked (μ M)	MP found (μ M)	Recovery (%)	RSD (%)
Onion	0.5	0.513	102.6	1.26
	2	1.974	98.7	3.32
	8	7.86	96.2	2.18
Cabbage	0.5	0.463	92.6	2.64
	2	1.943	97.15	3.14
	8	8.04	97.8	2.48
Spinach	0.5	0.476	95.2	3.36
	2	2.027	101.35	2.53
	8	7.93	98.5	1.98

7.3.3 Comparative evaluation on electrochemical sensor based on SJPCS@ β -CD and HPLC for MP detection in Vegetables

According to the above experimental results, both the electrochemical sensor detection method based on SJPCS@ β -CD/GCE and the HPLC detection method realized the actual detection of MP residue in vegetable samples, and the recovery rates were 96.5%~100.5% and 92.6%~102.6% respectively, with low RSD less than 5%. This indicates that the new electrochemical sensor method is relatively accurate and reliable, and can be used as an alternative method for detecting MP residues in vegetable samples. In addition, the electrochemical sensor is simple and fast to operate, which provides the possibility for the realization of on-site detection of plant products.

7.4. Conclusion in section 7

The expired sugarcane juice (SJ)-derived porous carbon spheres (PCS) were prepared by hydrothermal method and further modified with β -cyclodextrin (β -CD). The SJPCS@ β -CD nanocomposite was used to modify the glassy carbon electrode

(GCE) for the fabrication of SJPCS@ β -CD/GCE sensor towards methyl parathion (MP). SJPCS with interconnected porous structure exhibits excellent electrical conductivity, strong adsorption property, and high specific surface area, while β -CD with molecular recognition property achieves the uniform dispersion of SJPCS and promotes the recognition and adsorption of MP molecules. Thanks to the synergistic combination of SJPCS and β -CD, the SJPCS@ β -CD/GCE sensor exhibited respectable MP determination performance with low limit of detection of 5.87 nM in the MP concentration range of 0.01-10 μ M. For the MP detection in vegetables (onion, cabbage, spinach), the fabricated sensor showed good practicability with adequate relative standard deviation of 1.06% to 4.25% and satisfactory recoveries of 96.5 to 100.5%. A promising strategy for the rapid determination of methyl parathion in food products was developed. Moreover, it can be found that the obtained recoveries of MP are well comparable with the recoveries obtained from HPLC. These results indicate that the good practical feasibility of the fabricated SJPCS@ β -CD/GCE sensor can be achieved for the MP determination in vegetables. The sensor method was simple and fast to operate, providing the possibility of realizing the convenient field detection of pesticide residues.

CONCLUSIONS

Excessive pesticides residues usually produce serious negative impact on human health and environmental safety. Therefore, the differences and laws of pesticide absorption and transport of leafy vegetables are studied in this dissertation, which are important for pesticide pollution control. Additionally, a series of electrochemical sensor are prepared by using several nanocomposite materials as modification materials of sensing electrodes to detect the pesticide residues in agricultural products, fruits and vegetables. Electrochemical sensor technology as a new type of pesticide residue detection technology, because of its detection of low cost, simple operation, short test time, high sensitivity, strong stability, and other advantages, has attracted much attention in the field of pesticide residue detection. Under the optimal conditions, the fabricated electrochemical sensors showed highly sensitive pesticide detection performance with satisfactory recovery rates and low limit of detection (LOD) values. The good repeatability, reproducibility, stability, anti-interference can be achieved at the fabricated sensors. Moreover, the accurate and sensitive quantitative analysis performance can be obtained at the fabricated sensor for the detection of pesticide residues in real samples, and then evaluated by using HPLC to confirm the accuracy of pesticide electrochemical detection. The conclusions are as follows:

(1) The distribution, dynamic transfer differences and rules of IMI in leafy vegetables-water system were preliminarily proved through hydroponic experiments, and leafy vegetables with high and low residues of IMI were screened out. That is the residue concentration of IMI in the root of Greengrocery was the highest, and the residue concentration of IMI in the root of Pakchoi-Jimaocai was the least. The residue concentration of IMI was the highest in the leaves of Pakchoi-Shanghaiqing, and relatively less in the leaves of Gaogenbai. The dynamic test results of IMI enrichment and transfer in lettuce showed that IMI could be quickly absorbed and

transferred by lettuce, and the residual concentration of IMI in different parts of lettuce varied with the collection site and collection time.

(2) MWCNT-COOH was used to modify the glassy carbon electrode (GCE) for the fabrication of MWCNT-COOH/GCE sensor towards carbendazim (CBZ). Under the optimal conditions, the fabricated MWCNT-COOH/GCE sensor exhibited good CBZ detection performance with low LOD value (6.7 nM). The good practical feasibility can be obtained at the fabricated sensor for the detection of CBZ in cabbage, cucumber and potato samples, and then the results are evaluated by using HPLC to confirm the accuracy of CBZ electrochemical detection.

(3) Soybean-derived porous carbon (SDPC) with three-dimensional (3D) interconnected porous structure was prepared by using the expired soybean as carbon source through a high-temperature carbonization process. SDPC was used to modify the glassy carbon electrode (GCE) for the fabrication of SDPC/GCE sensor towards imidacloprid (IMI). Under the optimal conditions, the fabricated SDPC/GCE sensor exhibited a low LOD value (5.18 μ M) in wide IMI linear concentration range of 0.3-75 μ M. Moreover, the sensor has been successfully applied to the determination of IMI in cabbage, cucumber and potato samples, and its recovery rate is in good agreement with that of HPLC, indicating that the constructed sensor has good practical application value in the analysis of IMI in complex matrices.

(4) The multifunctional nanocomposite of superconductive carbon black (SCB) and ZrO₂ was prepared by a simple and efficient ultrasound-assisted strategy. The SCB@ZrO₂ nanocomposite was used to modify the glassy carbon electrode (GCE) for the fabrication of SCB@ZrO₂/GCE sensor towards methyl parathion (MP). Under the optimal conditions, the fabricated SCB@ZrO₂/GCE sensor exhibited a low LOD value (16 nM) in MP linear concentration range of 0.03-10 μ M. The good practical feasibility can be obtained at the fabricated sensor for the detection of MP

in lettuce, cucumber and tomato samples, and then the results are evaluate by using HPLC to confirm the accuracy of MP electrochemical detection.

(5) The expired sugarcane juice (SJ)-derived porous carbon spheres (PCS) were prepared by hydrothermal method and further modified with β -cyclodextrin (β -CD). The SJPCS@ β -CD nanocomposite was used to modify the glassy carbon electrode (GCE) for the fabrication of SJPCS@ β -CD/GCE sensor towards MP. Thanks to the synergistic combination of SJPCS and β -CD, the SJPCS@ β -CD/GCE sensor exhibited respectable MP determination performance with low limit of detection of 5.87 nM in the MP concentration range of 0.01-10 μ M. For the MP detection in vegetables (onion, cabbage, spinach), the fabricated sensor showed good practicability with adequate relative standard deviation of 1.06% to 4.25% and satisfactory recoveries of 96.5 to 100.5%. A promising strategy for the rapid determination of methyl parathion in food products was developed. The good practical feasibility can be obtained at the fabricated sensor for the detection of MP in onion, cabbage and spinach samples, and then the results are evaluate by using HPLC to confirm the accuracy of MP electrochemical detection.

Reference

1. Addrah, M. E., Zhang, Y. Y., Zhang, J., Liu, L., Zhou, H. Y., Chen, W. D., & Zhao, J. (2020). Fungicide Treatments to Control Seed-borne Fungi of Sunflower Seeds. *Pathogens*, 9(1). Retrieved from <Go to ISI>://WOS:000513130300007. doi:10.3390/pathogens9010029
2. Adeleye, A. O., Sosan, M. B., & Oyekunle, J. A. O. (2019). Dietary exposure assessment of organochlorine pesticides in two commonly grown leafy vegetables in South-western Nigeria. *Heliyon*, 5(6). Retrieved from <Go to ISI>://WOS:000473818300058. doi:10.1016/j.heliyon.2019.e01895
3. Akdag, A., Isik, M., & Goktas, H. (2020). Conducting polymer-based electrochemical biosensor for the detection of acetylthiocholine and pesticide via acetylcholinesterase. *Biotechnology and Applied Biochemistry*. Retrieved from <Go to ISI>://WOS:000578756000001. doi:10.1002/bab.2030
4. Akilarasan, M., Tamilalagan, E., Chen, S. M., Maheshwaran, S., Chen, T. W., Al-Mohaimed, A. M., . . . Elshikh, M. S. (2021). An eco-friendly low-temperature synthetic approach towards micro-pebble-structured GO@SrTiO₃ nanocomposites for the detection of 2,4,6-trichlorophenol in environmental samples. *Microchimica Acta*, 188(3). Retrieved from <Go to ISI>://WOS:000617410700002. doi:10.1007/s00604-021-04729-w
5. Al-Hamry, A., Ega, T. K., Pasti, I. A., Bajuk-Bogdanovic, D., Lazarevic-Pasti, T., Rodriguez, R. D., . . . Kanoun, O. (2019, Oct 30-31). *Electrochemical Sensor based on Reduced Graphene Oxide/PDAC for Dimethoate Pesticide Detection*. Paper presented at the 5th International Conference on Nanotechnology for Instrumentation and Measurement (NanofIM), Sfax, TUNISIA.
6. Albaiges, J. (2016). High performance liquid chromatography in pesticide residue analysis. *International Journal of Environmental Analytical Chemistry*, 96(15), 1507-1508. Retrieved from <Go to ISI>://WOS:000392438400008. doi:10.1080/03067319.2016.1257708
7. Alex, A. V., & Mukherjee, A. (2021). Review of recent developments (2018-2020) on acetylcholinesterase inhibition based biosensors for organophosphorus pesticides detection. *Microchemical Journal*, 161. Retrieved from <Go to ISI>://WOS:000605201300010. doi:10.1016/j.microc.2020.105779
8. Arduini, F., Cinti, S., Caratelli, V., Amendola, L., Palleschi, G., & Moscone, D. (2019). Origami multiple paper-based electrochemical biosensors for pesticide detection. *Biosensors & Bioelectronics*, 126, 346-354. Retrieved from <Go to ISI>://WOS:000457659500045. doi:10.1016/j.bios.2018.10.014
9. Aslan, S., Cakir, Z., Emet, M., Serinken, M., Karcioglu, O., Kandis, H., & Uzkeser, M. (2011). ACUTE ABDOMEN ASSOCIATED WITH ORGANOPHOSPHATE POISONING. *Journal of Emergency Medicine*, 41(5), 507-512. Retrieved from <Go to ISI>://WOS:000297233300012.

doi:10.1016/j.jemermed.2010.05.072

10. Ayat, M., Ayouz, K., Yaddadene, C., Berouaken, M., & Gabouze, N. (2021). Porous silicon-modified electrode for electrochemical pesticide biosensor. *Journal of Coatings Technology and Research*, 18(1), 53-62. Retrieved from <Go to ISI>://WOS:000565115400003. doi:10.1007/s11998-020-00381-w
11. Azzouz, A., Colon, L. P., Souhail, B., & Ballesteros, E. (2019). A multi-residue method for GC-MS determination of selected endocrine disrupting chemicals in fish and seafood from European and North African markets. *Environ Res*, 178, 108727. Retrieved from <https://www.ncbi.nlm.nih.gov/pubmed/31520833>. doi:10.1016/j.envres.2019.108727
12. Balasubramanian, P., Annalakshmi, M., Chen, S. M., Sathesh, T., & Balamurugan, T. S. T. (2019). Ultrasonic energy-assisted preparation of beta-cyclodextrin-carbon nanofiber composite: Application for electrochemical sensing of nitrofurantoin. *Ultrason Sonochem*, 52, 391-400. Retrieved from <https://www.ncbi.nlm.nih.gov/pubmed/30591361>. doi:10.1016/j.ultsonch.2018.12.014
13. Ben Brahim, M., Belhadj Ammar, H., Abdelhédi, R., & Samet, Y. (2016). Electrochemical behavior and analytical detection of Imidacloprid insecticide on a BDD electrode using square-wave voltammetric method. *Chinese Chemical Letters*, 27(5), 666-672. doi:10.1016/j.ccllet.2015.12.032
14. Ben Messaoud, N., Ghica, M. E., Dridi, C., Ben Ali, M., & Brett, C. M. A. (2017). Electrochemical sensor based on multiwalled carbon nanotube and gold nanoparticle modified electrode for the sensitive detection of bisphenol A. *Sensors and Actuators B-Chemical*, 253, 513-522. Retrieved from <Go to ISI>://WOS:000411124800060. doi:10.1016/j.snb.2017.06.160
15. Bi, Z., Kong, Q., Cao, Y., Sun, G., Su, F., Wei, X., . . . Chen, C.-M. (2019). Biomass-derived porous carbon materials with different dimensions for supercapacitor electrodes: a review. *Journal of Materials Chemistry A*, 7(27), 16028-16045. doi:10.1039/c9ta04436a
16. Bi, Z. H., Kong, Q. Q., Cao, Y. F., Sun, G. H., Su, F. Y., Wei, X. X., . . . Chen, C. M. (2019). Biomass-derived porous carbon materials with different dimensions for supercapacitor electrodes: a review. *Journal of Materials Chemistry A*, 7(27), 16028-16045. Retrieved from <Go to ISI>://WOS:000475689800002. doi:10.1039/c9ta04436a
17. Bolat, G., Abaci, S., Vural, T., Bozdogan, B., & Denkbas, E. B. (2018). Sensitive electrochemical detection of fenitrothion pesticide based on self-assembled peptide-nanotubes modified disposable pencil graphite electrode. *Journal of Electroanalytical Chemistry*, 809, 88-95. Retrieved from <Go to ISI>://WOS:000424309900013. doi:10.1016/j.jelechem.2017.12.060
18. Brandt, A., Gorenflo, A., Siede, R., Meixner, M., & Buchler, R. (2016). The neonicotinoids thiacloprid, imidacloprid, and clothianidin affect the immunocompetence of honey bees (*Apis mellifera* L.). *Journal of Insect Physiology*, 86, 40-47. Retrieved from <Go to

- ISI>://WOS:000384779500006. doi:10.1016/j.jinsphys.2016.01.001
19. Calaf, G. M., Bleak, T. C., & Roy, D. (2021). Signs of carcinogenicity induced by parathion, malathion, and estrogen in human breast epithelial cells. *Oncology Reports*, *45*(4). Retrieved from <Go to ISI>://WOS:000623987000001. doi:10.3892/or.2021.7975
 20. Camara, M. A., Fuster, A., & Oliva, J. (2020). Determination of pesticide residues in edible snails with QuEChERS coupled to GC-MS/MS. *Food Additives and Contaminants Part a-Chemistry Analysis Control Exposure & Risk Assessment*, *37*(11), 1881-1887. Retrieved from <Go to ISI>://WOS:000567581500001. doi:10.1080/19440049.2020.1809720
 21. Cao, J., Wang, M., Yu, H., She, Y. X., Cao, Z., Ye, J. M., . . . Lao, S. B. (2020). An Overview on the Mechanisms and Applications of Enzyme Inhibition-Based Methods for Determination of Organophosphate and Carbamate Pesticides. *Journal of Agricultural and Food Chemistry*, *68*(28), 7298-7315. Retrieved from <Go to ISI>://WOS:000551495300003. doi:10.1021/acs.jafc.0c01962
 22. Caratelli, V., Ciampaglia, A., Guiducci, J., Sancesario, G., Moscone, D., & Arduini, F. (2020). Precision medicine in Alzheimer's disease: An origami paper-based electrochemical device for cholinesterase inhibitors. *Biosensors & Bioelectronics*, *165*. Retrieved from <Go to ISI>://WOS:000566444800006. doi:10.1016/j.bios.2020.112411
 23. Castilla-Fernandez, D., Moreno-Gonzalez, D., Gilbert-Lopez, B., Garcia-Reyes, J. F., & Molina-Diaz, A. (2021). Worldwide survey of pesticide residues in citrus-flavored soft drinks. *Food Chem*, *365*, 130486. Retrieved from <https://www.ncbi.nlm.nih.gov/pubmed/34237571>. doi:10.1016/j.foodchem.2021.130486
 24. Chen, D., Zhou, H., Li, H., Chen, J., Li, S., & Zheng, F. (2017). Self-template synthesis of biomass-derived 3D hierarchical N-doped porous carbon for simultaneous determination of dihydroxybenzene isomers. *Sci Rep*, *7*(1), 14985. Retrieved from <https://www.ncbi.nlm.nih.gov/pubmed/29101387>. doi:10.1038/s41598-017-15129-7
 25. Chen, L., Dang, X., Ai, Y., & Chen, H. (2018). Preparation of an acryloyl beta-cyclodextrin-silica hybrid monolithic column and its application in pipette tip solid-phase extraction and HPLC analysis of methyl parathion and fenthion. *J Sep Sci*, *41*(18), 3508-3514. Retrieved from <https://www.ncbi.nlm.nih.gov/pubmed/29736920>. doi:10.1002/jssc.201701273
 26. Chen, M. L., Zhao, Z. M., Lan, X. F., Chen, Y. M., Zhang, L., Ji, R. D., & Wang, L. X. (2015). Determination of carbendazim and metiram pesticides residues in reapeseed and peanut oils by fluorescence spectrophotometry. *Measurement*, *73*, 313-317. Retrieved from <Go to ISI>://WOS:000359309900031. doi:10.1016/j.measurement.2015.05.006
 27. Chen, Z., Zhang, Y., Yang, Y., Shi, X., Zhang, L., & Jia, G. (2021). Hierarchical nitrogen-doped holey graphene as sensitive electrochemical

- sensor for methyl parathion detection. *Sensors and Actuators B: Chemical*, 336. doi:10.1016/j.snb.2021.129721
28. Chen, Z. F., Zhang, Y., Yang, Y. Q., Shi, X. R., Zhang, L., & Jia, G. W. (2021). Hierarchical nitrogen-doped holey graphene as sensitive electrochemical sensor for methyl parathion detection. *Sensors and Actuators B-Chemical*, 336. Retrieved from <Go to ISI>://WOS:000639153000005. doi:10.1016/j.snb.2021.129721
29. Chouichit, P., Whangsuk, W., Sallabhan, R., Mongkolsuk, S., & Loprasert, S. (2020). A highly sensitive biosensor with a single-copy evolved sensing cassette for chlorpyrifos pesticide detection. *Microbiology-Sgm*, 166(11), 1019-1024. Retrieved from <Go to ISI>://WOS:000603436200003. doi:10.1099/mic.0.000979
30. Chu, Y., Tong, Z., Dong, X., Sun, M. N., Gao, T. C., Duan, J. S., & Wang, M. (2020). Simultaneous determination of 98 pesticide residues in strawberries using UPLC-MS/MS and GC-MS/MS. *Microchemical Journal*, 156. Retrieved from <Go to ISI>://WOS:000543430700061. doi:10.1016/j.microc.2020.104975
31. Covaciu, F. D., Magdas, D. A., Marincas, O., & Moldovan, Z. (2017). Determination of Pesticides in Carrots by Gas Chromatography-Mass Spectrometry. *Analytical Letters*, 50(17), 2665-2676. Retrieved from <Go to ISI>://WOS:000415951900002. doi:10.1080/00032719.2016.1263313
32. Dai, H. (2018). *Study on Functionalized Polypyrrole Nanocomposites-based Electrochemical Sensors*. (Doctor), Shandong University, Available from Cnki
33. Dai, Y., Zhu, G. D., Shang, X. H., Zhu, T. Z., Yang, J. M., & Liu, J. Y. (2017). Electrospun zirconia-embedded carbon nanofibre for high-sensitive determination of methyl parathion. *Electrochemistry Communications*, 81, 14-17. Retrieved from <Go to ISI>://WOS:000406947200004. doi:10.1016/j.elecom.2017.05.017
34. Davie-Martin, C. L., Hageman, K. J., Chin, Y. P., Rouge, V., & Fujita, Y. (2015). Influence of Temperature, Relative Humidity, and Soil Properties on the Soil-Air Partitioning of Semivolatile Pesticides: Laboratory Measurements and Predictive Models. *Environmental Science & Technology*, 49(17), 10431-10439. Retrieved from <Go to ISI>://WOS:000360773600020. doi:10.1021/acs.est.5b02525
35. Davletshina, R., Ivanov, A., Shamagsumova, R., Evtugyn, V., & Evtugyn, G. (2020). Electrochemical Biosensor Based on Polyelectrolyte Complexes with Dendrimer for the Determination of Reversible Inhibitors of Acetylcholinesterase. *Analytical Letters*. Retrieved from <Go to ISI>://WOS:000572799200001. doi:10.1080/00032719.2020.1821700
36. de Medeiros, J. F., Acayaba, R. D., & Montagner, C. C. (2021). THE CHEMISTRY IN THE HUMAN HEALTH RISK ASSESSMENT DUE PESTICIDES EXPOSURE. *Quimica Nova*, 44(5), 584-598. Retrieved from <Go to ISI>://WOS:000678535800006. doi:10.21577/0100-4042.20170699

37. Ding, C., & Cao, X. (2005). Present situation and countermeasures of pesticide residues in agricultural products. *Guangdong Agricultural Sciences*(03), 101-182. doi:10.16768/j.issn.1004-874x.2005.03.038
38. Ding, H., Zheng, X. Z., Zhang, J., Zhang, Y. S., Yu, J. H., & Chen, D. L. (2019). Influence of chlorothalonil and carbendazim fungicides on the transformation processes of urea nitrogen and related microbial populations in soil. *Environmental Science and Pollution Research*, 26(30), 31133-31141. Retrieved from <Go to ISI>://WOS:000494047900051. doi:10.1007/s11356-019-06213-8
39. Dominguez, J. W. O. R. R. P. E. (2003). Electrochemical detection of DNA hybridization based on DNA-templated assembly of silver cluster. *Electrochemistry Communications*, 5(1), 83-86. doi:https://doi.org/10.1016/S1388-2481(02)00542-8
40. Farina, Y., Abdullah, M. P., Bibi, N., & Khalik, W. (2017). Determination of pesticide residues in leafy vegetables at parts per billion levels by a chemometric study using GC-ECD in Cameron Highlands, Malaysia. *Food Chemistry*, 224, 55-61. Retrieved from <Go to ISI>://WOS:000394631400008. doi:10.1016/j.foodchem.2016.11.113
41. Feng, X., Li, R., Yang, X., & Hou, W. (2012). Application of Novel Carbon Nanomaterials to Electrochemistry. *PROGRESS IN CHEMISTRY*, 24(11), 2158-2166.
42. Feng, X., Qiu, B., Dang, Y., & Sun, D. (2021). Enhanced adsorption of naproxen from aquatic environments by β -cyclodextrin-immobilized reduced graphene oxide. *Chemical Engineering Journal*, 412. doi:10.1016/j.cej.2021.128710
43. Ferro, E., Otsuki, T., & Wilson, J. S. (2015). The effect of product standards on agricultural exports. *Food Policy*, 50, 68-79. Retrieved from <Go to ISI>://WOS:000348748600007. doi:10.1016/j.foodpol.2014.10.016
44. Gallart-Mateu, D., Armenta, S., & de la Guardia, M. (2016). Indoor and outdoor determination of pesticides in air by ion mobility spectrometry. *Talanta*, 161, 632-639. Retrieved from <Go to ISI>://WOS:000386989500081. doi:10.1016/j.talanta.2016.09.020
45. Gao, J. J., Gai, Q. G., Liu, B. B., & Shi, Q. H. (2021). Farm size and pesticide use: evidence from agricultural production in China. *China Agricultural Economic Review*, 13(4), 912-929. Retrieved from <Go to ISI>://WOS:000691602000001. doi:10.1108/caer-11-2020-0279
46. Gao, N., He, C. H., Ma, M. Y., Cai, Z. W., Zhou, Y., Chang, G., . . . He, Y. B. (2019). Electrochemical co-deposition synthesis of Au-ZrO₂-graphene nanocomposite for a nonenzymatic methyl parathion sensor. *Analytica chimica acta*, 1072, 25-34. Retrieved from <Go to ISI>://WOS:000469021200003. doi:10.1016/j.aca.2019.04.043
47. Ghorbani, A., Ojani, R., Ganjali, M. R., & Raoof, J. Direct voltammetric determination of carbendazim by utilizing a nanosized imprinted polymer/MWCNTs-modified electrode. *Journal of the Iranian Chemical*

- Society*. Retrieved from <Go to ISI>://WOS:000648506600002. doi:10.1007/s13738-021-02255-3
48. Golge, O. (2021). Validation of Quick Polar Pesticides (QuPPE) Method for Determination of Eight Polar Pesticides in Cherries by LC-MS/MS. *Food Analytical Methods*, 6. Retrieved from <Go to ISI>://WOS:000620433800001. doi:10.1007/s12161-021-01966-w
49. Gong, Z. L., Guo, Y. M., Sun, X., Cao, Y. Y., & Wang, X. Y. (2014). Acetylcholinesterase biosensor for carbaryl detection based on interdigitated array microelectrodes. *Bioprocess and Biosystems Engineering*, 37(10), 1929-1934. Retrieved from <Go to ISI>://WOS:000342171500001. doi:10.1007/s00449-014-1195-4
50. Govindasamy, M., Mani, V., Chen, S. M., Chen, T. W., & Sundramoorthy, A. K. (2017a). Methyl parathion detection in vegetables and fruits using silver@graphene nanoribbons nanocomposite modified screen printed electrode. *Scientific Reports*, 7. Retrieved from <Go to ISI>://WOS:000399696800001. doi:10.1038/srep46471
51. Govindasamy, M., Mani, V., Chen, S. M., Chen, T. W., & Sundramoorthy, A. K. (2017b). Methyl parathion detection in vegetables and fruits using silver@graphene nanoribbons nanocomposite modified screen printed electrode. *Sci Rep*, 7, 46471. Retrieved from <https://www.ncbi.nlm.nih.gov/pubmed/28425441>. doi:10.1038/srep46471
52. Guzsány, V., Kádár, M., Papp, Z., Bjelica, L., Gaál, F., & Tóth, K. (2008). Monitoring of Photocatalytic Degradation of Selected Neonicotinoid Insecticides by Cathodic Voltammetry with a Bismuth Film Electrode. *Electroanalysis*, 20(3), 291-300. doi:10.1002/elan.200704057
53. Guzsany, V. J., Papp, Z. J., Lazic, S. D., Gaal, F. F., Bjelica, L. J., & Abramovic, B. F. (2009). A rapid spectrophotometric determination of imidacloprid in selected commercial formulations in the presence of 6-chloronicotinic acid. *Journal of the Serbian Chemical Society*, 74(12), 1455-1465. Retrieved from <Go to ISI>://WOS:000275494600011. doi:10.2298/jsc0912455g
54. Han, X. (2022). Study on residue degradation and influencing factors of imidacloprid and acetamiprid in agricultural soils from *Lycium barbarum* L. of Ningxia. *Journal of Ningxia Normal University*, 43(4), 41-50. Retrieved from <https://d.wanfangdata.com.cn/periodical/ChlQZXJpb2RpY2FsQ0hJTmV3UzIwMjMwNDI2Eg9neXN6eGIyMDIyMDQwMDYaCGpqY2J3bDQ0>. doi:10.3969/j.issn.1674-1331.2022.04.006
55. Hou, J., Dong, J., Zhu, H., Teng, X., Ai, S., Mang, M. J. B., & Bioelectronics. (2015). A simple and sensitive fluorescent sensor for methyl parathion based on l-tyrosine methyl ester functionalized carbon dots. 68, 20-26.
56. Huang, B. A., Zhang, W. D., Chen, C. H., & Yu, Y. X. (2010). Electrochemical determination of methyl parathion at a Pd/MWCNTs-modified electrode. *Microchimica Acta*, 171(1-2), 57-62. Retrieved from <Go to ISI>://WOS:000281669900008. doi:10.1007/s00604-010-0408-z

57. Huang, S. M., Hu, Y. F., Chen, Y. L., Li, G. K., & Xia, L. (2020). Magnetic Solid-phase Extraction Coupled with High-Performance Liquid Chromatography for Pesticide Residues Analysis in Citrus Sample. *Chinese Journal of Analytical Chemistry*, 48(10), 1392-1399. Retrieved from <Go to ISI>://WOS:000574774500016. doi:10.19756/j.issn.0253-3820.201359
58. Hughes, D., Thongkum, W., Tudpor, K., Turnbull, N., Yukalang, N., Sychareun, V., . . . Jordan, S. (2021). Pesticides use and health impacts on farmers in Thailand, Vietnam, and Lao PDR: Protocol for a survey of knowledge, behaviours and blood acetyl cholinesterase concentrations. *Plos One*, 16(9). Retrieved from <Go to ISI>://WOS:000743903000085. doi:10.1371/journal.pone.0258134
59. Hui, N. (2017). *The Fabrication and application of electrochemical sensors based on novel conducting polymer nanocomposites*. (Doctor), Qingdao University of Science and Technology, Available from Cnki
60. Huo, D. Q., Li, Q., Zhang, Y. C., Hou, C. J., & Lei, Y. (2014). A highly efficient organophosphorus pesticides sensor based on CuO nanowires-SWCNTs hybrid nanocomposite. *Sensors and Actuators B-Chemical*, 199, 410-417. Retrieved from <Go to ISI>://WOS:000336878000056. doi:10.1016/j.snb.2014.04.016
61. Jain, M., Yadav, P., Joshi, B., Joshi, A., & Kodgire, P. (2021). A novel biosensor for the detection of organophosphorus (OP)-based pesticides using organophosphorus acid anhydrolase (OPAA)-FL variant. *Applied Microbiology and Biotechnology*, 105(1), 389-400. Retrieved from <Go to ISI>://WOS:000589560800001. doi:10.1007/s00253-020-11008-w
62. Jia, Y. M., Ahmed, A., Jiang, X. Y., Zhou, L., Fan, Q. G., & Shao, J. Z. (2020). Microfluidic fabrication of hierarchically porous superconductive carbon black/graphene hybrid fibers for wearable supercapacitor with high specific capacitance. *Electrochimica Acta*, 354. Retrieved from <Go to ISI>://WOS:000569141400004. doi:10.1016/j.electacta.2020.136731
63. Jian-yong, F. (2018). Application of Gas Chromatography in the Analysis of Pesticide Residues. *Chemical Engineering Design Communications*, 44(03), 113.
64. Jing, H. (2017). *Study on Detection System and Method of Pesticide Residues Based on Double light response*. Chongqing university,
65. Jones, K., Everard, M., & Harding, A. H. (2014). Investigation of gastrointestinal effects of organophosphate and carbamate pesticide residues on young children. *International Journal of Hygiene and Environmental Health*, 217(2-3), 392-398. Retrieved from <Go to ISI>://WOS:000331595500035. doi:10.1016/j.ijheh.2013.07.015
66. Jorfi, S., Atashi, Z., Akhbarizadeh, R., Khorasgani, Z. N., & Ahmadi, M. (2019). Distribution and health risk assessment of organochlorine pesticides in agricultural soils of the Aghili plain, Southwest Iran. *Environmental Earth Sciences*, 78(20). Retrieved from <Go to ISI>://WOS:000488965000005. doi:10.1007/s12665-019-8605-5

67. Kaewvimol, L. (2018). Pencil Graphite Based Biosensor for Rapid Malathion Pesticide Detection. *Chiang Mai Journal of Science*, 45(6), 2374-2380. Retrieved from <Go to ISI>://WOS:000445605500012.
68. Kalinke, C., Mangrich, A. S., Marcolino, L. H., & Bergamini, M. F. (2016). Carbon Paste Electrode Modified with Biochar for Sensitive Electrochemical Determination of Paraquat. *Electroanalysis*, 28(4), 764-769. Retrieved from <Go to ISI>://WOS:000374135700015. doi:10.1002/elan.201500640
69. Kang, T.-F., Wang, F., Lu, L.-P., Zhang, Y., & Liu, T.-S. (2010). Methyl parathion sensors based on gold nanoparticles and Nafion film modified glassy carbon electrodes. *Sensor. Actuat. B-Chem.*, 145(1), 104-109. doi:10.1016/j.snb.2009.11.038
70. Karimi-Takallo, A., Dianat, S., & Hatefi-Mehrjardi, A. (2021). Fabrication and electrochemical study of K(1,10-(1,4 Butanediyl) dipyridinium)(2) PW11O39Co(H2O) /MWCNTs-COOH nanohybrid immobilized on glassy carbon for electrocatalytic detection of nitrite. *Journal of Electroanalytical Chemistry*, 886. Retrieved from <Go to ISI>://WOS:000636273400015. doi:10.1016/j.jelechem.2021.115139
71. Ko, A. Y., Rahman, M. M., Abd El-Aty, A. M., Jang, J., Park, J. H., Cho, S. K., & Shim, J. H. (2014). Development of a simple extraction and oxidation procedure for the residue analysis of imidacloprid and its metabolites in lettuce using gas chromatography. *Food Chemistry*, 148, 402-409. Retrieved from <Go to ISI>://WOS:000328810500058. doi:10.1016/j.foodchem.2013.10.055
72. Koo, Y. C., Lee, K. W., Yang, S. Y., Kim, H., & Shin, H. S. (2010). Multiresidual Pesticide Analysis of Four Sulfonylurea Pesticides by High-Performance Liquid Chromatography with Diode-Array Detection. *Faseb Journal*, 24. Retrieved from <Go to ISI>://WOS:000208675507386.
73. Kumar, P., Kim, K. H., & Deep, A. (2015). Recent advancements in sensing techniques based on functional materials for organophosphate pesticides. *Biosensors & Bioelectronics*, 70, 469-481. Retrieved from <Go to ISI>://WOS:000356554400065. doi:10.1016/j.bios.2015.03.066
74. Kumaravel, A., & Chandrasekaran, M. (2011). A biocompatible nano TiO₂/nafion composite modified glassy carbon electrode for the detection of fenitrothion. *Journal of Electroanalytical Chemistry*, 650(2), 163-170. Retrieved from <Go to ISI>://WOS:000285656000001. doi:10.1016/j.jelechem.2010.10.013
75. Lah, N. F. C., Ahmad, A. L., & Low, S. C. (2021). Molecular imprinted membrane biosensor for pesticide detection: Perspectives and challenges. *Polymers for Advanced Technologies*, 32(1), 17-30. Retrieved from <Go to ISI>://WOS:000574855800001. doi:10.1002/pat.5098
76. Li, F., Liu, R., Dubovyk, V., Ran, Q., Li, B., Chang, Y., . . . Komarneni, S. (2022a). Three-dimensional hierarchical porous carbon coupled with chitosan based electrochemical sensor for sensitive determination of niclosamide. *Food Chem*, 366, 130563. Retrieved from

<https://www.ncbi.nlm.nih.gov/pubmed/34289441>.

doi:10.1016/j.foodchem.2021.130563

77. Li, F., Liu, R. Q., Dubovyk, V., Ran, Q. W., Li, B., Chang, Y. Q., . . . Komarneni, S. (2022b). Three-dimensional hierarchical porous carbon coupled with chitosan based electrochemical sensor for sensitive determination of niclosamide. *Food Chemistry*, 366. Retrieved from <Go to ISI>://WOS:000696903000005. doi:10.1016/j.foodchem.2021.130563
78. Li, J. (2014). *Nanocomposite modified electrodes for the determination of phenols*. (Master), Xinan University, Available from Cnki
79. Li, J., Michalkiewicz, B., Min, J., Ma, C., Chen, X., Gong, J., . . . Tang, T. (2019). Selective preparation of biomass-derived porous carbon with controllable pore sizes toward highly efficient CO₂ capture. *Chemical Engineering Journal*, 360, 250-259. doi:10.1016/j.cej.2018.11.204
80. Li, J. X., Michalkiewicz, B., Min, J. K., Ma, C. D., Chen, X. C., Gong, J., . . . Tang, T. (2019). Selective preparation of biomass-derived porous carbon with controllable pore sizes toward highly efficient CO₂ capture. *Chemical Engineering Journal*, 360, 250-259. Retrieved from <Go to ISI>://WOS:000460964000027. doi:10.1016/j.cej.2018.11.204
81. Li, P. L., Sun, P. Y., Dong, X. L., & Li, B. H. (2020). Residue analysis and kinetics modeling of thiophanate-methyl, carbendazim, tebuconazole and pyraclostrobin in apple tree bark using QuEChERS/HPLC-VWD. *Biomedical Chromatography*, 34(9). Retrieved from <Go to ISI>://WOS:000542619500001. doi:10.1002/bmc.4851
82. Li, W., Wang, Y. N., Huang, L. M., Wu, T., Hu, H. L., & Du, Y. P. (2015). Rapid determination of trace thiabendazole in apple juice utilizing dispersive liquid-liquid microextraction combined with fluorescence spectrophotometry. *Luminescence*, 30(6), 872-877. Retrieved from <Go to ISI>://WOS:000364639900026. doi:10.1002/bio.2835
83. Li, Y., Du, C., Liu, X., Wang, K., Yang, H., & Li, Y. (2021). Non-Enzymatic Methyl Parathion Electrochemical Sensor Based on Hydroxyl Functionalized Ionic Liquid/Zeolitic Imidazolate Framework Composites Modified Glassy Carbon Electrode. *Journal of The Electrochemical Society*, 168(7). doi:10.1149/1945-7111/ac13d4
84. Li, Y. H., Hu, J., Yao, Z. L., Wang, Q., & Zhang, H. (2020). Transfer assessment of carbendazim residues from rapeseed to oil production determined by HPLC-MS/MS. *Journal of Environmental Science and Health Part B-Pesticides Food Contaminants and Agricultural Wastes*, 55(8), 726-731. Retrieved from <Go to ISI>://WOS:000546170400001. doi:10.1080/03601234.2020.1780869
85. Iijima, S. (1991). Helical microtubules of graphitic carbon. *Nature*, 354, 56-58. doi:10.1038/354056a0
86. Liu, L., Guo, J., & Ding, L. (2021). Polyaniline Nanowire Arrays Deposited on Porous Carbon Derived from Raffia for Electrochemical Detection of Imidacloprid. *Electroanalysis*, 33(9), 2048-2052.

doi:10.1002/elan.202100162

- 87.Liu, L., Guo, J. W., & Ding, L. H. (2021). Polyaniline Nanowire Arrays Deposited on Porous Carbon Derived from Raffia for Electrochemical Detection of Imidacloprid. *Electroanalysis*, 33(9), 2048-2052. Retrieved from <Go to ISI>://WOS:000669909900001. doi:10.1002/elan.202100162
- 88.Liu, N. (2018). *Green fabrication of carbon nanomaterials and the study of their electrochemical properties*. (doctor), Suzhou University, Available from Cnki
- 89.Liu, P., Guo, Y. Z., & Iop. (2019). Current situation of pesticide residues and their impact on exports in China. In *Third International Conference on Energy Engineering and Environmental Protection* (Vol. 227).
- 90.Liu, R., Wang, Y., Li, D., Dong, L., Li, B., Liu, B., . . . Chen, X. (2019). A Simple, Low-Cost and Efficient β -CD/MWCNTs/CP-based Electrochemical Sensor for the Rapid and Sensitive Detection of Methyl Parathion. *Int. J. Electrochem. Sci.*, 9785-9795. doi:10.20964/2019.10.28
- 91.Liu, R., Wang, Y., Li, D., Li, B., Liu, B., & Ma, H. (2019). A Simple, Low-Cost and Efficient β -CD/MWCNTs/CP-based Electrochemical Sensor for the Rapid and Sensitive Detection of Methyl Parathion. *International Journal of Electrochemical Science*, 9785-9795. doi:10.20964/2019.10.28
- 92.Liu, S., Liao, Y., Guo, S., Lai, X., Xie, Z., & Deng, J. (2021). Present situation and reasons of pesticide residues in three major types of leafy vegetables. *Horticulture & Seed*, 41(4), 57-59. Retrieved from <https://d.wanfangdata.com.cn/periodical/ChlQZXJpb2RpY2FsQ0hJTmV3UzIwMjMwNDI2Eg16bHp3MjAyMTA0MDI0GghkOWlocDN5bA%3D%3D>. doi:10.16530/j.cnki.cn21-1574/s.2021.04.023
- 93.Liu, Y., Cao, B., Zhang, X., Luo, R., Luo, C. H., Lin, H. C., & Peng, H. (2021). Preparation of alpha-Co(OH)(2)@MWCNTs-COOH nanocomposites and their application for supercapacitors. *Journal of Materials Science-Materials in Electronics*. Retrieved from <Go to ISI>://WOS:000645184700001. doi:10.1007/s10854-021-05970-y
- 94.Liu, Z. J., & Cao, Z. M. (2015, May 30-31). *The pollution of chemical pesticides and safe production of vegetables*. Paper presented at the International Conference on Energy Equipment Science and Engineering (ICEESE), Guangzhou, PEOPLES R CHINA.
- 95.Liu, Z. Y., Chen, Y., Han, J. H., Chen, D., Yang, G. Q., Lan, T. T., . . . Zhang, K. K. (2021). Determination, dissipation dynamics, terminal residues and dietary risk assessment of thiophanate-methyl and its metabolite carbendazim in cowpeas collected from different locations in China under field conditions. *Journal of the Science of Food and Agriculture*. Retrieved from <Go to ISI>://WOS:000630337100001. doi:10.1002/jsfa.11198
- 96.Lu, H., & Zhao, X. S. (2017). Biomass-derived carbon electrode materials for supercapacitors. *Sustainable Energy & Fuels*, 1(6), 1265-1281. Retrieved from <Go to ISI>://WOS:000422787100004. doi:10.1039/c7se00099e
- 97.Luo, Q., Lai, J., Qiu, P., Wang, X. J. S., & Chemical, A. B. (2018). An

- ultrasensitive fluorescent sensor for organophosphorus pesticides detection based on RB-Ag/Au bimetallic nanoparticles. *263*, 517-523.
98. Lyu, L., Seong, K., Ko, D., Choi, J., Lee, C., Hwang, T., . . . Piao, Y. (2019). Recent development of biomass-derived carbons and composites as electrode materials for supercapacitors. *Materials Chemistry Frontiers*, *3*(12), 2543-2570. Retrieved from <Go to ISI>://WOS:000499250700001. doi:10.1039/c9qm00348g
 99. Mahmoudian, M. R., Basirun, W. J., & Alias, Y. (2016). A sensitive electrochemical Hg²⁺ ions sensor based on polypyrrole coated nanospherical platinum. *Rsc Advances*, *6*(43), 36459-36466. Retrieved from <Go to ISI>://WOS:000374561300029. doi:10.1039/c6ra03878f
 100. Mammana, S. B., Berton, P., Camargo, A. B., Lascalea, G. E., & Altamirano, J. C. (2017). Coprecipitation-assisted coacervative extraction coupled to high-performance liquid chromatography: An approach for determining organophosphorus pesticides in water samples. *Electrophoresis*, *38*(9-10), 1334-1343. Retrieved from <Go to ISI>://WOS:000401166900011. doi:10.1002/elps.201600335
 101. Marichi, R. B., Goel, S., Tomar, A. K., Sahu, V., Lalwani, S., Singh, G., & Sharma, R. K. (2020). Direct hydrothermal treatment of sugarcane juice for 3D oxygen-rich carbon Aerogel/NiCo₂O₄ based supercapacitor. *Materials Chemistry and Physics*, *239*. doi:10.1016/j.matchemphys.2019.121957
 102. Mei-yang, Z. (2015). A study on Progress in Pre-processing Technology Related to Pesticide Residue Detection According to Gas Chromatography. *Times Agricultural Machinery*, *42*(09), 134-135.
 103. Merkoci, J. W. G. L. R. P. A. (2002). Electrochemical stripping detection of DNA hybridization based on cadmium sulfide nanoparticle tags. *Electrochemistry Communications*, *4*(9), 722-726. doi:https://doi.org/10.1016/S1388-2481(02)00434-4
 104. Mie, A., Andersen, H. R., Gunnarsson, S., Kahl, J., Kesse-Guyot, E., Rembialkowska, E., . . . Grandjean, P. (2017). Human health implications of organic food and organic agriculture: a comprehensive review. *Environmental Health*, *16*. Retrieved from <Go to ISI>://WOS:000414019200001. doi:10.1186/s12940-017-0315-4
 105. Migliorini, F. L., Sanfelice, R. C., Mercante, L. A., Facure, M. H. M., & Correa, D. S. (2020). Electrochemical sensor based on polyamide 6/polypyrrole electrospun nanofibers coated with reduced graphene oxide for malathion pesticide detection. *Materials Research Express*, *7*(1). Retrieved from <Go to ISI>://WOS:000499456700001. doi:10.1088/2053-1591/ab5744
 106. Mouskeftara, T., Virgiliou, C., Iakovakis, A., Raikos, N., & Gika, H. G. (2021). Liquid chromatography tandem mass spectrometry for the determination of nine insecticides and fungicides in human postmortem blood and urine. *J Chromatogr B Analyt Technol Biomed Life Sci*, *1179*, 122824. Retrieved from https://www.ncbi.nlm.nih.gov/pubmed/34218092. doi:10.1016/j.jchromb.2021.122824

107. Niu, X., Huang, Y., Zhang, W., Yan, L., Wang, L., Li, Z., & Sun, W. (2021). Synthesis of gold nanoflakes decorated biomass-derived porous carbon and its application in electrochemical sensing of luteolin. *Journal of Electroanal. Chem.*, 880, 114832. doi:10.1016/j.jelechem.2020.114832
108. Niu, X. L., Huang, Y., Zhang, W. L., Yan, L. J., Wang, L. K., Li, Z. F., & Sun, W. (2021). Synthesis of gold nanoflakes decorated biomass-derived porous carbon and its application in electrochemical sensing of luteolin. *Journal of Electroanalytical Chemistry*, 880. Retrieved from <Go to ISI>://WOS:000639615600007. doi:10.1016/j.jelechem.2020.114832
109. Noori, J. S., Mortensen, J., & Geto, A. (2021). Rapid and Sensitive Quantification of the Pesticide Lindane by Polymer Modified Electrochemical Sensor. *Sensors*, 21(2). Retrieved from <Go to ISI>://WOS:000611714800001. doi:10.3390/s21020393
110. Oliveira, A. E. F., Bettio, G. B., & Pereira, A. C. (2018). An Electrochemical Sensor Based on Electropolymerization of ss-Cyclodextrin and Reduced Graphene Oxide on a Glassy Carbon Electrode for Determination of Neonicotinoids. *Electroanalysis*, 30(9), 1918-1928. Retrieved from <Go to ISI>://WOS:000443938300006. doi:10.1002/elan.201800236
111. Ouyang, Q., Wang, L., Ahmad, W., Rong, Y. W., Li, H. H., Hu, Y. Q., & Chen, Q. S. (2021). A highly sensitive detection of carbendazim pesticide in food based on the upconversion-MnO₂ luminescent resonance energy transfer biosensor. *Food Chemistry*, 349. Retrieved from <Go to ISI>://WOS:000621597800013. doi:10.1016/j.foodchem.2021.129157
112. Pan, D., Ma, S., Bo, X., & Guo, L. (2011). Electrochemical behavior of methyl parathion and its sensitive determination at a glassy carbon electrode modified with ordered mesoporous carbon. *Microchimica Acta*, 173(1-2), 215-221. doi:10.1007/s00604-011-0551-1
113. Papp, Z., Švancara, I., Guzsvány, V., Vytrás, K., & Gaál, F. (2009). Voltammetric determination of imidacloprid insecticide in selected samples using a carbon paste electrode. *Microchimica Acta*, 166(1-2), 169-175. doi:10.1007/s00604-009-0181-z
114. Paula, S. A., Ferreira, O. A. E., & Cesar, P. A. (2020). Determination of Imidacloprid Based on the Development of a Glassy Carbon Electrode Modified with Reduced Graphene Oxide and Manganese (II) Phthalocyanine. *Electroanalysis*, 32(1), 86-94. Retrieved from <Go to ISI>://WOS:000483130400001. doi:10.1002/elan.201900227
115. Pinho, G. P., Neves, A. A., Queiroz, M., & Silverio, F. O. (2009). MATRIX EFFECT IN PESTICIDE QUANTIFICATION BY GAS CHROMATOGRAPHY. *Quimica Nova*, 32(4), 987-995. Retrieved from <Go to ISI>://WOS:000267331400030. doi:10.1590/s0100-40422009000400030
116. Popp, J., Peto, K., & Nagy, J. (2013). Pesticide productivity and food security. A review. *Agronomy for Sustainable Development*, 33(1), 243-255. Retrieved from <Go to ISI>://WOS:000312738100012. doi:10.1007/s13593-

117. Pundir, C. S., Malik, A., & Preety. (2019). Bio-sensing of organophosphorus pesticides: A review. *Biosensors & Bioelectronics*, 140, 5-17. Retrieved from <Go to ISI>://WOS:000472990500001. doi:10.1016/j.bios.2019.111348
118. Rasheed, T., Bilal, M., Nabeel, F., Adeel, M., & Iqbal, H. M. N. (2019). Environmentally-related contaminants of high concern: Potential sources and analytical modalities for detection, quantification, and treatment. *Environment International*, 122, 52-66. Retrieved from <Go to ISI>://WOS:000454356400006. doi:10.1016/j.envint.2018.11.038
119. Razzino, C. A., Sgobbi, L. F., Canevari, T. C., Cancino, J., & Machado, S. A. S. (2015). Sensitive determination of carbendazim in orange juice by electrode modified with hybrid material. *Food Chemistry*, 170, 360-365. Retrieved from <Go to ISI>://WOS:000343780400049. doi:10.1016/j.foodchem.2014.08.085
120. ReddyPrasad, P., Naidoo, E. B., & Sreedhar, N. Y. (2019). Electrochemical preparation of a novel type of C-dots/ZrO₂ nanocomposite onto glassy carbon electrode for detection of organophosphorus pesticide. *Arabian Journal of Chemistry*, 12(8), 2300-2309. Retrieved from <https://www.sciencedirect.com/science/article/pii/S1878535215000465>. doi:<https://doi.org/10.1016/j.arabjc.2015.02.012>
121. Renganathan, V., Balaji, R., Chen, S. M., & Kokulnathan, T. (2020). Coherent design of palladium nanostructures adorned on the boron nitride heterojunctions for the unparalleled electrochemical determination of fatal organophosphorus pesticides. *Sensors and Actuators B-Chemical*, 307. Retrieved from <Go to ISI>://WOS:000508110400017. doi:10.1016/j.snb.2019.127586
122. Saka, M. (2010). Application of gas chromatograph with selected detector for pesticide residue analysis in food. *Journal of Pesticide Science*, 35(4), 580-586. Retrieved from <Go to ISI>://WOS:000286408400025. doi:10.1584/jpestics.35.580
123. Sakdarat, P., Chongsuebsirikul, J., Phongphut, A., Klinthingchai, Y., Prichanont, S., Thanachayanont, C., . . . Ieee. (2019, Jul 22-26). *Copper Oxide Nanorods Pesticide Sensor For Methyl Parathion Detection*. Paper presented at the IEEE 19th International Conference on Nanotechnology (IEEE-NANO), Macau, PEOPLES R CHINA.
124. Samnani, P., Vishwakarma, K., & Pandey, S. Y. (2011). Simple and Sensitive Method for Determination of Imidacloprid Residue in Soil and Water by HPLC. *Bulletin of Environmental Contamination and Toxicology*, 86(5), 554-558. Retrieved from <Go to ISI>://WOS:000289897400020. doi:10.1007/s00128-011-0245-8
125. Sarangapani, C., O'Toole, G., Cullen, P. J., & Bourke, P. (2017). Atmospheric cold plasma dissipation efficiency of agrochemicals on blueberries. *Innovative Food Science & Emerging Technologies*, 44, 235-241.

- Retrieved from <Go to ISI>://WOS:000418217000031.
doi:10.1016/j.ifset.2017.02.012
126. Sgobbi, L. F., & Machado, S. A. S. (2018). Functionalized polyacrylamide as an acetylcholinesterase-inspired biomimetic device for electrochemical sensing of organophosphorus pesticides. *Biosensors & Bioelectronics*, *100*, 290-297. Retrieved from <Go to ISI>://WOS:000416187600038. doi:10.1016/j.bios.2017.09.019
 127. Shams, N., Lim, H. N., Hajian, R., Yusof, N. A., Abdullah, J., Sulaiman, Y., . . . Pandikumar, A. (2016). A promising electrochemical sensor based on Au nanoparticles decorated reduced graphene oxide for selective detection of herbicide diuron in natural waters. *Journal of Applied Electrochemistry*, *46*(6), 655-666. doi:10.1007/s10800-016-0950-4
 128. Si, W. M., Lei, W., Hao, Q. L., Xia, X. F., Zhang, H., Li, J., . . . Cong, R. M. (2016). Facile Synthesis of Nitrogen-doped Graphene Derived from Graphene Oxide and Vitamin B3 as High-performance Sensor for Imidacloprid Determination. *Electrochimica Acta*, *212*, 784-790. Retrieved from <Go to ISI>://WOS:000382250200086. doi:10.1016/j.electacta.2016.07.063
 129. Silva Junior, G. J., Selva, J. S. G., Sukeri, A., Goncalves, J. M., Regiart, M., & Bertotti, M. (2021). Fabrication of dendritic nanoporous gold via a two-step amperometric approach: Application for electrochemical detection of methyl parathion in river water samples. *Talanta*, *226*, 122130. Retrieved from <https://www.ncbi.nlm.nih.gov/pubmed/33676684>. doi:10.1016/j.talanta.2021.122130
 130. Silva, T. S. E., Soares, I. P., Lacerda, L. R. G., Cordeiro, T. A. R., Ferreira, L. F., & Franco, D. L. (2020). Electrochemical modification of electrodes with polymers derived from hydroxybenzoic acid isomers: Optimized platforms for an alkaline phosphatase biosensor for pesticide detection. *Materials Chemistry and Physics*, *252*. Retrieved from <Go to ISI>://WOS:000566398000015. doi:10.1016/j.matchemphys.2020.123221
 131. Silva, V., Mol, H. G. J., Zomer, P., Tienstra, M., Ritsema, C. J., & Geissen, V. (2019). Pesticide residues in European agricultural soils - A hidden reality unfolded. *Science of the Total Environment*, *653*, 1532-1545. Retrieved from <Go to ISI>://WOS:000458626800144. doi:10.1016/j.scitotenv.2018.10.441
 132. Singh, A. P., Balayan, S., Hooda, V., Sarin, R. K., & Chauhan, N. (2020). Nano-interface driven electrochemical sensor for pesticides detection based on the acetylcholinesterase enzyme inhibition. *International Journal of Biological Macromolecules*, *164*, 3943-3952. Retrieved from <Go to ISI>://WOS:000588093700376. doi:10.1016/j.ijbiomac.2020.08.215
 133. Singh, S., Singh, N., Kumar, V., Datta, S., Wani, A. B., Singh, D., . . . Singh, J. (2016). Toxicity, monitoring and biodegradation of the fungicide carbendazim. *Environmental Chemistry Letters*, *14*(3), 317-329. Retrieved from <Go to ISI>://WOS:000383054400003. doi:10.1007/s10311-016-0566-2

134. Sjerps, R. M. A., Kooij, P. J. F., van Loon, A., & Van Wezel, A. P. (2019). Occurrence of pesticides in Dutch drinking water sources. *Chemosphere*, 235, 510-518. Retrieved from <Go to ISI>://WOS:000487567000054. doi:10.1016/j.chemosphere.2019.06.207
135. Su, D. D., Li, H. X., Yan, X., Lin, Y. H., & Lu, G. Y. (2021). Biosensors based on fluorescence carbon nanomaterials for detection of pesticides. *Trac-Trends in Analytical Chemistry*, 134. Retrieved from <Go to ISI>://WOS:000611899600013. doi:10.1016/j.trac.2020.116126
136. Su, L. T., Wang, S., Wang, L. M., Yan, Z. Y., Yi, H. Y., Zhang, D. W., . . . Ma, Y. (2020). Fluorescent aptasensor for carbendazim detection in aqueous samples based on gold nanoparticles quenching Rhodamine B. *Spectrochimica Acta Part a-Molecular and Biomolecular Spectroscopy*, 225. Retrieved from <Go to ISI>://WOS:000504048200025. doi:10.1016/j.saa.2019.117511
137. Sulak, M. T. (2010). Acetylcholinesterase-Polyprrole Modified Gold Electrode for Determination of Pesticides. *Sensor Letters*, 8(2), 273-279. Retrieved from <Go to ISI>://WOS:000276808500011. doi:10.1166/sl.2010.1263
138. Sun, Z., Chen, D., Jia, F., Zhang, C., Tang, S., Ren, G., & Liu, X. (2014). Effect of six conventional insecticides on *Aphidius gifuensis* Ashmead in tobacco fields. *Plant protection*, 40(4), 185-189. Retrieved from <https://d.wanfangdata.com.cn/periodical/ChlQZXJpb2RpY2FsQ0hJTmV3UzIwMjMwNDI2Eg16d2JoMjAxNDA0MDM4Ggg3OGVodmk5Ng==>. doi:10.3969/j.issn.0529-1542.2014.04.038
139. Syafrudin, M., Kristanti, R. A., Yuniarto, A., Hadibarata, T., Rhee, J., Al-onazi, W. A., . . . Al-Mohaimed, A. M. (2021). Pesticides in Drinking Water-A Review. *International Journal of Environmental Research and Public Health*, 18(2). Retrieved from <Go to ISI>://WOS:000611281900001. doi:10.3390/ijerph18020468
140. Szpyrka, E., Kurdziel, A., Matyaszek, A., Podbielska, M., Rugar, J., & Slowik-Borowiec, M. (2015). Evaluation of pesticide residues in fruits and vegetables from the region of south-eastern Poland. *Food Control*, 48, 137-142. Retrieved from <Go to ISI>://WOS:000343961100021. doi:10.1016/j.foodcont.2014.05.039
141. Taghizadeh, S. F., Rezaee, R., Azizi, M., Hayes, A. W., Giesy, J. P., & Karimi, G. (2021). Pesticides, metals, and polycyclic aromatic hydrocarbons in date fruits: A probabilistic assessment of risk to health of Iranian consumers. *Journal of Food Composition and Analysis*, 98. Retrieved from <Go to ISI>://WOS:000632888700010. doi:10.1016/j.jfca.2021.103815
142. Tan, L. S., Ahmad, A. L., Abd Shukor, S. R., & Yeap, S. P. (2019). Impact of Solute Properties and Water Matrix on Nanofiltration of Pesticides. *Chemical Engineering & Technology*, 42(9), 1780-1787. Retrieved from <Go to ISI>://WOS:000481801600008. doi:10.1002/ceat.201800475
143. Tang, F., Wang, L., & Liu, Y.-N. (2019). Biomass-derived N-doped

- porous carbon: an efficient metal-free catalyst for methylation of amines with CO₂. *Green Chemistry*, 21(23), 6252-6257. doi:10.1039/c9gc03277k
144. Tang, F. H. M., Lenzen, M., McBratney, A., & Maggi, F. (2021). Risk of pesticide pollution at the global scale. *Nature Geoscience*, 14(4), 206-+. Retrieved from <Go to ISI>://WOS:000634737700001. doi:10.1038/s41561-021-00712-5
145. Tang, J., Li, J. J., Xiong, P. Y., Sun, Y. F., Zeng, Z. Y., Tian, X. C., & Tang, D. P. (2020). Rolling circle amplification promoted magneto-controlled photoelectrochemical biosensor for organophosphorus pesticides based on dissolution of core-shell MnO₂ nanoflower@CdS mediated by butyrylcholinesterase. *Microchimica Acta*, 187(8). Retrieved from <Go to ISI>://WOS:000552412800005. doi:10.1007/s00604-020-04434-0
146. Tao, H. P., Bao, Z. W., Jin, C. Y., Miao, W. Y., Fu, Z. W., & Jin, Y. X. (2020). Toxic effects and mechanisms of three commonly used fungicides on the human colon adenocarcinoma cell line Caco-2. *Environmental Pollution*, 263. Retrieved from <Go to ISI>://WOS:000539427600116. doi:10.1016/j.envpol.2020.114660
147. Teixeira, A., Oostingh, G., Valado, A., Osorio, N., Caseiro, A., Gabriel, A., . . . Figueiredo, J. P. (2018). *The impact of pesticides on the cholinesterase-activity in serum samples*.
148. Tertis, M., Cernat, A., Lacatis, D., Florea, A., Bogdan, D., Suci, M., . . . Cristea, C. (2017). Highly selective electrochemical detection of serotonin on polypyrrole and gold nanoparticles-based 3D architecture. *Electrochemistry Communications*, 75, 43-47. Retrieved from <Go to ISI>://WOS:000393249700011. doi:10.1016/j.elecom.2016.12.015
149. Theurillat, X., Dubois, M., & Huertas-Perez, J. F. (2021). A multi-residue pesticide determination in fatty food commodities by modified QuEChERS approach and gas chromatography-tandem mass spectrometry. *Food Chemistry*, 353. Retrieved from <Go to ISI>://WOS:000656155500007. doi:10.1016/j.foodchem.2021.129039
150. Thota, R., & Ganesh, V. (2016). Selective and sensitive electrochemical detection of methyl parathion using chemically modified overhead projector sheets as flexible electrodes. *Sensors and Actuators B-Chemical*, 227, 169-177. Retrieved from <Go to ISI>://WOS:000369944200022. doi:10.1016/j.snb.2015.12.008
151. Tian, X., Liu, L., Li, Y., Yang, C., Zhou, Z., Nie, Y., & Wang, Y. (2018). Nonenzymatic electrochemical sensor based on CuO-TiO₂ for sensitive and selective detection of methyl parathion pesticide in ground water. *Sensors and Actuators B: Chemical*, 256, 135-142. doi:10.1016/j.snb.2017.10.066
152. Tu, X. L., Gao, F., Ma, X., Zou, J., Yu, Y. F., Li, M. F., . . . Lu, L. M. (2020). Mxene/carbon nanohorn/beta-cyclodextrin-Metal-organic frameworks as high-performance electrochemical sensing platform for sensitive detection of carbendazim pesticide. *Journal of Hazardous Materials*, 396. Retrieved from <Go to ISI>://WOS:000541924000087.

doi:10.1016/j.jhazmat.2020.122776

153. Tudi, M., Ruan, H. D., Wang, L., Lyu, J., Sadler, R., Connell, D., . . . Phung, D. T. (2021). Agriculture Development, Pesticide Application and Its Impact on the Environment. *International Journal of Environmental Research and Public Health*, 18(3). Retrieved from <Go to ISI>://WOS:000615222800001. doi:10.3390/ijerph18031112
154. Ueno, E. (2011). Application of gas chromatography/mass spectrometry for residue analysis of pesticides Residue analysis of pesticides in foods using GC-MS and GC-MS/MS (Part I). *Journal of Pesticide Science*, 36(4), 554-558. Retrieved from <Go to ISI>://WOS:000299448100020. doi:10.1584/jpestics.W11-42
155. Upadhyay, L. S. B., & Verma, N. (2013). Enzyme Inhibition Based Biosensors: A Review. *Analytical Letters*, 46(2), 225-241. Retrieved from <Go to ISI>://WOS:000312984400001. doi:10.1080/00032719.2012.713069
156. Urbanova, V., Bakandritsos, A., Jakubec, P., Szambo, T., & Zboril, R. (2017). A facile graphene oxide based sensor for electrochemical detection of neonicotinoids. *Biosens Bioelectron*, 89(Pt 1), 532-537. Retrieved from <https://www.ncbi.nlm.nih.gov/pubmed/27020063>. doi:10.1016/j.bios.2016.03.039
157. Vijver, M. G., & van den Brink, P. J. (2014). Macro-Invertebrate Decline in Surface Water Polluted with Imidacloprid: A Rebuttal and Some New Analyses. *Plos One*, 9(2). Retrieved from <Go to ISI>://WOS:000332396200086. doi:10.1371/journal.pone.0089837
158. Wang, B., Li, X. L., Zhang, L., Wang, G. M., Cao, S. R., & Zhang, J. Z. (2010). Simultaneous Determination of Organochlorine and Pyrethroid Pesticide Residues in Hotpot Condiment by Gas Chromatography. *Chinese Journal of Analytical Chemistry*, 38(10), 1433-1438. Retrieved from <Go to ISI>://WOS:000283904400010. doi:10.3724/sp.J.1096.2010.01433
159. Wang, C., Xiong, Y., Wang, H. W., & Sun, Q. F. (2018). All-round utilization of biomass derived all-solid-state asymmetric carbon-based supercapacitor. *Journal of Colloid and Interface Science*, 528, 349-359. Retrieved from <Go to ISI>://WOS:000440127000037. doi:10.1016/j.jcis.2018.05.103
160. Wang, D. Y., Huang, B. T., Liu, J., Guo, X., Abudukeyoumu, G., Zhang, Y., . . . Li, Y. C. (2018). A novel electrochemical sensor based on Cu@Ni/MWCNTs nanocomposite for simultaneous determination of guanine and adenine. *Biosensors & Bioelectronics*, 102, 389-395. Retrieved from <Go to ISI>://WOS:000424176600052. doi:10.1016/j.bios.2017.11.051
161. Wang, H. B., Su, Y. C., Kim, H. J., Yong, D. M., Wang, L., & Han, X. J. (2015). A Highly Efficient ZrO₂ Nanoparticle Based Electrochemical Sensor for the Detection of Organophosphorus Pesticides. *Chinese Journal of Chemistry*, 33(10), 1135-1139. Retrieved from <Go to ISI>://WOS:000363218000005. doi:10.1002/cjoc.201500460
162. Wang, M., & Li, Z. (2008). Nano-composite ZrO₂/Au film electrode

- for voltammetric detection of parathion. *Sensor. Actuat. B-Chem.*, *133*(2), 607-612. doi:10.1016/j.snb.2008.03.023
163. Wang, N., Hei, Y., Liu, J., Sun, M., Sha, T., Hassan, M., . . . Zhou, M. (2019). Low-cost and environment-friendly synthesis of carbon nanorods assembled hierarchical meso-macroporous carbons networks aerogels from natural apples for the electrochemical determination of ascorbic acid and hydrogen peroxide. *Analytica chimica acta*, *1047*, 36-44.
164. Wang, Q., Yin, Q. B., Fan, Y., Zhang, L., Xu, Y., Hu, O., . . . She, Y. B. (2019). Double quantum dots-nanoporphyrin fluorescence-visualized paper-based sensors for detecting organophosphorus pesticides. *Talanta*, *199*, 46-53. Retrieved from <Go to ISI>://WOS:000465050000008. doi:10.1016/j.talanta.2019.02.023
165. Wang, S., Chen, H. Y., Xie, H. L., Wei, L. N., Xu, L., Zhang, L., . . . Fu, H. Y. (2021). A novel thioctic acid-carbon dots fluorescence sensor for the detection of Hg²⁺ and thiophanate methyl via S-Hg affinity. *Food Chemistry*, *346*. Retrieved from <Go to ISI>://WOS:000614807500018. doi:10.1016/j.foodchem.2020.128923
166. Wang, S., Wang, R., Zhang, Y., Jin, D., & Zhang, L. (2018). Scalable and sustainable synthesis of carbon microspheres via a purification-free strategy for sodium-ion capacitors. *Journal of Power Sources*, *379*, 33-40. doi:10.1016/j.jpowsour.2018.01.019
167. Wang, S. Y., Shi, X. C., Liu, F. Q., & Laborda, P. (2020). Chromatographic Methods for Detection and Quantification of Carbendazim in Food. *Journal of Agricultural and Food Chemistry*, *68*(43), 11880-11894. Retrieved from <Go to ISI>://WOS:0005868886500002. doi:10.1021/acs.jafc.0c04225
168. Wang, Y. L., Jin, J., Yuan, C. X., Zhang, F., Ma, L. L., Qin, D. D., . . . Lu, X. Q. (2015). A novel electrochemical sensor based on zirconia/ordered macroporous polyaniline for ultrasensitive detection of pesticides. *Analyst*, *140*(2), 560-566. Retrieved from <Go to ISI>://WOS:000346304200021. doi:10.1039/c4an00981a
169. Wu, S., Lan, X., Cui, L., Zhang, L., Tao, S., Wang, H., . . . Meng, C. (2011). Application of graphene for preconcentration and highly sensitive stripping voltammetric analysis of organophosphate pesticide. *Anal Chim Acta*, *699*(2), 170-176. Retrieved from https://www.ncbi.nlm.nih.gov/pubmed/21704771. doi:10.1016/j.aca.2011.05.032
170. Xue, X., Wei, Q., Wu, D., Li, H., Zhang, Y., Feng, R., & Du, B. (2014). Determination of methyl parathion by a molecularly imprinted sensor based on nitrogen doped graphene sheets. *Electrochim. Acta*, *116*, 366-371. doi:10.1016/j.electacta.2013.11.075
171. Yang, J., & Liang, J. Z. (2011). A modified model of electrical conduction for carbon black-polymer composites. *Polymer International*, *60*(5), 738-742. Retrieved from <Go to ISI>://WOS:000289516300004.

doi:10.1002/pi.3002

172. Yang, X.-m., Gu, Y.-p., Wu, S.-j., Feng, L., & Xie, F. (2019). *Research on a rapid detection method of pesticide residues in milk by enzyme inhibition*. Paper presented at the E3S Web of Conferences.
173. Yang, Y. X., Huo, D. Q., Wu, H. X., Wang, X. F., Yang, J. S., Bian, M. H., . . . Hou, C. J. (2018). N, P-doped carbon quantum dots as a fluorescent sensing platform for carbendazim detection based on fluorescence resonance energy transfer. *Sensors and Actuators B-Chemical*, 274, 296-303. Retrieved from <Go to ISI>://WOS:000443960000032. doi:10.1016/j.snb.2018.07.130
174. Yao, Y., Zhang, L., Xu, J., Wang, X., Duan, X., & Wen, Y. (2014). Rapid and sensitive stripping voltammetric analysis of methyl parathion in vegetable samples at carboxylic acid-functionalized SWCNTs- β -cyclodextrin modified electrode. *J. Electroanal. Chem.*, 713, 1-8. doi:10.1016/j.jelechem.2013.11.024
175. Ye, X. L., Gu, Y. G., & Wang, C. M. (2012). Fabrication of the Cu₂O/polyvinyl pyrrolidone-graphene modified glassy carbon-rotating disk electrode and its application for sensitive detection of herbicide paraquat. *Sensors and Actuators B-Chemical*, 173, 530-539. Retrieved from <Go to ISI>://WOS:000311248100075. doi:10.1016/j.snb.2012.07.047
176. Yu, G. X., Zhang, W. N., Zhao, Q., Wu, W. X., Wei, X. Y., & Lu, Q. (2016). Enhancing the sensitivity of hexachlorobenzene electrochemical sensor based on nitrogen-doped graphene. *Sensors and Actuators B-Chemical*, 235, 439-446. Retrieved from <Go to ISI>://WOS:000380823400055. doi:10.1016/j.snb.2016.05.072
177. Yu, Q. W., Sun, H., Wang, K., He, H. B., & Feng, Y. Q. (2017). Monitoring of Carbendazim and Thiabendazole in Fruits and Vegetables by SiO₂@NiO-Based Solid-Phase Extraction Coupled to High-Performance Liquid Chromatography-Fluorescence Detector. *Food Analytical Methods*, 10(8), 2892-2901. Retrieved from <Go to ISI>://WOS:000405821500028. doi:10.1007/s12161-017-0837-y
178. Yuan, Y. Y., Wang, S. T., Liu, S. Y., Cheng, Q., Wang, Z. F., & Kong, D. M. (2020). Green approach for simultaneous determination of multi-pesticide residue in environmental water samples using excitation-emission matrix fluorescence and multivariate calibration. *Spectrochimica Acta Part a-Molecular and Biomolecular Spectroscopy*, 228. Retrieved from <Go to ISI>://WOS:000513010500099. doi:10.1016/j.saa.2019.117801
179. Yue, X., Han, P., Zhu, W., Wang, J., & Zhang, L. (2016). Facile and sensitive electrochemical detection of methyl parathion based on a sensing platform constructed by the direct growth of carbon nanotubes on carbon paper. *Rsc Advances*, 6(63), 58771-58779. doi:10.1039/c6ra09335c
180. Zambianco, N. A., Silva, T. A., Zanin, H., Fatibello-Filho, O., & Janegitz, B. C. (2019). Novel electrochemical sensor based on nanodiamonds and manioc starch for detection of diquat in environmental samples. *Diamond and Related Materials*, 98. doi:10.1016/j.diamond.2019.107512

181. Zeng, W. J., Li, C., Feng, Y., Zeng, S. H., Fu, B. X., & Zhang, X. L. (2021). Carboxylated multi-walled carbon nanotubes (MWCNTs-COOH)-intercalated graphene oxide membranes for highly efficient treatment of organic wastewater. *Journal of Water Process Engineering*, 40. Retrieved from <Go to ISI>://WOS:000632958500006. doi:10.1016/j.jwpe.2020.101901
182. Zhai, X. C., Zhang, M., Chen, P., Siriphithakyothin, T., Liu, J. Y., Zhao, H. T., . . . Wang, J. (2020). Oligochitosan-modified three-dimensional graphene free-standing electrode for electrochemical detection of imidacloprid insecticide. *Journal of the Chinese Chemical Society*, 67(6), 1078-1088. Retrieved from <Go to ISI>://WOS:000503149600001. doi:10.1002/jccs.201900395
183. Zhai, Y., Xuan, T., Wu, Y. P., Guo, X. Y., Ying, Y., Wen, Y., & Yang, H. F. (2021). Metal-organic-frameworks-enforced surface enhanced Raman scattering chip for elevating detection sensitivity of carbendazim in seawater. *Sensors and Actuators B-Chemical*, 326. Retrieved from <Go to ISI>://WOS:000582806300045. doi:10.1016/j.snb.2020.128852
184. Zhang, B., Jiang, Y. Q., & Balasubramanian, R. (2021). Synthesis, formation mechanisms and applications of biomass-derived carbonaceous materials: a critical review. *Journal of Materials Chemistry A*, 9(44), 24759-24802. Retrieved from <Go to ISI>://WOS:000714174700001. doi:10.1039/d1ta06874a
185. Zhang, W., Liu, L., Li, Y., Wang, D., Ma, H., Ren, H., . . . Ye, B. C. (2018). Electrochemical sensing platform based on the biomass-derived microporous carbons for simultaneous determination of ascorbic acid, dopamine, and uric acid. *Biosens Bioelectron*, 121, 96-103. Retrieved from <https://www.ncbi.nlm.nih.gov/pubmed/30199714>. doi:10.1016/j.bios.2018.08.043
186. Zhang, X., Du, J., Wu, D. P., Long, X. Y., Wang, D., Xiong, J. H., . . . Liao, X. N. (2021). Anchoring Metallic MoS₂ Quantum Dots over MWCNTs for Highly Sensitive Detection of Postharvest Fungicide in Traditional Chinese Medicines. *Acs Omega*, 6(2), 1488-1496. Retrieved from <Go to ISI>://WOS:000612348300048. doi:10.1021/acsomega.0c05253
187. Zhang, Y., Waterhouse, G. I. N., Xiang, Z. P., Che, J., Chen, C., & Sun, W. (2020). A highly sensitive electrochemical sensor containing nitrogen-doped ordered mesoporous carbon (NOMC) for voltammetric determination of l-tryptophan. *Food Chem*, 326, 126976. Retrieved from <https://www.ncbi.nlm.nih.gov/pubmed/32413756>. doi:10.1016/j.foodchem.2020.126976
188. Zhao, G., Wang, H., & Liu, G. (2015). Advances in Biosensor-Based Instruments for Pesticide Residues Rapid Detection. *International Journal of Electrochemical Science*, 10(12), 9790-9807. Retrieved from <Go to ISI>://WOS:000366307100001.
189. Zhao, H., Ji, X., Wang, B., Wang, N., Li, X., Ni, R., . . . bioelectronics.

- (2015). An ultra-sensitive acetylcholinesterase biosensor based on reduced graphene oxide-Au nanoparticles- β -cyclodextrin/Prussian blue-chitosan nanocomposites for organophosphorus pesticides detection. *65*, 23-30.
190. Zhao, H., Li, B., Liu, R., Chang, Y., Wang, H., Zhou, L., & Komarneni, S. (2021). Ultrasonic-assisted preparation of halloysite nanotubes/zirconia/carbon black nanocomposite for the highly sensitive determination of methyl parathion. *Materials Science and Engineering: C*, *123*. doi:10.1016/j.msec.2021.111982
191. Zhao, H., Liu, B., Li, Y., Li, B., Ma, H., & Komarneni, S. (2020). One-pot green hydrothermal synthesis of bio-derived nitrogen-doped carbon sheets embedded with zirconia nanoparticles for electrochemical sensing of methyl parathion. *Ceram. Int.*, *46*(12), 19713-19722. doi:10.1016/j.ceramint.2020.04.277
192. Zhao, H., Ma, H., Li, X., Liu, B., Liu, R., & Komarneni, S. (2021). Nanocomposite of halloysite nanotubes/multi-walled carbon nanotubes for methyl parathion electrochemical sensor application. *Appl. Clay Sci.*, *200*. doi:10.1016/j.clay.2020.105907
193. Zhao, H., Ran, Q., Li, Y., Li, B., Liu, B., Ma, H., . . . Komarneni, S. (2020). Highly sensitive detection of gallic acid based on 3D interconnected porous carbon nanotubes/carbon nanosheets modified glassy carbon electrode. *J. Mater. Res. Technol.*, *9*(4), 9422-9433. doi:10.1016/j.jmrt.2020.05.102
194. Zhao, H. Y., Ji, X. P., Wang, B. B., Wang, N., Li, X. R., Ni, R. X., & Ren, J. J. (2015). An ultra-sensitive acetylcholinesterase biosensor based on reduced graphene oxide-Au nanoparticles-beta-cyclodextrin/Prussian blue-chitosan nanocomposites for organophosphorus pesticides detection. *Biosensors & Bioelectronics*, *65*, 23-30. Retrieved from <Go to ISI>://WOS:000348880000005. doi:10.1016/j.bios.2014.10.007
195. Zhao, H. Y., Li, B., Liu, R. Q., Chang, Y. Q., Wang, H. L., Zhou, L., & Komarneni, S. (2021). Ultrasonic-assisted preparation of halloysite nanotubes/zirconia/carbon black nanocomposite for the highly sensitive determination of methyl parathion. *Materials Science & Engineering C-Materials for Biological Applications*, *123*. Retrieved from <Go to ISI>://WOS:000637805000008. doi:10.1016/j.msec.2021.111982
196. Zheng, Y., Liu, Z., Zhan, H., Li, J., & Zhang, C. J. A. m. (2016). Studies on electrochemical organophosphate pesticide (OP) biosensor design based on ionic liquid functionalized graphene and a Co₃O₄ nanoparticle modified electrode. *8*(26), 5288-5295.
197. Zhou, H., Wei, C., Fang, J., Fu, L., Liu, G., & Liu, Q. (2019). Poly 3,4-ethylenedioxythiophene and zirconia nanoparticles composite modified sensor for methyl parathion determination. *Journal of Electroanalytical Chemistry*, *848*. doi:10.1016/j.jelechem.2019.113282
198. Zhou, H. H., Wei, C. H. N., Fang, J., Fu, L. K., Liu, G., & Liu, Q. M. (2019). Poly 3,4-ethylenedioxythiophene and zirconia nanoparticles

- composite modified sensor for methyl parathion determination. *Journal of Electroanalytical Chemistry*, 848. Retrieved from <Go to ISI>://WOS:000504505400038. doi:10.1016/j.jelechem.2019.113282
199. Zhou, W., Li, W., Xie, Y., Wang, L., Pan, K., Tian, G., . . . Fu, H. (2014). Fabrication of noncovalently functionalized brick-like β -cyclodextrins/graphene composite dispersions with favorable stability. *RSC Adv.*, 4(6), 2813-2819. doi:10.1039/c3ra45666h
200. Zhou, X. F., He, K. Y., Wang, Y., Zheng, H. T., & Suye, S. (2015). Amperometric Determination of Ascorbic Acid on an Au Electrode Modified by a Composite Film of Poly(3,4-ethylenedioxythiophene) and Superconductive Carbon Black. *Analytical Sciences*, 31(5), 429-436. Retrieved from <Go to ISI>://WOS:000355361700012. doi:10.2116/analsci.31.429
201. ZHOU, Y.-z., WANG, X., LIU, B.-l. J. S., & Industry, T. o. F. (2018). Progress of functionalized nano probe based on aptamer in food safety and detection. (10), 62.
202. Zhou, Y., Cheng, F., Hong, Y., Huang, J., Zhang, X., & Liao, X. (2020). Rapid and Sensitive Detection of Isoproturon Via an Electrochemical Sensor Based on Highly Water-Dispersed Carbon Hybrid Material. *Food Analytical Methods*, 13(4), 839-849. doi:10.1007/s12161-020-01707-5
203. Zhou, Y., Jiang, T., Xiong, X., & Liu, G. (2018). Application of HPLC Method for Detecting Pesticides Residues in Vegetables. *Fram Products Processing*(08), 73-74+77. doi:10.16693/j.cnki.1671-9646(X).2018.04.051
204. Zou, N., Yuan, C. H., Liu, S. W., Han, Y. T., Li, Y. J., Zhang, J. L., . . . Pan, C. P. (2016). Coupling of multi-walled carbon nanotubes/polydimethylsiloxane coated stir bar sorptive extraction with pulse glow discharge-ion mobility spectrometry for analysis of triazine herbicides in water and soil samples. *Journal of Chromatography A*, 1457, 14-21. Retrieved from <Go to ISI>://WOS:000380080000003. doi:10.1016/j.chroma.2016.06.043
205. Zuniga-Venegas, L., Saracini, C., Pancetti, F., Munoz-Quezada, M. T., Lucero, B., Foerster, C., & Cortes, S. (2021). Exposicion a plaguicidas en Chile y salud poblacional: urgencia para la toma de decisiones. *Gaceta Sanitaria*, 35(5), 480-487. Retrieved from <Go to ISI>://WOS:000700785000012. doi:10.1016/j.gaceta.2020.04.020